ENHANCING CAROTENOIDS PRODUCTION OF *Rhodotorula paludigena* CM33 USING CRUDE GLYCEROL AS THE SUBSTRATE AND ITS APPLICATION IN DIETARY SUPPLEMENT OF *Litopenaeus vannamei*

CHEERANAN SRIPHUTTHA

A Thesis Submitted in Partial Fulfillment of the Requirements for the

Degree of Doctor of Philosophy in Biotechnology

Suranaree University of Technology

Academic Year 2022

การเพิ่มการผลิตแคโรทีนอยด์ของ *Rhodotorula paludigena* CM33 โดยใช้กลีเซอรอลดิบเป็นสารตั้งต้น และการประยุกต์ใช้ในผลิตภัณฑ์เสริมอาหารของ *Litopenaeus vannamei*

นางสาวจีรนันท์ ศรีพุทธา

วิทยานิพนธ์นี้เป็นส่วนหนึ่งของการศึกษาตามหลักสูตรปริญญาวิทยาศาสตรดุษฎีบัณฑิต
สาขาวิชาเทคโนโลยีชีวภาพ
มหาวิทยาลัยเทคโนโลยีสุรนารี
ปีการศึกษา 2565

ENHANCING CAROTENOIDS PRODUCTION OF *Rhodotorula paludigena* CM33 USING CRUDE GLYCEROL AS THE SUBSTRATE AND ITS APPLICATION IN DIETARY SUPPLEMENT OF *Litopenaeus vannamei*

Suranaree University of Technology has approved this thesis submitted in partial fulfillment of the requirements for the Degree of Doctor of Philosophy.

Thesis Examining Committee
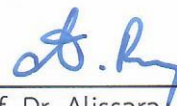
_____
(Prof. Dr. Alissara Reungsang)
Chairperson

_____
(Assoc. Prof. Dr. Apichat Boontawan)
Member (Thesis Advisor)

_____
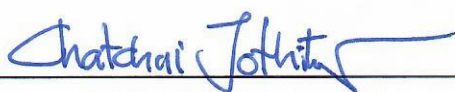(Assoc. Prof. Dr. Mariena Ketudat-Cairns)
Member

_____
(Assoc. Prof. Dr. Panlada Tittabutr)
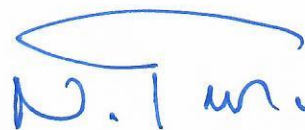Member

_____
(Dr. Pakpoom Boonchuen)
Member

_____
(Assoc. Prof. Dr. Chatchai Jothityangkoon)
Vice Rector for Academic Affairs
and Quality Assurance

_____
(Prof. Dr. Neung Teaumroong)
Dean of Institute of Agricultural
Technology

จีรนันท์ ศรีพุทธา: การเพิ่มการผลิตแคโรทีนอยด์ของ *Rhodotorula paludigena* CM33
โดยใช้กลีเซอรอลดิบเป็นสารตั้งต้นและการประยุกต์ใช้ในผลิตภัณฑ์เสริมอาหารของ
Litopenaeus vannamei (ENHANCING CAROTENOIDS PRODUCTION OF
Rhodotorula paludigena CM33 USING CRUDE GLYCEROL AS THE SUBSTRATE
AND ITS APPLICATION IN DIETARY SUPPLEMENT OF *Litopenaeus vannamei*)
อาจารย์ที่ปรึกษา: รองศาสตราจารย์ ดร. อภิชาติ บุญทาวัน, 112 หน้า.

คำสำคัญ: แคโรทีนอยด์/*Rhodotorula paludigena* CM33/กลีเซอรอลดิบ/*Litopenaeus
vannamei*/โปรไบโอติก

Rhodotorula paludigena CM33 เป็น oleaginous yeast ที่มีการสะสมไขมันและ
แคโรทีนอยด์ภายในเซลล์ ในการศึกษานี้มีวัตถุประสงค์ที่หนึ่งเพื่อการปรับปรุงการใช้ประโยชน์ของ
กลีเซอรอลดิบเป็นสารตั้งต้นในการเพาะเลี้ยง *R. paludigena* CM33 โดยใช้วิธีการพื้นผิวตอบสนอง
(Response Surface Methodology: RSM) ออกแบบการทดลองเพื่อปรับปรุงปัจจัยที่ส่งผลต่อ
การเจริญเติบโตและเพื่อเพิ่มการผลิตแคโรทีนอยด์ของยีสต์ชนิดนี้ จากการทดลองพบว่า วิธีการพื้นผิว
ตอบสนองการใช้กลีเซอรอลดิบเท่ากับ 40 กรัมต่อลิตร ร่วมกับสารสกัดจากยีสต์ 0.72 กรัมต่อลิตร,
และ $(NH_4)_2SO_4$ 0.43 กรัมต่อลิตร มีค่าแคโรทีนอยด์สูงสุดเท่ากับ 328 ไมโครกรัมต่อกรัม
และหลังจากผ่านการหมักแบบกึ่งกะในถังหมักขนาด 500 ลิตร มีผลน้ำหนักแห้งของเซลล์ และ
แคโรทีนอยด์สูงสุดเท่ากับ 45.38±1.05 กรัมต่อลิตร และ 15.39±0.03 มิลลิกรัมต่อกรัม ตามลำดับ
ซึ่งผลการวิจัยแสดงให้เห็นว่าการเพาะเลี้ยง *R. paludigena* CM33 ด้วยกลีเซอรอลดิบร่วมกับการ
หมักแบบกึ่งกะในถังหมักขนาด 500 ลิตรส่งผลต่อความเข้มข้นของแคโรทีนอยด์ได้อย่างมี
ประสิทธิภาพ

วัตถุประสงค์ที่สองปรับปรุงกระบวนการเก็บเกี่ยว สกัด และแยกแคโรทีนอยด์จากเซลล์ของ
R. paludigena CM33 โดยทำการเก็บเกี่ยวเซลล์ด้วยกระบวนการกรองขนาดเล็ก (Microfiltration)
และทำการทำลายผนังเซลล์และสกัดแคโรทีนอดย์ด้วยเครื่องลดขนาดอนุภาค (high-pressure
homogenizer : HPH) โดยใช้วิธีการพื้นผิวตอบสนองออกแบบการทดลอง และทำการแยก
แคโรทีนอยด์ด้วยเครื่องโครมาโทกราฟีสำหรับวิเคราะห์เตรียมสารสำคัญ (preparative high-
performance liquid chromatography : prep HPLC) และสุดท้ายวิเคราะห์ชนิดของแคโรทีนอยด์
ที่ได้ด้วยเทคนิค HPLC, LC-MS, และ NMR ผลการวิจัยพบว่าส่วนต้านทานของของแข็งที่ค้างบนแผ่น
กรอง (Cake) มีค่าเท่ากับร้อยละ 85.38 และสำหรับส่วนต้านทานจากการดูดซับมีค่าเท่ากับร้อยละ
12.62 ในส่วนของผลการทำลายผนังเซลล์และสกัดแคโรทีนอยด์ด้วย HPH โดยใช้วิธีการพื้นผิว
ตอบสนองในการออกแบบการทดลอง พบว่าการใช้ความดัน 30,000 psi, การทำการผ่าน 4 ครั้ง,

และการใช้เซลล์ยีสต์ร้อยละ 5 นำไปสู่การทำลายเซลล์ที่เพิ่มขึ้น และหลังจากผ่าน prep HPLC ผล
การวิเคราะห์ด้วยเทคนิค HPLC, LC-MS, และ NMR ยืนยันการตรวจพบแคโรทีนอยด์หลักคือเบต้า-
แคโรทีน แสดงให้เห็นถึงศักยภาพของกระบวนการกรองขนาดเล็ก ทำลายผนังเซลล์และสกัดแคโรที
นอยด์ด้วยเครื่องลดขนาดอนุภาค และเครื่องโครมาโทกราฟีสำหรับวิเคราะห์เตรียมสารสำคัญ มีการ
เพิ่มประสิทธิภาพในกระบวนการเก็บเกี่ยว สกัดและแยกแคโรทีนอยด์ในเซลล์ *R. paludigena* CM33

นอกจากนี้วัตถุประสงค์ที่สามคือการศึกษาศักยภาพของ *R. paludigena* CM33 สำหรับเป็น
โปรไบโอติกสำหรับกุ้งขาว โดยการศึกษานี้ได้ประเมินผลของระดับต่างๆ ของ *R. paludigena* CM33
(RD) ที่ผสมกับอาหารกุ้งต่อการเติบโตของกุ้งขาว (*Litopenaeus vannamei*) ต่อการเจริญเติบโต
การแสดงของยีนในระบบภูมิคุ้มกัน สุขภาพลำไส้ ความต้านทานต่อการติดเชื้อ *Vibrio
parahaemolyticus* (VP$_{AHPND}$) และส่วนประกอบของเนื้อกุ้ง ผลการวิจัยพบว่า กุ้งที่ได้รับอาหารผสม
ยีสต์ร้อยละ 1, 2 และ 5 มีอัตราการเจริญเติบโต น้ำหนัก และอัตรารอดสูงกว่าชุดควบคุม และการให้
อาหารผสมยีสต์ร้อยละ 5 ส่งผลทำให้มีการลดการตายสะสมเมื่อถูกทดสอบกับ VP$_{AHPND}$ อีกทั้งยังมี
การแสดงของ immune-responsive genes เช่น โปรฟีนอลออกซิเดส (prophenoloxidase-2:
PO2) และเอนไซม์ต้านอนุมูลอิสระ (superoxide dismutase: SOD, glutathione peroxidase:
GPX, และ catalase: CAT), JAK/STAT pathway (signal transducer และ activator of
transcription: STAT, gamma interferon inducible lysosomal thiol reductase: GILT), IMD
pathway (inhibitor of nuclear factor kappa-B kinase subunit beta และ epsilon: IKKb and
IKKe) และ Toll pathway (Lysozyme) เพิ่มสูงขึ้นในกลุ่มที่ได้รับอาหารผสมยีสต์ร้อยละ 5 และ
นอกจากนี้การวิเคราะห์จุลินทรีย์ในลำไส้กุ้ง แสดงให้เห็นถึงผลของระดับของสายพันธุ์ *Vibrio* ลดลงใน
กลุ่มที่ได้รับอาหารผสมยีสต์ร้อยละ 5 ในขณะที่มีการเพิ่มจำนวนของแบคทีเรียที่มีประโยชน์อย่างสาย
พันธุ์ *Bifidobacterium* ในกลุ่มที่ได้รับอาหารผสมยีสต์ร้อยละ 5 เช่นเดียวกัน ในส่วนของการ
วิเคราะห์ส่วนประกอบของเนื้อกุ้ง แสดงให้เห็นถึงการเพิ่มขึ้นของโปรตีนและไขมัน ซึ่งส่วนประกอบ
ดังกล่าวเป็นสารอาหารที่สำคัญ ดังนั้น ผลการวิจัยทั้งหมดแสดงให้เห็นถึงความสามารถของ
R. paludigena CM33 ในการเป็นโปรไบโอติกในอาหารกุ้งที่สามารถเพิ่มการเจริญเติบโต
ความต้านทานต่อโรค VP$_{AHPND}$ และเพิ่มคุณภาพเนื้อกุ้งโดยการเพิ่มความเข้มข้นของโปรตีนและไขมัน
ในกุ้งได้

สาขาวิชาเทคโนโลยีชีวภาพ   ลายมือชื่อนักศึกษา _____
ปีการศึกษา 2565   ลายมือชื่ออาจารย์ที่ปรึกษา _____
                                           ลายมือชื่ออาจารย์ที่ปรึกษาร่วม _____
                                           ลายมือชื่ออาจารย์ที่ปรึกษาร่วม _____

CHEERANAN SRIPHUTTHA: ENHANCING CAROTENOIDS PRODUCTION OF
Rhodotorula paludigena CM33 USING CRUDE GLYCEROL AS THE SUBSTRATE
AND ITS APPLICATION IN DIETARY SUPPLEMENT OF *Litopenaeus vannamei*.
THESIS ADVISOR: ASSOC. PROF. APICHAT BOONTAWAN, Ph.D., 112 PP.

Keyword: Carotenoids/*Rhodotorula paludigena* CM3/Crude glycerol/*Litopenaeus vannamei*/Probiotic

Rhodotorula paludigena CM33 is an oleaginous yeast that accumulates lipids and carotenoids intracellularly. The first objective of this study was to improve the utilization of crude glycerol, as a substrate for cultivating *R. paludigena* CM33 and to use the Response Surface Methodology (RSM) to optimize factors influencing its growth and enhance carotenoid production. The results of this study revealed that the optimal conditions for carotenoid production were achieved by using 40 g/L of crude glycerol, 0.72 g/L of yeast extract, and 0.43 g/L of $(NH_4)_2SO_4$, resulting in a carotenoid yield of 382 µg/g. The maximum dry cell weight and carotenoid concentration obtained were 45.38±1.05 g/L and 15.39±0.03 mg/g, respectively, in 500-L fed-batch fermentation. The findings demonstrate that culturing *R. paludigena* CM33 with crude glycerol, combined with fed-batch fermentation in a 500-liter fermenter, efficiently enhances the carotenoid concentration.

The second objective was to improve the harvesting, extraction, and separation of carotenoids from the cells of *R. paludigena* CM33. This was achieved by harvesting the cells through a microfiltration process, then disrupting the cell walls and extracting carotenoids using a high-pressure homogenizer (HPH) in experiment design with the RSM. The carotenoids were subsequently separated using preparative high-performance liquid chromatography (prep HPLC), and their types were analyzed using HPLC, LC-MS, and NMR techniques. The results revealed that the cake accounted for 85.38% of the overall resistance, while the adsorption resistance accounted for 12.62%. The use of HPH for cell disruption and carotenoid extraction, along with RSM, revealed that a pressure of 30,000 psi, 4 passes, and a 5% feed led to increased cell disruption. After passing through prep HPLC, the analysis using HPLC, LC-MS, and NMR techniques confirmed the identification of the main carotenoid as β-carotene. These results

demonstrated the potential of microfiltration, cell disruption, and carotenoid extraction using a high-pressure homogenizer, as well as preparative HPLC for efficient carotenoid extraction and separation in *R. paludigena* CM33 cells.

The third objective was to assess the effects of incorporating different levels of *R. paludigena* CM33 (RD) in the dietary composition on the growth, immune-related gene expression, intestinal health, resistance to *Vibrio parahaemolyticus* (VP_{AHPND}) infection, and meat composition of shrimp (*Litopenaeus vannamei*). The results demonstrated significant improvements in the specific growth rate, weight gain, and survival of shrimp fed with 1% RD, 2% RD, and 5% RD. Administration of 5% RD led to a reduction in cumulative mortality following the VP_{AHPND} challenge. Furthermore, the expression levels of immune-responsive genes, such as the proPO system (prophenoloxidase-2: PO2), antioxidant enzymes (superoxide dismutase: SOD, glutathione peroxidase: GPX, and catalase: CAT), JAK/STAT pathway (signal transducer and activator of transcription: STAT, gamma interferon-inducible lysosomal thiol reductase: GILT), IMD pathway (inhibitor of nuclear factor kappa-B kinase subunit beta and epsilon: IKKb and IKKe), and Toll pathway (Lysozyme) genes, were up-regulated in the 5% RD group. Microbiome analysis revealed that the genus level, *Vibrio* was found to be reduced in the 5% RD group, whereas the abundance of potentially beneficial bacteria, such as *Bifidobacterium*, increased. The 5% RD group exhibited a significant increase in crude protein and crude lipid levels, which are essential nutrients. These results indicate that *R. paludigena* CM33 has the potential to serve as a probiotic supplement in shrimp feed, improving growth, disease resistance against VP_{AHPND}, and meat quality by increasing protein and lipid content in shrimp.

School of Biotechnology

Academic Year 2022

Student's Signature_____

Advisor's Signature_____

Co-Advisor's Signature_____

Co-Advisor's Signature_____

ACKNOWLEDGEMENTS

Upon the completion of my thesis, I would like to extend my sincere gratitude to my exceptional supervisor, Associate Professor Dr. Apicaht Boontawan, for his superb guidance, supervision, encouragement, and support throughout my three-year study. His invaluable advice and our insightful conversations have played a pivotal role in shaping the conclusions of my research. I want to express my heartfelt appreciation for all that you have done to facilitate my learning, growth, and development as a more proficient researcher.

To Associate Professor Dr. Mariena Ketudat-Cairns, my co-supervisor, I would like to express my gratitude for the opportunity to be a part of your pleasant, large, and exceptional laboratory research group. Thank you for welcoming me and allowing me to contribute to the valuable research conducted in the group.

A special thanks goes to Dr. Pakpoom Boonchuen, my co-supervisor, for providing me with the opportunity to join a supportive, dynamic, and exceptional laboratory research group. Your constant support and guidance have been invaluable throughout my journey. I have not only acquired profound scientific knowledge from you but also gained valuable scientific experiences that you generously shared with me. Additionally, I would like to express my gratitude to the members of AB's and PB's labs for their valuable suggestions and engaging discussions regarding my work.

Additional great appreciation is extended to Professor Dr. Alissara Reungsang and Associate Professor Dr. Panlada Tittabutr for generously dedicating your valuable time to serve as members of my thesis defense committee. Your expertise and insights have greatly contributed to the successful completion of my thesis. Thank you for your valuable feedback and constructive criticism.

Finally, I would like to express my heartfelt appreciation to indispensable individuals, such as my parents, my husband, my son, and all members of my family, for their invaluable advice, understanding, encouragement, unwavering love, care, and support throughout my life. Their presence and support have been instrumental in my personal and academic growth, and I am truly grateful for their constant belief in me.

Cheeranan Sriphuttha

TABLE OF CONTENTS

TABLE OF CONTENTS (Continued)

TABLE OF CONTENTS (Continued)

TABLE OF CONTENTS (Continued)

LIST OF TABLES

LIST OF FIGURES

LIST OF FIGURES (Continued)

LIST OF ABBREVIATIONS

β	=	Beta
OD_{600}	=	Optical density measured at 600 nm
DI	=	Deionized water
μL	=	Microliters
YPD	=	Yeast Peptone Dextrose medium
h	=	Hour
$Y_{carotenoid}$	=	Carotenoids (mg/g)
°C	=	Degree Celsius
%	=	Percent
w/w	=	Weight per Weight
w/v	=	Weight per Volume
g/L	=	Gram per Liter
$L/m^2/h$	=	Liter per Square meter per Hour
g	=	Gram
s	=	Second
mg/g	=	Microgram per Gram
mL/min	=	Milliliter per Minute
mM	=	Millimolar
et al.,	=	and other
mL	=	Milliliter
rpm	=	Round per Minute
vvm	=	Volume per Volume per Liter
min	=	Minute
C18:1	=	Oleic acid
C16:0	=	Palmitic acid
SD	=	Standard deviation
SE	=	Standard error
TCBS	=	Thiosulfate-citrate-bile salts-sucrose agar

LIST OF ABBREVIATIONS (Continued)

GC-MS	=	Gas Chromatography-Mass Spectrometry
HPH	=	High-pressure homogenizer
prep HPLC	=	Preparative High Performance Liquid Chromatography
HPLC	=	High Performance Liquid Chromatography
LC-MS	=	Liquid Chromatography-Mass Spectrometer
NMR	=	Nuclear Magnetic Resonance
MF	=	Microfiltration
RSM	=	Response Surface methodology
Pa	=	Pascal
VP_{AHPND}	=	*Vibrio parahaemolyticus* AHPND
AHPND	=	Acute hepatopancreatic necrosis disease
DNA	=	Deoxyribonucleic acid
cDNA	=	Complementary Deoxyribonucleic acid
dsRNA	=	Double-stranded RNA
LD_{50}	=	Lethal Dose fifty
$CFU.mL^{-1}$	=	Colony Forming Unit per Milliliter
qRT- PCR	=	Quantitative real-time Polymerase chain reaction
L	=	Liter
TSB	=	Tryptic Soy Broth
OTUs	=	operational taxonomic units

CHAPTER 1

INTRODUCTION

1.1 Background

Carotenoids are vibrant organic compounds that exhibit colors ranging from yellow to red. They can be found in various organisms, including plants, animals, algae, bacteria, and yeast (Maldonade et al., 2008; Mata-Gómez et al., 2014). There are two groups consist of carotene and xanthophylls (Bhosale & Bernstein, 2005). Furthermore, carotenoid pigments have recently become widely used in industries such as cosmetics, pharmaceuticals, chemicals, and food supplements, making them expensive (Mata-Gómez et al., 2014). Commercial carotenoids can be produced through vegetable extraction or chemical synthesis. However, chemical synthesis can result in hazardous waste that can negatively impact the environment. Plant-based production of carotenoids can be challenging due to geographic variability and seasonal limitations. In contrast, microbial production can utilize low-cost substrates, resulting in a more cost-effective method for producing carotenoids (Maldonade et al., 2008). Using oleaginous yeast for carotenoids production is a promising alternative that could help reduce costs in the industry (Valduga et al., 2014).

Oleaginous yeast cultivation has the potential to utilize industry waste to accumulate intracellular carotenoids and produce lipids. In addition, these yeasts can utilize agricultural waste products such as crude glycerol and wastewater, making them a sustainable option for carotenoid production (Mata-Gómez et al., 2014). Oleaginous yeast is known to accumulate high levels of intracellular lipids, with some strains capable of producing up to 20 – 25% lipid content (Breil et al., 2016). The yeast strain *Rhodotorula paludigena* CM33 has been successfully used to produce a high lipid content of 23.9% dry cell weight when grown on glucose (Gosalawit et al., 2021). In addition, several oleaginous yeast strains have been found to produce carotenoids, including *Rhodotorula* spp., *Sporobolomyces roseus*, *S. salmonicolor*, and *Phaffia rohdozyma*. The majority of these products are β-carotene, astaxanthin, torulene,

α-carotene, and torularodine (Mata-Gómez et al., 2014; Valduga et al., 2014). The carotenoid profiles of yeast cultures can be significantly influenced by various factors, including nitrogen and carbon sources, pH levels, light exposure, temperature, and other environmental conditions (Mata-Gómez et al., 2014). Furthermore, *R. glutinis* 32 was found to utilize glucose as a carbon source and produce a mixture of carotenoids. Specifically, the carotenoid profile consisted of approximately 80% β-carotene, 17% torulene, and 2.3% torularodine (Bhosale & Gadre, 2001a). When beet molasses was used as a carbon source, *R. glutinis* DBVPG 3853 was found to produce a mixture of carotenoids. The carotenoid profile was comprised of approximately 3.1% β-carotene, 9.6% torulene, and 80.7% torularodine (Buzzini & Martini, 2000). Furthermore, the use of alternative substrates derived from agricultural waste materials can significantly reduce the production costs of carotenoids. These substrates include potato medium, whey, chicken feathers, and crude glycerol. For example, *R. glutinis* was successfully used to produce β-carotene (at a concentration of 46 mg/L) when cultivated in whey (Marova et al., 2012). *R. glutinis* MT-5 has been demonstrated to be capable of producing β-carotene at a concentration of 92 mg/L when cultivated using chicken feathers as a substrate (Taskin et al., 2011). Moreover, *R. glutinis* has been employed to produce β-carotene (at a concentration of 135.2 mg/L) using crude glycerol as a substrate. Crude glycerol is a waste byproduct of biodiesel production that is both low-cost and readily available (Anitha et al., 2016). Therefore, crude glycerol enhances the carotenoids production while decreasing the costs of cultivation (Mata-Gómez et al., 2014; Saenge et al., 2011). Based on the aforementioned research, it is therefore interesting to consider cultivating *R. paludigena* CM33 using crude glycerol in order to enhance carotenoid production.

Shrimp farming, particularly of *Litopenaeus vannamei*, is among the most economical aquaculture practices worldwide (Landsman et al., 2019). In Thailand, the total shrimp market value for July 2020 and June 2021 was $885 million (Schmitz & Nguyen, 2022). Major markets for the exports include Japan, the US, China, ASEAN countries, and South Korea (Asche et al., 2022). Despite its economic significance, large-scale shrimp farming faces several challenges, notably outbreaks of diseases such as acute hepatopancreatic necrosis disease (AHPND), early mortality syndrome (EMS), and hepatopancreas necrosis syndrome (HPNS), which significantly affect shrimp yield

(Kumar et al., 2020).Yeast (probiotic) offer positive impacts on the animal gut, provide health benefits to the host, mitigate diseases in shrimp aquaculture, and have gained popularity among shrimp farmers (Knipe et al., 2021). Regarding yeast, several studies have indicated its beneficial effects on growth, stress resistance, immune responses, and disease resistance against aquaculture pathogens (Ayiku et al., 2020). Additionally, It is reported that dietary supplementation with carotenoids contributes to a higher survival rate than the control group (Yu et al., 2020). *R. paludigena* has gained recognition as a dependable producer of carotenoids (Wang et al., 2019a). Published studies on the application of *R. paludigena* have mainly focused on accumulating neutral lipids for biodiesel production (Gosalawit et al., 2021). However, there is a lack of literature reports regarding the effects of *R. paludigena* on growth, immune response, intestinal health, and disease resistance in shrimp and other aquatic animals. Such studies could provide valuable guidance for shrimp production practices.

The objective of this study is to develop a carotenoid production process for *R. paludigena* CM33 using crude glycerol as the substrate in a 500-L fermenter. The goal is to increase the quality of the products with crude glycerol as a substrate and reduce cultivation costs. Additionally, this study explores two applications for the produced carotenoids. The first application, after developing the cultivation process to obtain higher yields of carotenoids, is to investigate efficient methods for harvesting, extraction, and separation to enhance the effectiveness of the obtained carotenoids. The subsequent application involves using *R. paludigena* CM33 as a probiotic to enhance growth rates, disease resistance, and improve the quality of shrimp meat.

1.2 Research objectives

1.2.1 Optimizing the utilization of crude glycerol in the cultivation of *R. paludigena* CM33 for carotenoid production in a 500-L fermenter.

1.2.2 Optimization of the harvesting, extraction, and separation of carotenoids from *R. paludigena* CM33 cells.

1.2.3 The potential of *R. paludigena* CM33 as a probiotic for white shrimp.

CHAPTER 2

LITERATURE REVIEW

2.1 *Rhodotorula* sp.

Rhodotorula is a genus of pigmented unicellular yeasts that belongs to the family Cryptococcaceae within the phylum Basidiomycota, as well as the subfamily Rhodotorulodae (Hawksworth et al., 1996). These yeasts are anamorphic, and certain species among them are important in food spoilage or the fermentation industry (Yeeh, 1999). These *Rhodotorula* strains have polyphyletic cells that exhibit various shapes, including ovoid, subglobose, elongated, and ellipsoidal. Asexual reproduction in *Rhodotorula* predominantly occurs through multilateral and polar budding, although some strains occasionally undergo the sexual reproduction life cycle, which can involve the formation of pseudohyphae (Kurtzman et al., 2011). As a result of carotenoid pigment synthesis, the colonies exhibit shades of red, orange, or yellow (Yeeh, 1999). As widespread saprophytic yeasts, *Rhodotorula* species can be found in a wide range of habitats, spanning from the equator to the poles and encompassing both land and water. *Rhodotorula* strains can develop on various surfaces and thrive in diverse ecological settings, including the soil, air, and manure, as well as within the bodies of plants, animals, and some lower species (Wirth & Goldani, 2012).

Rhodotorula can grow in solid minimal synthesis medium without the need for vitamins. It grows well at 30°C and does not produce ethanol when cultivated on high-glucose media under aerobic conditions (Yeeh, 1999). The production of natural carotenoids through biosynthesis is one of the most prominent qualities of *Rhodotorula.* The biomass of *Rhodotorula*, with its rich colors, can also be utilized as a high-quality, single-cell protein source, making it a desirable addition to animal feed (Tang et al., 2019). Moreover, the *Rhodotorula* strain, being oleaginous, produces lipids and fatty acids. In a previous study, *Rhodotorula paludigena* CM33 was screened using NR fluorescent dye labeling and flow cytometry techniques, with castor beans (*Ricinus* sp.) serving as the substrate. The study also demonstrated the ability of *R. paludigena*

CM33 to utilize industrial byproducts such as molasses and crude glycerol as carbon sources. The resulting biomass exhibited concentrations of 16.5 g/L of lipid, 37.1% DCW (dry cell weight) of lipid, and 6.1 g/L of lipid concentration (Gosalawit et al., 2021). Furthermore, depending on the carbon substrates, the oleaginous yeast *R. paludigena* CM33 can intracellularly accumulate 20–27% lipids. The majority of these lipids consist of oleic acid (C18:1) and palmitic acid (C16:0), along with a few other fatty acids. The bio-oil, as determined by simulated distillation gas chromatography, exhibited a composition of 2.6% heavy naphtha, 20.7% kerosene, 24.3% biodiesel, and 52.4% fuel oil (Poopisut et al., 2023).

2.2 Carotenoid production in *Rhodotorula* sp.

Carotenoids play a crucial role in pharmaceuticals, chemicals, and cosmetics, serving as important compounds. Some carotenoids also act as precursors of vitamin A (Prabhala et al., 1993). Furthermore, carotenoids have long been utilized as natural colorants in the food industry (Rodrigues et al., 2019). *Neurospora crassa* and Blakeslea trispora are fungi that accumulate carotenoids, while the genera *Rhodotorula* sp., *Rhodosporidium* sp., and *Sporobolomyces* sp. are yeasts that produce carotenoids. The carotenoids in fungi are produced through the ergosterol pathway and accumulate when exposed to light conditions (Schweiggert & Carle, 2016). Yeasts are the primary producers of β-carotene, along with other carotenoids such as torulene, torularhodin, and γ-carotene (Moliné et al., 2010). Some researchers have reported the production of carotenoids from various *Rhodotorula* species using different substrates as carbon sources, as summarized in Table 2.1.

Table 2.1 Comparison of carotenoid production by *Rhodotorula* species grown on various substrates as carbon sources.

Rhodotorula species	Carbon source	Total carotenoids (mg/g dry cells)	Reference
R. glutinis 32	Glucose	5.4	(Bhosale & Gadre, 2001a)
R. glutinis KCTC	Sugar cane molasses	0.295	(Park et al., 2007)
R. glutinis 32	Sugar cane molasses	2.36	(Bhosale & Gadre, 2001b)
R. mucilaginosa NRRR-2502	Whey	29.2	(Aksu & Eren, 2005)
R.glutinis DBVPG 3853 + *Debaryomyces castellii* DBVPG 3503	Corn syrup	0.535	(Buzzini, 2001)

These terpenoid pigments consist of 40 carbon atoms and can be classified into two groups: carotenes and xanthophylls. They are soluble in nonpolar solvents. Xanthophylls, such as astaxanthin and canthaxanthin, contain more than one oxygen functional group, whereas carotenes, such as β-carotene and torulene, consist of hydrocarbon skeletons (Britton, 2008). The biosynthetic pathway of carotenoids in yeasts consists of three steps. In the first step, acetyl CoA is converted to β-Hydroxy β-methylglutaryl-CoA (HMG-CoA) by HMG-CoA synthase. HMG-CoA is then converted into mevalonic acid (MVA). Mevalonic acid (MVA) is further converted to Isopentenyl pyrophosphate (IPP) by MVA kinase. In the second step, three IPP molecules combine to form dimethylallyl pyrophosphate (DMAPP) through the action of prenyltransferase. DMAPP is then catalyzed to geranylgeranyl-diphosphate (GGPP). Two molecules of GGPP are involved in the synthesis of phytoene, which undergoes a desaturation process to form lycopene. In the final step, lycopene serves as a precursor for carotenoid cyclic compounds, leading to the production of γ-carotene. γ-carotene is a major branching point and a precursor for the synthesis of β-carotene and torulene.

Torulene can be further transformed into torularhodin through hydroxylation and oxidation. Astaxanthin biosynthesis involves several steps, including the conversion of lycopene, β-carotene, and echinenone to astaxanthin (Frengova & Beshkova, 2009). 4-keto-torulene converts to 3-hydroxy-3',4'-didehydro-β, phi-carotene-4-one (HDCO), and HDCO further converts to 3,3'-dihydroxy-β, phi-carotene-4,4'-dione (DCD), ultimately resulting in the production of trans-astaxanthin, as shown in Figure 2.1.
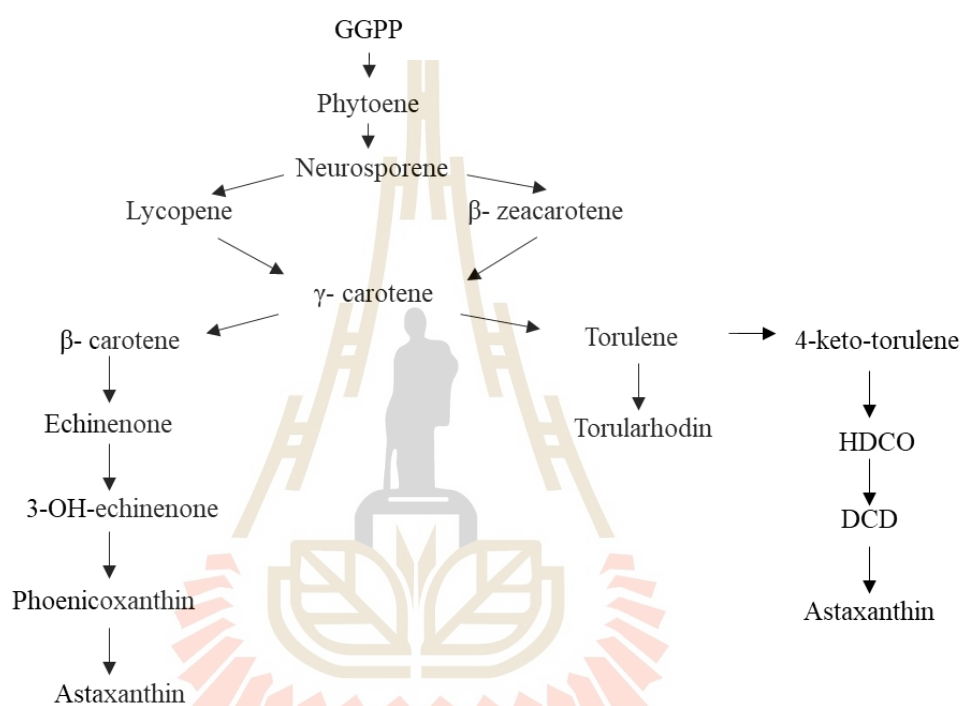
Figure 2.1 Biosynthetic pathway in *Rhodotorula* species (Frengova & Beshkova, 2009).

2.3 Factors affecting carotenoid production in *Rhodotorula* sp.

The most crucial element in carotenoid formation is the availability of carbon. Under aerobic fermentation conditions, the glycolytic process utilizes glucose or other carbohydrates to enhance pigment synthesis (Hannibal et al., 2000). When *R. glutinis* is grown with sodium acetate as the carbon source and exposed to light, it enhances β-carotene accumulation (Gong et al., 2020). The β-carotene content was 24.6 μg/g when exposed to LED lamps, whereas in the absence of light, it was 14.69 μg/g (Yen & Zhang, 2011). Temperature has a significant impact on cell growth and metabolite production, including carotenogenesis, as it influences the biosynthetic pathways. *R. glutinis* DM 28

exhibited the highest carotenoid production when cultured at 29 and 30 °C (Malisorn & Suntornsuk, 2008). The growth rate, cell mass, and carotenogenesis are influenced by the airflow rate. Additionally, low oxygen levels have an impact on carotenoid and xanthophyll production. The biomass reached 8.17 g/L when the aeration was increased from 0 to 2 vvm (Saenge et al., 2011). Additionally, when 10 g/L of ethanol and 5 g/L of acetic acid were added to the media of *P. Rhodozyma*, the carotenoid concentrations reached 45.62 mg/L and 43.87 mg/L, respectively (Kim et al., 2003). Many factors have been implicated in the increasing buildup of carotenoid concentrations in yeast. Factors such as growth rate and biomass should be considered while cultivating yeast for carotenoid synthesis.

2.4 Upstream and Downstream

2.4.1 Fermenter

Microorganisms predigest or break down complex organic compounds into simpler forms during fermentation. Alcohol and other key byproducts of some fermentations are gases. Beer, wine, leavened bread, and cheese were the first foods to be fermented. Pickles, sauerkraut, vinegar, butter, and a variety of traditional alcoholic beverages are just a few examples of the fermented foods that are popular throughout East Asia (Krishna, 2005). Microorganisms in the industry are capable of producing chemical compounds, enzymes, and pharmaceuticals. These tiny organisms can be cultivated in fermenters using either solid or liquid media. Additionally, they have a fast growth rate and can yield significant quantities within a short period of time. Moreover, they can thrive under unique growth conditions. Products can be obtained through batch or continuous cultivation methods. Figure 2.2 illustrates a diagram of a fermenter.
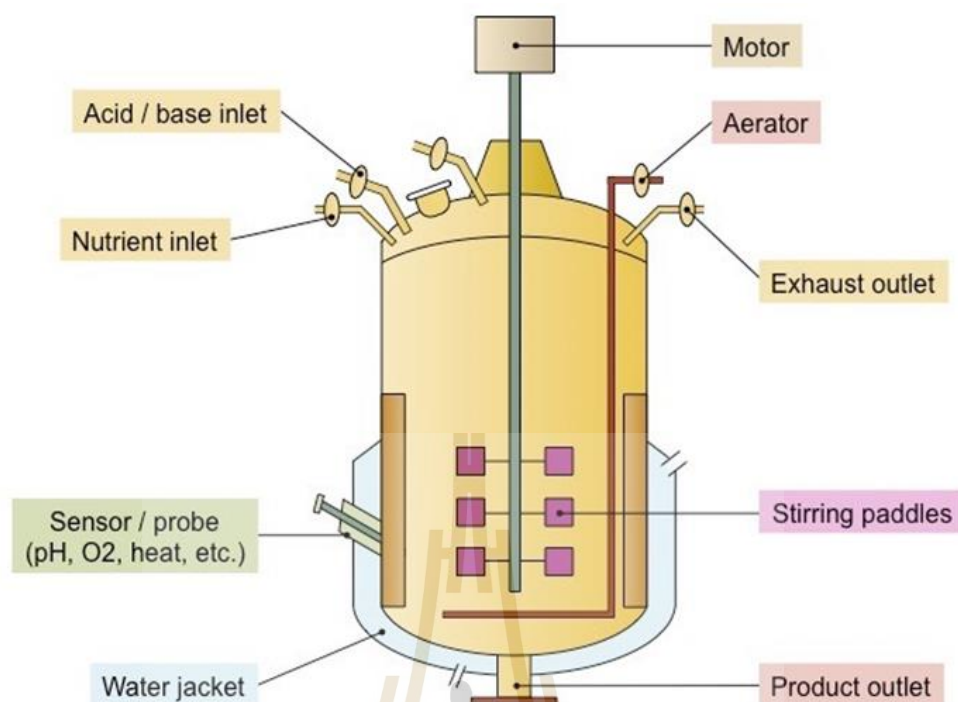
Figure 2.2 A diagram of fermenter (Bioninja, 2021).

The fermenter is equipped with probes and sensors to monitor cell cultivation conditions. Motorized stirring paddles are responsible for distributing heat and ensuring the even stirring of materials within the reaction chamber. An aerator is used to introduce compressed air into the chamber, while a defoamer is employed to prevent the formation of foam. Acid/base inlets are provided to regulate the pH levels within the chamber, as the formation of the product may alter the pH (Bioninja, 2021). These components and their functions are depicted in Figure 2.2.

2.4.2 High Pressure Homogenizer or microfluidics

High-pressure homogenization (HPH) reduces particle size and enhances homogeneity, resulting in highly efficient emulsions or suspensions. This process involves applying high pressure to push sample fluids through a narrow gap over a very short distance. The shear effects caused by liquid fluid shear can increase the temperature by 14–18 °C per 100 MPa (Lammari et al., 2021). High-pressure homogenization (HPH) involves shear forces and cavitation, resulting in the reduction of particle size and the formation of emulsions or suspensions, as depicted in

Figure 2.3 HPH finds application in various areas such as nano-emulsion preparation, enzymatic inactivation, and the food sector. The potential of HPH is significant due to its diverse range of applications. Furthermore, the development of HPH technology for particle size reduction is an area of growing interest, including its application in yeast preparation (Comuzzo & Calligaris, 2019). In a previous study, In the HPH method, three homogenization cycles were conducted at a pressure of 80 MPa and a bacterial liquid concentration of 8% (Liu et al., 2019). The yeast strain GYB40-10s utilized HPH with a pressure of up to 100 MPa to enhance energy yield, yielding similar results (Ekpeni et al., 2015). Furthermore, autolysis using HPH treatment (200 - 600 bar, 3 passes) enhanced the extraction of β-glucan from *Saccharomyces cerevisiae* cells (Dimopoulos et al., 2020). In a previous study, carotenoid extraction was performed using HPH at a pressure of 80 MPa (11,603 psi) applied to an 8% biomass concentration and with 3 passes of *Sporidiobolus pararoseus* cells (Liu et al., 2019). Additionally, HPH was explored as a cell disruption method for extracting carotenoids from *Desmodesmus* sp. F51 (Xie et al., 2016). To achieve the desired results, the samples are often subjected to multiple passes through a high-pressure homogenizer (Nemer et al., 2021).

Figure 2.3 Characteristics of the high-pressure homogenizer.

2.4.3 Pure Flash/Prep HPLC

The Pure Flash/Prep HPLC Model C-850 is a high-purity chromatography system used for processing and analytical methods. It offers both Flash and Prep modes, allowing users to select from flash systems or combination flash/prep HPLC for small to large-scale purification of complex mixtures. The system comes with standard UV detection, and users also have the option to add ELS detection to detect all compounds. It features purification and high-resolution steps, making it capable of separating various compounds such as cannabinoids, essential oils, lipids, amino acids, sugars, polymers, and natural products, among others (AG, 2020). The characteristics of the equipment, as shown in Figure 2.4 of the Pure Flash/Prep HPLC Model C-850, allow for the efficient separation of the target peak from impurities. The equipment is designed to handle sample particles of medium to large size (15 - 60 μm). Its primary objective is to separate and purify the sample (AG, 2020). In addition, a 95.8% purity was achieved by Nie at et al.'s (Nie et al., 2021) use of Prep HPLC to separate partially purified terpenoids obtained by high-speed countercurrent chromatography (HSCCC) fractionation.

Figure 2.4 The characteristics of the Pure Flash/Prep HPLC Model C-850.

2.4.4 Microfiltration

Microfiltration is a highly accurate filtration process that is used to clean or separate macromolecules. It operates by separating particles from mixtures, eliminating particles with sizes ranging from 0.1 to 1.5 m. Microfiltration is a low-pressure membrane filtration technology with an inlet pressure of less than 0.2 MPa. Microfiltration has a filtration precision that sits somewhere between traditional filtration and heat filtration. It can separate components with diameters ranging from 0.03 to 15 m, allowing it to remove dust, turbidity, bacteria, viruses, algae, and other impurities (Koyuncu et al., 2015). In the food sector, microfiltration processing is commonly used. Microfiltration is used in the biotechnology industry for a variety of purposes, such as cell recycling and harvesting, process purification, and the separation of recombinant proteins from cell detritus (Cassano & Basile, 2013). The characteristics of microfiltration are shown in Figure 2.5. In addition, in a previous study, stamped ceramic membranes were utilized for microfiltration of beer yeast solutions. Both membranes had an outside diameter of approximately 9 mm and featured an active layer composed of zirconia oxide with a mean pore size of 0.23 mm. When a 5% yeast suspension was microfiltered using the smooth membrane, a steady flow of permeate was achieved in approximately 1000 seconds. In contrast, the stamped membrane required nearly 2000 seconds to reach a constant flux (Stopka et al., 2001).

Figure 2.5 Characteristics of microfiltration.

2.5 White Shrimp (*Litopenaeus vannamei*)

L. vannamei (Boone), commonly known as Pacific white shrimp, is the most significant shrimp species cultivated in the Americas (Cuzon et al., 2004). Shrimp farming is a significant industry in tropical and subtropical regions worldwide, with current production estimated at 1090 Mt per year (Tidwell & Allan, 2001). The Pacific white shrimp has a high growth rate and is typically found in tropical and subtropical regions worldwide. It thrives in temperatures above 25°C, with a preferred salinity range of 2 to 45 ppt, and it tends to inhabit muddy bottom areas. In terms of growth, female shrimp exhibit faster growth rates compared to males, with an average weight ranging from 30 to 45 g. The life cycle of *L. vannamei* consists of 6 nauplii stages, followed by 3 protozoal and 3 mysis stages. Subsequently, they progress through post-larval stages and eventually adopt a benthic lifestyle (Wei et al., 2014). *L. vannamei* is translucent-white in color. However, as depicted in Figure 2.6, the body exhibits a bluish hue.

Figure 2.6 The characteristic of *Litopenaeus vannamei*.

Recent studies have shown the beneficial effects of astaxanthin on shrimp growth, hepatopancreas repair, and antioxidant properties. A diet supplemented with astaxanthin at a concentration of 275.2 mg/kg resulted in increased final body weight and caused certain visible histopathological changes in the hepatopancreas. Furthermore, a diet containing 450 mg/kg of astaxanthin showed improvements in

hepatopancreatic health (Yu et al., 2020). The inclusion of astaxanthin at concentrations of 50 and 100 ppm resulted in increased weight gain and specific growth rate (SGR) compared to the control group (Wang et al., 2020). Cultivating *L. vannamei* with 2% yeast extracts as feed for 8 weeks resulted in increased weight gain and specific growth rate compared to the control treatment (Zheng et al., 2021). Thus, the role of carotenoids in affecting the specific growth rate, antioxidant capacity, and protection against certain damages in shrimp is of great interest as it can contribute to increased shrimp production and high-quality shrimp exports.

2.5.1 Pathogen of shrimp

Shrimp are among the most important species in global aquaculture trade (H. Liu et al., 2021; Luo et al., 2007). However, worldwide shrimp production reached approximately 6.5 million tons in 2019, leading to the transformation of the shrimp farming sector into a large-scale operation. Nevertheless, the expansion of shrimp farming has been accompanied by numerous disease outbreaks, resulting in substantial losses in shrimp output. In addition to bacterial and fungal illnesses, several viral infections can cause significant damage (Lee et al., 2022). Vibriosis is the most common bacterial illness affecting shrimp aquaculture. It is caused by gram-negative bacteria from the Vibrionaceae family, including *V. harveyi*, *V. alginolyticus*, *V. parahaemolyticus*, *V. vulnificus*, *V. cholerae*, and *V. splendidus* (Jayasree et al., 2006). In addition, Vibriosis manifests in hatcheries as luminescence in pond water or within the shrimp body. Increased levels of *Vibrio* spp. in grow-out ponds are linked to internal and external necrosis, reduced feeding rates, gastrointestinal disturbance, red staining of shrimp (especially the tail), increased mortality, and decreased immunity, making shrimp more susceptible to secondary infections (El-Saadony et al., 2022).

On the other hand, viruses are highly prevalent and pervasive in the marine environment. Among these marine viruses, the White Spot Syndrome Virus (WSSV) has emerged as one of the most widespread and deadly threats to shrimp populations worldwide (Sánchez-Paz, 2010). When it was first discovered in Taiwan in 1992, it rapidly spread to Japan and almost every Asian nation. The first recorded incidence of WSSV in the Americas occurred in 1995 in a shrimp farm in South Texas. It was hypothesized that the introduction most likely happened through an Asian shipment of frozen-bait

shrimp. The most recent outbreak in a WSSV-free area was reported in Brazil in 2005, as per the guidelines of the World Organization for Animal Health (OIE) (Hasson et al., 2006; Sánchez-Paz, 2010). White spots ranging from 0.5 to 3.0 mm in diameter may suddenly appear on the appendages, exoskeleton, and internal surface of WSSV-infected shrimp. However, these spots are not considered a reliable indicator for a preliminary diagnosis of the condition. Their presence is inconsistent, and similar spots can be caused by bacterial infections, stress, or excessive alkalinity. Additional symptoms of WSSV include lethargy, a sudden decrease in food intake, a loose cuticle and red coloring of the body and appendages (Sánchez-Paz, 2010). In 1992, a shrimp RNA virus known as Taura Syndrome Virus (TSV) was first identified in Ecuadorian shrimp raised in aquaculture. Since the initial outbreak, Taura Syndrome Disease (TSD) has spread to the majority of shrimp-producing nations, primarily through the exchange of shrimp seed and broodstock for aquaculture or via frozen shrimp food products (Bamford & Zuckerman, 2021). In post-larval and juvenile phases, this disease can lead to mortality rates ranging from 40% to 95% (Lightner, 1999). It is most commonly associated with the nursery phase of *P. vannamei* and typically manifests 14 to 40 days after postlarvae are stocked in grow-out ponds or tanks (Dhar et al., 2004). Based on the above information, this represents only a portion of bacterial and viral infections in shrimp. Thus, highlighting the importance of prevention and treatment of these infections to enhance shrimp production to meet consumer demands.

2.5.2 Acute Hepatopancreatic Necrosis Disease (AHPND)

Acute Hepatopancreatic Necrosis Disease (AHPND) is a severe bacterial illness that affects shrimp, leading to high mortality rates and causing significant financial losses in the shrimp farming sector (Zhou et al., 2023). AHPND typically breaks out at 30–35 days after juveniles and is characterized by sudden mass mortality, reaching up to 100% (de la Peña et al., 2015). In AHPND-affected shrimp, symptoms such as lethargy, anorexia, slow growth, empty digestive tract, and pale to white hepatopancreas were observed. The causative agent of AHPND, *Vibrio parahaemolyticus* (VP_{AHPND}), was identified in 2013 (Tran et al., 2013). The first outbreak of AHPND was reported in China, and since then, the disease has spread to shrimp production in Mexico, Malaysia, Thailand, the Philippines, Vietnam, Bangladesh, and

the United States, resulting in significant economic losses (de la Peña et al., 2015; Dhar et al., 2019; Flegel, 2012; Tran et al., 2013). Among potential treatments, antibiotics can contribute to pathogen resistance, disinfectants or phages may result in environmental pollution, and while immunostimulants, probiotics, recombinant proteins, gold nanoparticles, and plant-based compounds have shown promising effects in the laboratory (Wang et al., 2020).

2.5.3 Immune system

As an invertebrate, shrimp lack a vertebrate-like adaptive immune system. Shrimp, on the other hand, has an effective innate immune system composed of physical barriers as well as cellular and humoral components. The recognition of different microbial cellular components (pathogen-associated molecular patterns, PAMPs) by host-associated pattern recognition receptors (PRRs) activates innate immunity, which triggers different signaling pathways and, as a result, different cellular and humoral immune responses (Ekasari et al., 2014). Cellular defense consists of a variety of mechanisms (phagocytosis, encapsulation, nodule formation, coagulation, death, and so on) that are directly mediated by haemocytes. The activation of cascade systems and humoral components in shrimp results in the release of various compounds, including the prophenoloxidase (proPO) activating system, antioxidant system, agglutinins, protease inhibitors, antimicrobial peptides, phosphatase, lysozyme, and other molecules accumulated within the haemocytes (Cerenius et al., 2008). Intriguingly, it has been discovered that comparable to insects like *Tenebrio molitor* and *Drosophila*, the prophenoloxidase (proPO) enzyme cascade and the Toll pathway are simultaneously activated by the same proteolytic enzymes (Hauton, 2012; Kan et al., 2008). Similar to this, reports on the simultaneous activation of the proPO and Toll pathways leading to the synthesis of AMPs in *P. monodon* have been made by gene silencing (Figure 2.7) (Kulkarni et al., 2021).
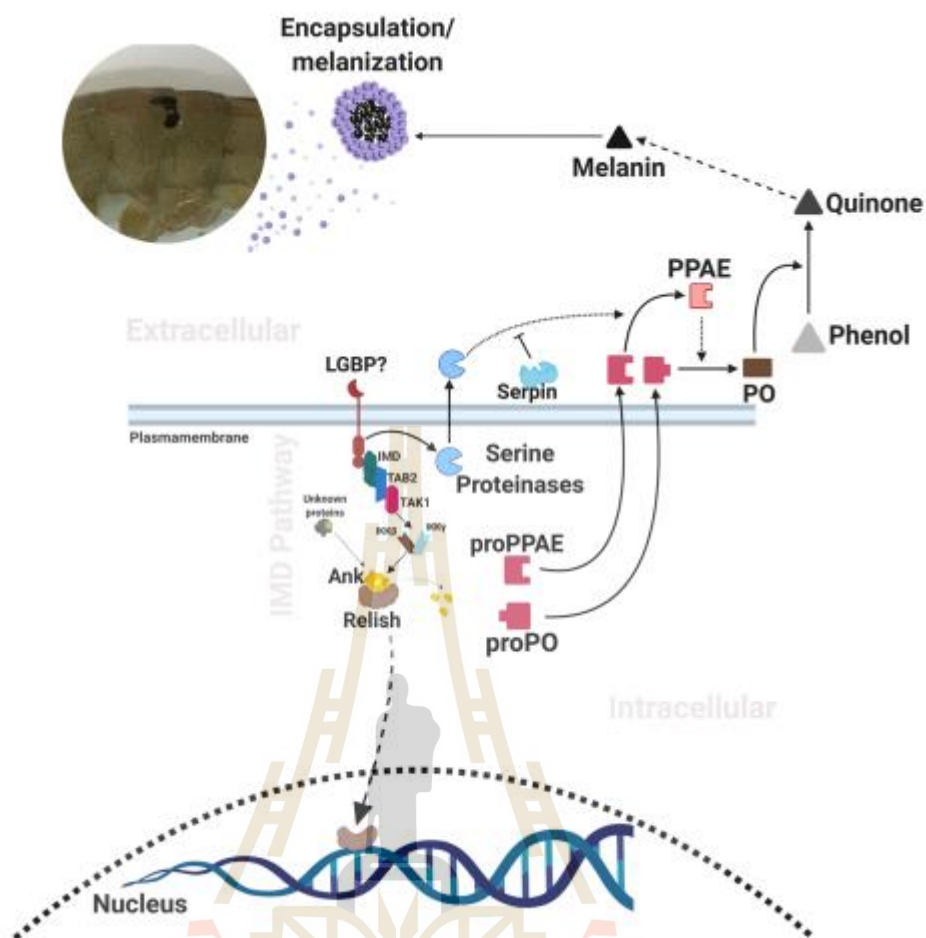
Figure 2.7 The shrimp immune system model (Kulkarni et al., 2021; Song & Li, 2014; Tassanakajon et al., 2013).

In invertebrates, activated PRRs directly or indirectly initiate a range of cellular or humoral responses, including the prophenoloxidase-activating system (proPO), clotting mechanism, phagocytosis, and the release of NF-kB dependent antimicrobial peptides (AMPs). These innate immune responses are controlled by signal transduction pathways that are activated when PRRs bind to specific PAMPs (Borregaard et al., 2000). In both the model organism *Drosophila* and shrimp, three major types of signaling pathways have been discovered: the Toll pathway, the immune deficiency (IMD) pathway, and the JAK/STAT pathway. In *Drosophila*, the Toll pathway primarily functions in defense against fungi, Gram-positive bacteria, and viruses. However, in shrimp, the Toll pathway also responds to Gram-negative bacteria (Deepika et al., 2022; Li & Xiang, 2013; Sreedharan et al., 2017). In controlling Gram-negative bacterial and

viral infections, the IMD pathway plays key roles, while the JAK/STAT pathway functions in antiviral defense (Li & Xiang, 2013). Similarly, various components of these pathways have been identified in other crustacean species (Figure 2.8).

Antioxidant enzymes, including superoxide dismutase (SOD), catalase (CAT), and glutathione peroxidase (GPX), are essential components within cells for the elimination of excessive reactive oxygen species, such as hydrogen peroxide (H_2O_2) (Wang et al., 2012). SOD plays a role in scavenging superoxide anions and converting them into hydrogen peroxide and oxygen, thus detoxifying them. Subsequently, CAT and GPX further transform hydrogen peroxide into water and oxygen (Nordberg & Arnér, 2001). CAT, present in virtually all oxygen-respiring organisms, holds a central position as an important antioxidant enzyme by eliminating excessive hydroperoxide and maintaining cellular redox balance (Ryu et al., 2006). GPX serves a significant role in detoxifying lipids and hydroperoxides, safeguarding biomembranes and other cellular components from oxidative damage. During processes like phagocytosis and physiological metabolism, GPX catalyzes the reduction of various hydroperoxides using glutathione as the reducing substrate (Liu et al., 2004; Wang et al., 2012).
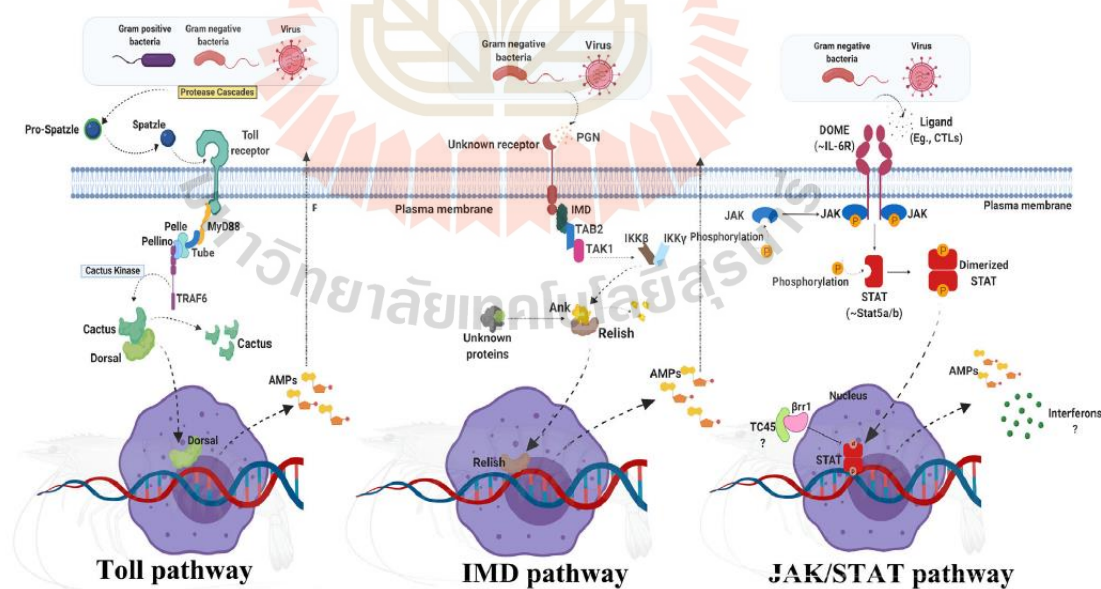
Figure 2.8 The shrimp immune system model, Toll pathway, immuno-deficiency (IMD) pathway, and Janus kinase/signal transducers and activators of transcription (JAK/STAT) pathway (Kulkarni et al., 2021).

2.5.4 Enhancement of shrimp immune system

In the Pacific white shrimp production chain, enhancing immunity and disease resistance has become crucial for the sustained and sustainable growth of the shrimp farming industry. Consequently, the utilization of immunostimulants has emerged as a significant ecological strategy for disease management and enhancing production in aquaculture (dos S Filho et al., 2023). Immunostimulants are any substances that have an effect on the immune response mechanisms in animals (Anderson, 1992). Bacterial cells and their components, or derivatives from bacteria, can effectively stimulate the immune system in shrimp due to the presence of protein molecules, specifically the receptor molecules PRRs or PRPs, known as lipopolysaccharide binding proteins (LGBPs) and peptidoglycan recognition proteins (PGRPs), located on the cell walls of shrimp hemocytes (Tassanakajon et al., 2013). Currently, various forms of bacterial immunostimulants are being prepared for use in stimulating the immune system. These include living bacteria, probiotic bacterial strains, bacterial extracts derived from bacterial cells, and extracts obtained from the cell walls of both Gram-positive and Gram-negative bacteria. *L. plantarum* exhibits enzymatic activity, such as phytase, which enhances phosphorus availability, and demonstrates effectiveness in suppressing *V. alginolyticus* infection (Chiu et al., 2007). *B. thermophilum* has been found to increase the activity of serine protease enzymes in hemocytes. These enzymes promote the functioning of the prophenoloxidase system (Rattanachai et al., 2005). In addition, supplementation with prebiotic carbohydrates can serve as a potent immunomodulator and effectively induce immune-related genes involved in host defense. Pure β-1,4-mannobiose (MNB) has demonstrated the ability to activate the prophenoloxidase system of shrimp hemocytes. These results provide evidence that supplementing with MNB can enhance the immune response and increase shrimp resistance against *V. parahaemolyticus* infection (Elshopakey et al., 2018). Likewise, yeast extracts from strains have contain components that can stimulate the immune system, such as antimicrobial extracts effective against pathogens or extracts that enhance the functioning of the immune system (Anderson, 1992). Similarly, nutritional factors and dietary supplements that have been reported to stimulate the immune system and have been used in shrimp include vitamin C, vitamin E, astaxanthin, animal extracts, and plant extracts etc. (Cipolatti et al., 2019; Manowattana et al., 2020; Zheng et al., 2021).

2.5.5 Probiotic

Microorganisms known as probiotics have positive impacts on either the body or the environment. There are already a number of aquatic probiotics that are marketed as mono- or multi-strain preparations. These probiotics can be delivered by adding the probiotic bacteria directly to the water in the culture system or by combining the probiotic bacteria with the feed. The former aids in the colonization of the host intestine by the probiotics, while the latter aids in keeping an environment free of pathogens (Chauhan & Singh, 2019; Mohapatra et al., 2013). By increasing the activity of host digestive enzymes, such as amylase and protease, probiotics enhance growth and feed utilization (Yu et al., 2009). For instance, *Lactobacillus* species produce hydrogen peroxide, short-chain fatty acids, and bacteriocins, all of which exhibit antagonistic effects against pathogens (Faramarzi et al., 2011). However, certain probiotic bacterial strains such as *Bifidobacterium* (*B. bifidum, B. animalis, B. lactis*), *Bacillus* (*B. cereus, B. toyoi*), and *Lactobacillus* (*L. acidophilus*) have the ability to disrupt pathogen signal molecules that facilitate this system. They achieve this by producing auto-inducer antagonists (Brown, 2011; Sahandi et al., 2019). Probiotics have demonstrated effectiveness in protecting shrimp against WSSV infection. For example, when probiotics are administered through the diet, it enhances shrimp's resistance to WSSV infection (Kumar et al., 2023).

CHAPTER 3

CAROTENOIDS PRODUCTION OF *Rhodotorula paludigena* CM33 USING CRUDE GLYCEROL AS A SUBSTRATE

3.1 Abstract

Rhodotorula paludigena CM33, an oleaginous yeast, has shown the capacity to accumulate significant amounts of intracellular carotenoids. The carbon sources that this yeast can use include glucose, sucrose, glycerol, and xylose. To increase the production of carotenoids in *R. paludigena* CM33, this study used crude glycerol, a by-product of the biodiesel industry, as a substrate in this study. Using response surface methods to optimize the growth conditions, this study found an increase in carotenoid content when 40 g/L of crude glycerol, 0.72 g/L yeast extract, and 0.43 g/L $(NH_4)_2SO_4$ was used. This study was obtained maximum concentrations of biomass (cell dry weight) and carotenoids at 45.38±1.05 g/L and 15.39±0.03 mg/g, respectively, in a fed-batch procedure carried out in a 500-L fermenter. Additionally, these results demonstrate the potential of crude glycerol as an alternative substrate for enhancing carotenoid production in *R. paludigena* CM33.

3.2 Introduction

Carotenoids, natural pigments utilized in high-value industries such as cosmetics, pharmaceuticals, food supplements, and chemical industries, have drawn significant interest. The biochemistry of carotenoid synthesis has been extensively reviewed in previous studies (Igreja et al., 2021). Carotenoids are commonly found in vegetables, fruits, microalgae, fungi, yeast, and bacteria (Mata-Gómez et al., 2014). The global carotenoids market was valued at 1.5 billion USD in 2019 and is projected to reach 2.0 billion USD by 2026 (Bccresearch, 2022). However, the production of carotenoids from plants has certain disadvantages. It is associated with high production costs due to the

requirement of extensive irrigation, time, land, fertilizers, and labor. Moreover, plant-based carotenoid production is often influenced by seasonal variations (C. Liu et al., 2021). Among carotenoid-producing microorganisms, red yeasts have been identified as potential carotenoid producers. They possess the ability to grow rapidly in various substrates, resulting in significantly reduced production times when implemented at an industrial scale (Chopra et al., 2022). Currently, extensive research is being conducted on the fermentation of microbial carotenoids using various red yeasts, including *Phaffia rhodozyma* (Mussagy et al., 2022), *Rhodotorula* sp. (Allahkarami et al., 2021), *R. mucilaginosa* (Li et al., 2022; Machado et al., 2022) and *R. glutinis* (Gong et al., 2020; Zhao & Li, 2022).

In a previous study, we isolated the yeast *R. paludigina* CM33 from our laboratory. This yeast demonstrated its capacity to utilize different carbon sources, namely glucose, sucrose, xylose, and glycerol, respectively (Gosalawit et al., 2021). For the advancement of process development, utilizing affordable agro-industrial substrates would result in reduced operational expenses and mitigate environmental contamination. Among the substrates examined, crude glycerol stands out as a compelling option due to its availability as a by-product of biodiesel production. Its utilization not only holds economic value by providing additional triglyceride feedstock for biodiesel and oleochemical production but also enables the production of carotenoids for high-value applications in the food industry. The bioprocess for carotenoid production entails both upstream and downstream processing. In the upstream phase, optimizing the yeast's growth and its capacity to accumulate substantial carotenoid levels is of great interest. Many techniques, including light irradiation (Gong et al., 2020; Manowattana et al., 2020), gene insertion (Breitenbach et al., 2019), and chemical treatments (Gassel et al., 2013), have been investigated for genetic modification aimed at enhancing carotenoid accumulation. Due to concerns about the safety of genetically modified foods, the majority of research in this field now emphasizes media optimization, culture conditions, and fermentation modes to produce natural carotenoids (Dias et al., 2020; Robles-Iglesias et al., 2023).

In this study, we initially investigated the process development by examining media formulation based on different concentrations of crude glycerol, salts, and nitrogen sources. Furthermore, we explored the effects of cultivation conditions on

cell growth and carotenoid concentration using response surface methodology (RSM). The optimized conditions obtained were then applied to a 500-L stirred tank bioreactor for batch, repeated batch, and fed-batch fermentations. The outcomes of this study have the potential to pave the way for the commercial production of carotenoids from oleaginous yeast.

3.3 Materials and methods

3.3.1 Microorganism and culture conditions

The oleaginous yeast *R. paludigena* CM33 was isolated from various natural habitats by our laboratory (Gosalawit et al., 2021). The microorganism was cultivated on yeast peptone dextrose (YPD) medium, which contained 20 g/L glucose, 10 g/L peptone, 10 g/L yeast extract, and 15 g/L agar (Gosalawit et al., 2021). For fermentation, the inoculum was prepared using 10 ml of minimal medium components, including 70 g/L glucose, 0.75 g/L yeast extract, 0.55 g/L $(NH_4)_2SO_4$, 2.0 g/L $MgSO_4 \cdot 7H_2O$, and 0.4 g/L KH_2PO_4 (Poontawee et al., 2023). The inoculated cultures were then incubated overnight at 30°C on a rotary shaker at 150 rpm for 48 h (Gosalawit et al., 2021).

3.3.2 Characteristics of chemical composition and elemental analysis of crude glycerol

Crude glycerol, obtained from BioSynergy (Nakhon Ratchasima, Thailand), was quantitatively determined using Gas Chromatography-Mass Spectrometry (GC-MS) (Agilent Technologies 7000B, California, USA). The pH of the crude glycerol was measured using a pH meter (Oakton pH700, Illinois, USA). The carbon, hydrogen, nitrogen, and sulfur elemental concentrations in the crude glycerol were determined using a CHNS/O (liquid sample) analyzer (LECO CHN628+TruSpecMicro, Michigan, USA). The concentrations of sodium (Na), magnesium (Mg), aluminum (Al), phosphorus (P), potassium (K), calcium (Ca), manganese (Mn), iron (Fe), cobalt (Co), copper (Cu), and zinc (Zn) were analyzed using an Inductively Coupled Plasma Optical Emission Spectrometer (ICP-OES) (Perkin Elmer Optima 8000, Massachusetts, USA).

3.3.3 Response Surface methodology (RSM) – Box-Behnken

The optimization of *R. paludigena* CM33 cultivation was studied using the Box-Behnken Design. The effects of the optimal conditions on carotenoid concentration were analyzed using Design Expert software (Version 13, Stat-Ease Inc., Minneapolis, MN, USA). The independent variables and their levels are presented in Table 3.1. A Box-Behnken design consisting of 15 factorial points was employed, as outlined in Table 3.2. The predicted and observed responses for carotenoid production were compared. The response variables were fitted into a quadratic polynomial model represented by Eq. (3.1). The response variable Y was measured for each combination of factorial levels. The regression coefficients β_0, β_i, β_{ii}, and β_{ij} represent the terms for linearity, intercept, interaction, and square, respectively. The independent variables X_1, X_2, and X_3 are the coded values of the independent variables.

$$y = \beta_0 + \sum_{i=1}^{3} \beta_i x_i + \sum_{i=1}^{3} \beta_{ii} x_i^2 + \Sigma_{i=1}^{2} \sum_{j=i+1}^{3} \beta_{ii} \, x_i x_j \qquad (3.1)$$

The fitness of the model can be assessed by several indicators, including the coefficient of determination (R^2), adjusted coefficient of determination (R^2_{adj}), *p*-value, and lack-of-fit. A model is considered well-fitted when the coefficient of determination (R^2) approaches unity (≈1) and the lack-of-fit test yields a non-significant *p*-value of 0.05. To determine the statistical significance of R^2 and the regression coefficient, F-test and *t*-test were employed, respectively.

Table 3.1 Evaluated factors, factor notation, and their levels in Box-Behnken.

Independent variables	codes	Factor levels		
		-1	0	1
Crude glycerol (g/L)	A (X_1)	20	40	80
Yeast extract (g/L)	B (X_2)	0.50	0.63	0.75
$(NH_4)_2SO_4$ (g/L)	C (X_3)	0.25	0.40	0.55

Table 3.2 Box-Behnken consisting of 15 experiments for three experimental factors for the carotenoid concentration by *R. paludigena* CM33.

Run	Independent variables			Dependent variables	
	Crude glycerol (g/L)	Yeast extract (g/L)	$(NH_4)_2SO_4$ (g/L)	Carotenoid concentration (ug/g)	
				observed	predicted
1	20	0.75	0.40	206.00	214.00
2	40	0.50	0.25	287.00	295.45
3	40	0.75	0.55	332.00	323.55
4	40	0.63	0.40	339.00	328.00
5	40	0.63	0.40	319.00	328.00
6	80	0.63	0.25	0	0.37
7	20	0.63	0.55	200.00	203.26
8	40	0.50	0.55	298.00	295.56
9	40	0.63	0.40	326.00	328.00
10	80	0.63	0.55	0	7.63
11	80	0.75	0.40	0	-2.00
12	80	0.50	0.40	0	-6.00
13	40	0.75	0.25	317.00	319.45
14	20	0.50	0.40	177.00	177.00
15	20	0.63	0.25	215.00	203.74

3.3.4 Cultivation of *R. paludigena* CM33 in a 500-L fermenter at pilot scale

The seed culture was made in the following manner: In a 5-L fermenter, *R. paludigena* CM33 was inoculated into a crude glycerol medium and grown there for 48 hours at 30 °C and 0.7 vvm. The same conditions were employed for cultivation in a 50-L fermenter as well. 10% (v/v) of the seed culture was added to the fermentation medium in order to carry out batch fermentation. With an airflow rate of 0.7 vvm, the batch fermentation process continued for 7 days at 30°C. For the repeated fermentation process, after the overall glycerol concentration decreased, approximately 70% of the fermentation broth was withdrawn, and an equal volume

of fresh medium was added. Finally, for the fed-batch fermentation with pulse addition, 10% (v/v) of cultures were inoculated into a 250 L medium and cultivated at 30 °C with a 0.7 vvm air flow level. The fed-batch culture took place in four stages. During the first stage, the fermenter received 25 L of medium, resulting in a total glycerol content of 40 g/L. After three days, the residual total glycerol concentration fell below 5 g/L, prompting the addition. Subsequently, 25 L of medium was added in each of the second to fourth stages to maintain a constant total glycerol concentration of 40 g/L. Daily, 25 mL samples of the fermentation broth were taken throughout the experiment to measure the levels of carotenoids, OD 600 nm, biomass, and glycerol. A spectrophotometer was used to measure the carotenoid levels (Ribeiro et al., 2019). 10N NaOH was used to keep the pH at 5.5 +/- 0.5. As required, foam generation was managed using silicone antifoam (Kemaus, Australia).

3.3.5 Analytical methods

The description of the extraction procedure by Ribeiro et al. (Ribeiro et al., 2019) is accurate. Cells were collected using a Denville microcentrifuge 260D from New Jersey, USA, by centrifuging them at 12,000 x g for 5 min. After discarding the supernatant, the cell pellets were then frozen at -20 °C for 24 hours. The frozen pellets were thawed, broken up, and then re-dissolved in 2 mL DMSO. After 15 minutes of incubation at 60°C, the mixture was vortexed for 2 minutes. The mixture was then successively treated with the addition of 2 mL of acetone, 2 mL of petroleum ether, and 2 mL of 20% NaCl. The entire mixture was vortexed for a total of 5 minutes, followed by 5 minutes of centrifugation at 12,000 x g. Thermo Scientific P1000 UV-Vis Wisconsin, USA spectrophotometer was used to detect the carotenoid concentration at 450 nm using β-carotene in PE's absorption coefficient ($A^{1\%}_{1cm}$ = 2592) (Ribeiro et al., 2019).

A spectrophotometer (Thermo Scientific Genesys10S UV-Vis Wisconsin, USA) was used to measure optical density (OD) at 600 nm. For each sample, the OD of the medium was removed (Campos et al., 2023). For biomass, a 2 mL sample was centrifuged at 12,000 x g for 2 minutes and the supernatant was discarded. Cells were washed three times with deionized water and dried for 24 hours at 65 °C to constant weight (Gong et al., 2020).

Glycerol was analyzed using HPLC (Hitachi Chromaster 5110 Tokyo, Japan), a Refractive Index (RI) detector (Model 5450 RI detector Tokyo, Japan), and an HPX-87C column (7.8 mm 150 mm i.d., 9 m). The samples were analyzed using a mobile phase of 5 mM sulfuric acid with a flow rate of 0.6 mL/min (Uprety et al., 2017).

3.4 Results and discussion

3.4.1 Crude glycerol characterization

The major portion of crude glycerol is utilized as feedstock for the manufacturing of various value-added chemicals (Yang et al., 2012). In this study, it was discovered that the crude glycerol used in this investigation had a pH value of 2.38 and comprised 58% glycerol in its chemical composition. The crude glycerol's element analysis revealed that it included 25.91% carbon, 7.44% hydrogen, 1% or fewer nitrogen atoms, 4.14% sulfur, and 11,769 ppm sodium (Table 3.3). Crude glycerol's chemical composition can change based on a number of variables, including transesterification efficiency, the type of catalyst utilized, and downstream processing techniques. During the biodiesel production process, crude glycerol is frequently refined using chemicals, leaving a pH value as low as 1 (Kongjao et al., 2010). These results are in line with earlier reports that stated crude glycerol had a carbon content of 24.3% (Hu et al., 2012). They discovered carbon content varying from 24 to 37% in seven different crude glycerol types (Thompson & He, 2006). The low nitrogen value reported in this study (1%), however, is consistent with prior research (Thompson & He, 2006). Because of the employment of basic catalysts and the harvesting of glycerol phase with 12.5 M NaOH during biodiesel production, the crude glycerol sample used in this investigation had a high sodium concentration (11,769 ppm) (Kongjao et al., 2010). In earlier research, oleaginous yeast was grown using crude glycerol as a carbon source to produce carotenoids (Sun et al., 2023). In this investigation, crude glycerol was employed as a substrate for *R. paludigena* CM33 fermentation. Additionally, we noted that the concentration of nitrogen sources in crude glycerol is low. As a result, in this study, we used response surface methodology (RSM) to improve the nitrogen sources using yeast extract and $(NH_4)_2SO_4$.

Table 3.3 Chemical composition and elemental analysis of crude glycerol.

Parameter	Unit	Crude glycerol
Free Glycerol	%	58
pH	-	2.38
C	%	25.909
H	%	7.440
N	%	<1
S	%	4.139
Na	ppm	11,769±0.10
Mg	ppm	31.29±0.12
Al	ppm	ND
P	ppm	38.7±0.50
K	ppm	118.8±0.13
Ca	ppm	2,050.080±0.14
Mn	ppm	3.22±0.42
Fe	ppm	31.6±0.34
Co	ppm	ND
Cu	ppm	4.960±0.14
Zn	ppm	25.79±0.31

3.4.2 Effects of crude glycerol, yeast extract, and $(NH_4)_2SO_4$ on carotenoid production in *R. paludigena* CM33.

Rhodotorula sp. is known to produce carotenoids and requires a medium that is rich in carbon but low in nitrogen (Saenge et al., 2011). Furthermore, a decrease in carotenoid synthesis may occur due to a reduced nitrogen concentration in the medium (Rodrigues et al., 2019). As a result, the primary independent variables in this investigation were crude glycerol (X_1), yeast extract (X_2), and $(NH_4)_2SO_4$ (X_3). These variables were selected to optimize carotenoid synthesis. The combined influence of the three independent variables on carotenoid concentration was assessed using the Response Surface Methodology (RSM) Central Composite Design.

The results were analyzed using Analysis of Variance (ANOVA), as shown in Table 3.4. From the table, it can be observed that X_1 has a positive effect on the responses ($P<0.05$). The Model F-value of 216.78 for carotenoid confirms that the model is highly significant, with a P-value less than 0.05. The lack of significance in the lack-of-fit test indicates the accuracy of the model in predicting carotenoid production. The model successfully predicted the variance observed in the test and fit well to the experimental data, as indicated by a obtained P-value of < 0.05 (Bezerra et al., 2008; Raviadaran et al., 2018). The coefficient of determination for carotenoid was calculated as $R^2 = 0.9974$. The adjusted R-squared value was determined as 0.9928 for carotenoids, as shown in Table 3.4. The collected data were analyzed using linear regression analysis with Design Expert software 13. A quadratic polynomial model was employed to describe the relationship between the variables. The model is represented by Eq. (3.2), where Y represents carotenoids and X_1, X_2, and X_3 represent the variables of crude glycerol, yeast extract, and $(NH_4)_2SO_4$, respectively.

$Y_{carotenoid}$ = -581.99 + 21.03 Crude glycerol + 1270.67 Yeast extract + 160.94 $(NH_4)_2SO_4$ − 2.20 Crude glycerol * Yeast extract + 0.43 Crude glycerol * $(NH_4)_2SO_4$ − 53.33 Yeast extract * $(NH_4)_2SO_4$ − 0.23 Crude glycerol^2 − 880.00 Yeast extract^2 − 255.56 $(NH_4)_2SO_4^2$ (3.2)

The regression equation depicting the relationship between significant parameters and carotenoid concentration was visually presented through RSM contour plots and 3D surface plots generated by Design Expert Software 13. Figure 3.1 (A-C) illustrates the effects and relationships between various significant variables and carotenoid concentration. The contour and 3D surface graphs were generated by plotting combinations of parameters while keeping the yeast extract concentration fixed and the remaining parameters at their maximum level. Figure 3.1 (A-B) illustrates that the highest carotenoid concentration was observed in the contours and 3D surface when the crude glycerol and $(NH_4)_2SO_4$ concentrations were within the middle range. The RSM predictions for the optimized parameters were 40 g/L of crude glycerol, 0.72 g/L of yeast extract, and 0.43 g/L of $(NH_4)_2SO_4$ concentration (Figure 3.1C). The carotenoid concentration obtained from the experiment closely matched the

predicted value. Similar findings were reported in the cultivation of *R. paludigenum* DMKU3-LPK4, where a glycerol concentration of 40 g/L was found to promote high carotenoid synthesis (Yimyoo et al., 2011). Additionally, Uprety et al. observed that the optimal concentration for lipid production in *R. toruloides* ATCC 10788 was 40 g/L of pure glycerol (Uprety et al., 2017). In a 5-L stirred tank, *Trichosporandoides spathulata* JU4-57 achieved a biomass yield of 13.8 g/L with a crude glycerol concentration of 32 g/L (Kitcha & Cheirsilp, 2013). Carotenoid and biomass production were observed during yeast culture on various substrates, as shown in Table 3.5 (Raviadaran et al., 2018; Uprety et al., 2017; Yimyoo et al., 2011). Based on the RSM results, the optimal concentrations of 40 g/L crude glycerol, 0.72 g/L yeast extract, and 0.43 g/L $(NH_4)_2SO_4$ can be employed for scaling up the production in a 500-L fermenter.

Table 3.4 Analysis of variance (ANOVA) and Significance level of the Response Surface Linear model exhibiting carotenoid concentration.

Source	Sum of squares	Degree of freedom	Mean square	F-value	p-value	
Carotenoid concentration (ug/L)						
Model	257800	9	28639.59	216.78	<0.0001	Significant
A	79600.50	1	79600.50	602.51	<0.0001	Significant
B	798.47	1	798.47	6.04	0.0573	not significant
C	21.90	1	21.90	0.1657	0.7008	not significant
Residual	660.58	5	132.12	–	–	
Lack of Fit	454.58	3	151.53	1.47	0.4291	not significant
Prue Error	206.00	2		–	–	
Cor Total	258400	14	–	–	–	
R^2 = 0.9974; R^2_{adj} = 0.9928						
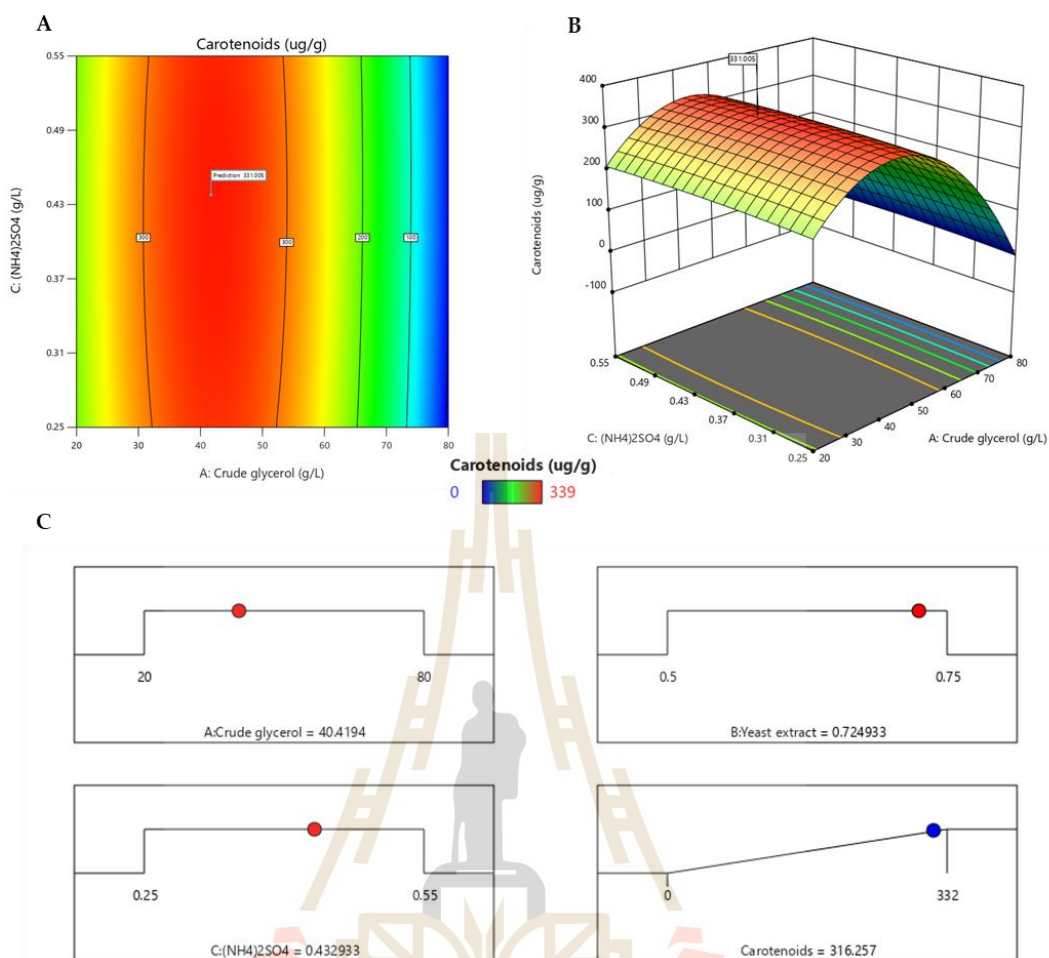
Figure 3.1 (A) The effect of different significant variables on the response surface contour plot was evaluated using Response Surface Methodology for carotenoids.; (B) The RSM 3D surface plots obtained using Design-Expert software illustrate the effects of different significant variables on carotenoids by *R. paludigena* CM33 (A) The optimized parameters predicted by RSM were 40 g/L of crude glycerol, 0.72 g/L of yeast extract and 0.43 g/L of $(NH_4)_2SO_4$ concentration.

Table 3.5 Presents the cultivation of yeast on various substrates, focusing on the production of biomass, and carotenoids.

Strain	Substrate	Cultivation method	Carotenoids	Biomass	Reference
R. paludigenum DMKU3-LPK4	40 g/L glycerol	Batch	3.42 mg/L	7.59 g/L	(Yimyoo et al., 2011)
R. toruloides ATCC 10788	40 g/L Pure glycerol	Batch	-	21.16 g/L	(Uprety et al., 2017)
T. spathulata JU4-57	40% crude glycerol	Fed-batch	-	13.80 g/L	(Kitcha & Cheirsilp, 2013)
R. mucilaginosa CCT 7688	70 g/L sugar cane molasses and 3.4 g/L corn steep liquor	Batch	1.25 mg/L	7.90 g/L	(Rodrigues et al., 2019)
R. mucilaginosa CCT 7688	30 g/L sugar cane molasses and 6.5 g/L corn steep liquor	Fed-batch	3.73 mg/L	16 g/L	(Rodrigues et al., 2019)
R. glutinis Rh-00301	400 g/L glycerol	Fed-batch	-	106 g/L	(Lorenz et al., 2017)
R. glutinis DBVPG 3853 and *D. castellii* DBVPG 3503	8.3 g/L glucose, 22.7 g/L maltose, and 4.65 g/L nitrogen	Fed-batch	8.20 mg/L	-	(Buzzini, 2001)
R. paludigena CM33	40 g/L Crude glycerol	Batch	1.27 mg/g	9.27 g/L	This work
R. paludigena CM33	40 g/L Crude glycerol	Repeated batch	14.64 mg/g	38.33 g/L	This work
R. paludigena CM33	40 g/L Crude glycerol	Fed-batch	15.39 mg/g	45.38 g/L	This work

3.4.3 In a 500-L fermenter pilot scale, the effects of different cultivation techniques on carotenoid production were examined using batch, repeated batch, and fed-batch cultivation.

In each operation, a 500-L fermenter was used with 40 g/L of crude glycerol, 0.72 g/L of yeast extract, and 0.43 g/L of $(NH_4)_2SO_4$. After 6 days of batch fermentation, *R. paludigena* CM33 produced a biomass of 9.27 ± 0.001 g/L using 40 g/L of crude glycerol (equivalent to 38.02 g/L of glycerol). The carotenoid concentration was 1.27 ± 4.27 mg/g of DCW (Figure 3.2A). A repeated batch method was employed to achieve high biomass, which resulted in a maximum biomass of 38.33 ± 0.02 g/L. Moreover, the maximum carotenoid concentration reached 14.64 ± 0.01 mg/g (after 8 days), respectively (Figure 3.2B). The results of the fed-batch fermentation procedures used to maximize the biomass, and carotenoid concentration in *R. paludigena* CM33 are illustrated in Figure 3.2C. The fermentation substrate used was 40 g/L of crude glycerol, equivalent to 32.98 g/L of glycerol. The highest carotenoid concentration was achieved during the fourth pulse, measuring 15.39 ± 0.03 mg/g of dry cell weight (DCW). These conditions led to a maximum biomass of 45.38 ± 1.05 g/L. The productivity of carotenoids in batch, repeated batch, and fed-batch cultivations was 0.054±0.001, 0.288±0.001, and 0.466±0.002, respectively (mg.L^{-1}.h^{-1}) and the total carotenoid yield was 0.025±0.002, 0.386±0.005, and 0.374±0.003, respectively (mg.g^{-1} DCW). According to this study, both the repeated batch and fed-batch fermentation techniques exhibited more than a 4-fold increase in biomass and a 12-fold increase in carotenoid synthesis compared to the batch process. In a similar previous study, the fed-batch co-culture of *R. glutinis* DBVPG 3853 and *Debaryomyces castellii* DBVPG 3503, using corn syrup as the carbon source, showed a 150% increase in carotenoid production and a 2-fold increase in biomass compared to the batch culture. These findings are consistent with previously reported carotenoid production (Buzzini, 2001). Additionally, in another study, a feeding strategy was implemented in the fed-batch method for *R. mucilaginosa* cultured in an agro-industrial medium, resulting in a 400% increase in carotenoid production compared to the batch process (Rodrigues et al., 2019). Furthermore, the addition of molasses as a supplement in a different study led to a 4-fold increase in biomass between the fed-batch culture and the batch culture (Bhosale & Gadre, 2001b) (Table 3.5) (Kitcha & Cheirsilp, 2013;

Lorenz et al., 2017; Yen & Zhang, 2011). Based on the findings, it can be concluded that fed-batch cultivation utilizing 40 g/L crude glycerol, 0.72 g/L yeast extract, and 0.43 g/L $(NH_4)_2SO_4$ in a 500-L fermenter pilot scale can significantly enhance both the carotenoid concentration.
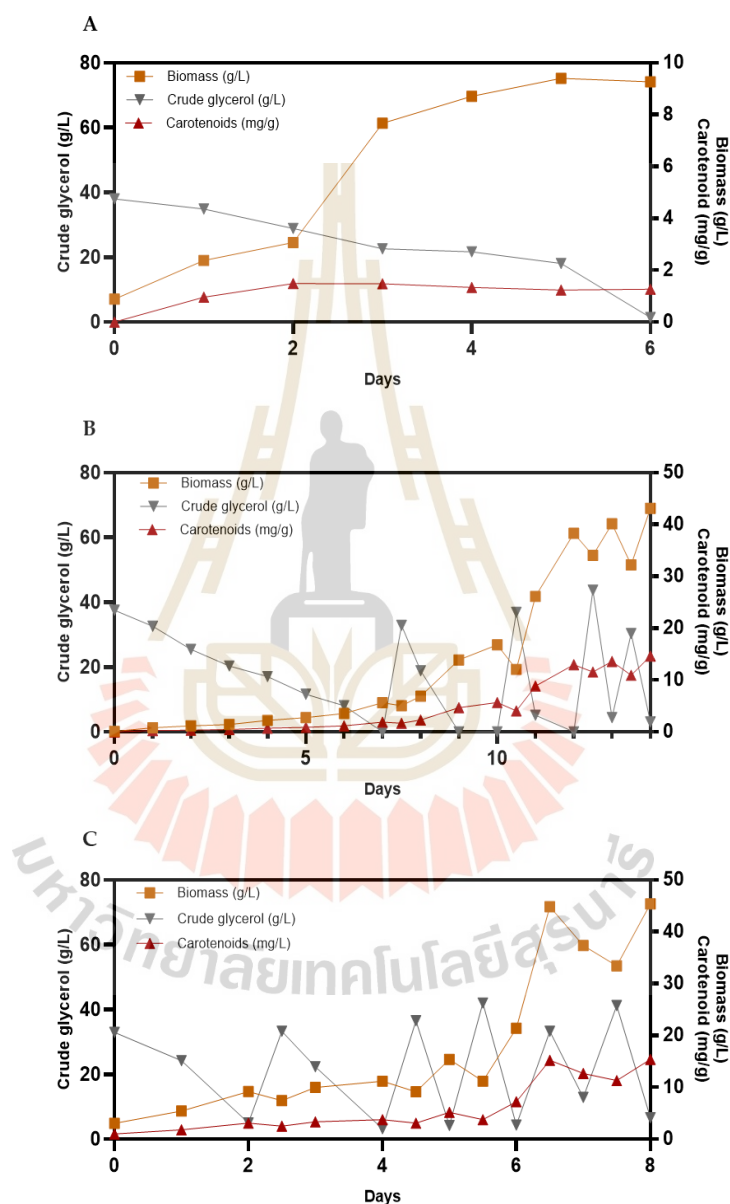
Figure 3.2 The effect of different fermentation modes: (A) batch, (B) repeated batch, and (C) fed batch, on carotenoid concentrations of *R. paludigena* CM33 grown on crude glycerol. Biomass (■), Carotenoid concentration (▲), and Crude glycerol (▼). Each experiment was conducted in triplicate.

3.5 Conclusion

The present study focused on investigating the utilization of crude glycerol as a substrate for biomass and carotenoid synthesis. The study found that feeding a 500-L fermenter with 40 g/L crude glycerol, 0.72 g/L yeast extract, and 0.43 g/L $(NH_4)_2SO_4$ led to increased cell density and carotenoid synthesis. According to this study, both the repeated batch and fed-batch fermentation techniques exhibited more than a 5 to 8-fold increase in carotenoids productivity and a 15-fold increase in total carotenoid yield compared to the batch process. Based on the results, it can be concluded that crude glycerol holds promise as an alternative substrate for enhancing carotenoid synthesis in *R. paludigena* CM33.
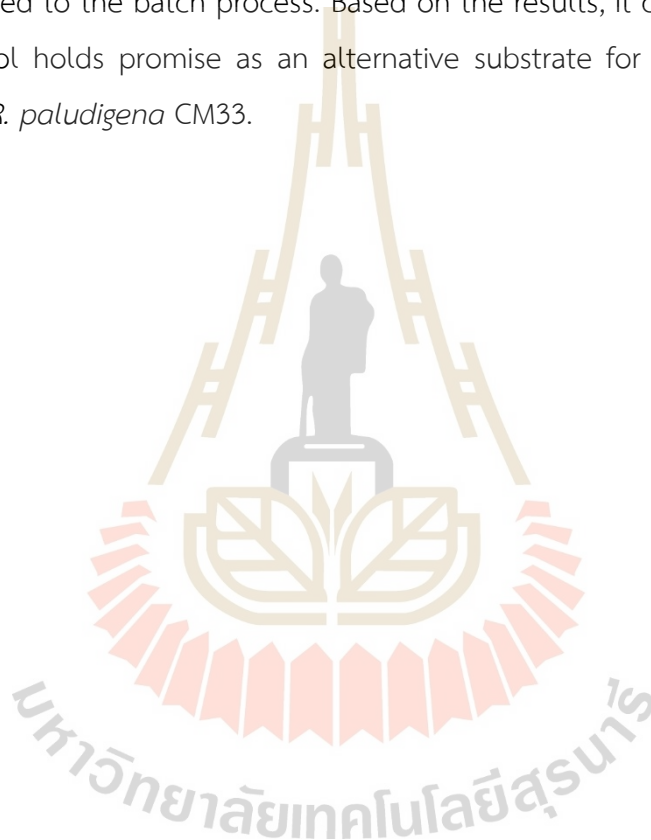
CHAPTER 4

EFFICIENT DOWNSTREAM PROCESSES FOR CAROTENOIDS

PRODUCTION IN *Rhodotorula paludigena* CM33

4.1 Abstract

In this study, the harvesting of *Rhodotorula paludigena* CM33 cells was examined through the analysis of the microfiltration process. The harvesting of carotenoids in *R. paludigena* CM33 was achieved by cell disruption using response surface methodology with a high-pressure homogenizer (HPH), followed by carotenoid purification with preparative high-performance liquid chromatography (prep HPLC). A microfiltration method was used for yeast harvesting. After fermentation, the recovery of yeast cells was explored using a cross-flow microfiltration (MF) method, which included concentration and diafiltration modes. To identify the primary causes of the flow rate drop, the fouling process of the membrane was examined using a cleaning approach. The observed flow rate of pure water was 80.00 L/m²/h, corresponding to a membrane resistance of 1.4×10^{15} m^{-1}. The flux exhibited a significant drop during the MF process for the entire broth and then gradually stabilized at around 25 L/m²/h until the completion of the experiment. Pure water was subsequently added during the diafiltration mode to remove any impurities. Following cell harvesting, a chemical washing technique was employed to measure the resistances of the cake and adsorption. After cleaning with water alone, the restored flux was measured at 68.40 L/m²/h; however, after washing with a 1 wt% NaOH solution, it increased to 80.00 L/m²/h. The results revealed that the cake accounted for 85.38% of the overall resistance, while the adsorption resistance accounted for 12.62%. In addition, The results of HPH revealed that applying a pressure of 30,000 psi, performing 4 passes, and using a 5% yeast cell feed led to an increase in cell disruption. Following the Prep HPLC, the compound was compared to a standard β-carotene. Subsequently, the analytical HPLC analysis exhibited excellent resolution for β-carotene, revealing a concentration of 12.76 mg/L and a purity of 94.80%. The carotenoids identified in this

study, primarily β-carotene, were confirmed through HPLC, LC-MS, and NMR analyses. These findings highlight the potential of microfiltration, high-pressure homogenization (HPH), and preparative HPLC in enhancing the downstream processing of carotenoids in *R. paludigena* CM33.

4.2 Introduction

Carotenoids are natural pigments that find applications in high-value industries, including cosmetics, medicines, dietary supplements, and chemical industries. Previous research has extensively investigated the biology of carotenoid production. (Igreja et al., 2021). In 2019, the global carotenoids market was estimated to be worth 1.5 billion USD, and it is projected to reach 2.0 billion USD by 2026.(Bccresearch, 2022). Red yeasts have been identified as potential carotenoid producers among microorganisms. Their ability to grow rapidly on various substrates makes them suitable for industrial-scale production, significantly reducing production times. (Chopra, Rangarajan, & Sen, 2022). Currently, extensive research is underway on the fermentation of microbial carotenoids using various red yeasts, including *Phaffia rhodozyma* (Mussagy et al., 2022), *Rhodotorula* sp. (Allahkarami, Sepahi, Hosseini, & Razavi, 2021), *R. mucilaginosa* (Li, Cui, Zhang, Meng, & Liu, 2022; Machado, Murari, Duarte, & Del Bianchi, 2022) and *R. glutinis* (Gong, Zhang, & Tan, 2020; Zhao & Li, 2022). We isolated the yeast *R. paludigena* CM33 from our laboratory for a previous study. This yeast demonstrated the ability to utilize various carbon sources, including glucose, sucrose, xylose, and glycerol, respectively (Gosalawit et al., 2021).

The bioprocess for carotenoid production entails both upstream and downstream processing. In the upstream phase, optimizing the yeast's growth and its capacity to accumulate substantial carotenoid levels is of great interest. Many techniques, including light irradiation (Gong et al., 2020; Manowattana, Techapun, Laokuldilok, Phimolsiripol, & Chaiyaso, 2020), gene insertion (Breitenbach, Pollmann, & Sandmann, 2019), and chemical treatments (Gassel, Schewe, Schmidt, Schrader, & Sandmann, 2013), have been investigated for genetic modification aimed at enhancing carotenoid accumulation. Due to concerns about the safety of genetically modified foods, the majority of research in this field now emphasizes media carotenoids (Dias, Reis, Santos, & da Silva, 2020; Robles-Iglesias, Naveira-Pazos, Fernández-Blanco, Veiga, & Kennes,

2023). In addition, several techniques have been explored for the downstream process to enhance the separation and purification of carotenoids. Physico-chemical extraction methods, including high-pressure homogenization (Dias, Nobre, Santos, da Silva, & Reis, 2022), ultrasound under pressure (Martínez, Delso, Aguilar, Álvarez, & Raso, 2020), and pulsed electric field (Martínez, Delso, Angulo, Álvarez, & Raso, 2018), have been studied. Chromatographic separation is subsequently employed as the final step to achieve high-purity carotenoid production (Latha & Jeevaratnam, 2010)

In this study, we initially investigated the process development for harvesting, extracting, and purifying carotenoids from a microfiltration process. We disrupted cells using a microfluidizer and employed response surface methodology (RSM) for optimization. Subsequently, preparative liquid chromatography techniques were employed. The presence of carotenoids was then confirmed through HPLC, LC-MS, and NMR analyses. The outcomes of this study have the potential to pave the way for the commercial production of carotenoids from oleaginous yeast.

4.3 Materials and methods

4.3.1 Microorganism and culture conditions

The oleaginous yeast *R. paludigena* CM33 was isolated from various natural habitats by our laboratory (Poopisut et al., 2023). The microorganism was grown on yeast peptone dextrose (YPD) medium (20 g/L glucose, 10 g/L peptone, 10 g/L yeast extract and 15 g/L agar) (Gosalawit et al., 2021). The inocula for fermentation were prepared by 10 ml minimal medium components: 70 g/L glucose, 0.4 g/L KH_2PO_4, 0.55 g/L $(NH_4)_2SO_4$, 2.0 g/L $MgSO_4 \cdot 7H_2O$ and 0.75 g/L yeast extract and incubated at 30°C overnight on rotary shaker at 150 rpm for 48 h (Poopisut et al., 2023). *R. paludigena* CM33 was inoculated into crude glycerol medium and cultivation for 48 h at 30 °C and 0.7 vvm in a 5-L and 50-L fermenter, respectively. The fed-batch culture was conducted in four stages. During the first stage, 25 L of the medium was added to the fermenter, reaching a total glycerol concentration of 40 g/L. This addition occurred when the residual total glycerol concentration dropped below 5 g/L after 3 days. Subsequently, in the second to fourth stages. The pH was maintained at 5.5 ± 0.5 using 10N NaOH. The silicone antifoam (Kemaus, Australia) was used to control foam formation as needed.

4.3.2 Harvesting *R. paludigena* CM33 cell using a microfiltration system

4.3.2.1 Microfiltration set up

R. parudigena CM33 cells were removed from fermentation both using cross-flow microfiltration and dead-end filtration for a study involving the volume concentration ratio (VCR) in the experiment. The schematic diagram of the dead-end and cross-flow microfiltration experiments were shown in Figure 4.1. A spiral-wound microfiltration (MF) element with a nominal pore size of 0.1 μm (Synder's Filtration, USA) was placed in a stainless-steel housing for the cross-flow MF experiment. The diameter and length of the membrane element were measured to be 10.2 cm and 96.5 cm, respectively. The feed spacer had a diameter of 3 mm, and the overall filter area was 4.27 m². The fermentation broth was recirculated using a 0.75 kW pump at a volumetric flow rate of 70 L/min, which corresponded to a calculated linear flow velocity of 0.09 m/s. (Russotti et al., 1995). A cooling coil, buried in the MF feed tank, was utilized to maintain the feed temperature at 30℃. Traditional pressure gauges were used to measure the feed, retentate, and permeate pressures, which were then used to calculate the transmembrane pressure. The membrane was initially cleaned with RO water after each run. Following 20 minutes of circulation with a 1% weight NaOH solution, it was thoroughly rinsed with RO water until neutral. Subsequently, it was cleaned with a 1.5% weight phosphoric acid solution and then rinsed with RO water until the pH reached 7.0.

4.3.2.2 Resistance Analysis

The flow through microporous membranes during the microfiltration stage is described by Darcy's Law. Due to the accumulation of oleaginous yeast cells and other particles on the membrane surface, as well as pore blockage, the permeate flux decreases (Juang et al., 2008). According to Darcy's law, the movement of cell through the membrane depends on the applied pressure (Redkar & Davis, 1993).

Darcy's law

$$Q = \frac{k\Delta p}{\mu l} \tag{4.1}$$

When Q = Volumatic filtration flowrate (m³/s)

k = Darcy's law permeability (m^2)

$\triangle p$ = Pressure drop across the filter medium (Pa)

μ = Viscosity of the broth (kg/m.s)

l = Thickness of the filter medium (m)

The permeability and thickness of filter can be combine into a medium resistance term.

$$R_m = \frac{l}{k} \qquad (4.2)$$

When R_m = medium resistance (m^{-1})

Equation (4.1) can be written as;

$$Q = \frac{A\Delta p}{\mu R_m} \text{ or } Q = \frac{dV}{dt} = \frac{A\Delta p}{\mu R_m} \qquad (4.3)$$

At any instant during filtration basing on the Darcy's law, rate of filtration is given by the equation;

$$J = \frac{1}{A}\frac{dV}{dt} = \frac{\Delta p}{\mu R} \qquad (4.4)$$

When J = Flux, and $R = R_{m+} R_c$

In this case R is a combination of resistance of filter medium (R_m) and resistance of cake solids (R_c). And the resistance of cake solids (R_c) can be written as;

$$R_c = \alpha p_c \frac{V}{A} \qquad (4.5)$$

When ρ_c is the mass of dry cake solids per volume of filtrate and α is specific cake resistance. Combination of equation (2) , and (3) results in the following equation;

$$\frac{1}{A}\frac{dV}{dt} = \frac{\Delta p}{\mu \left[\alpha p_c \frac{V}{A} + R_m\right]} \qquad (4.6)$$

And integration of the eqution (4) results in;

$$\frac{At}{V} = \frac{\mu \alpha p_c}{2\Delta p}\left(\frac{V}{A}\right) + \frac{\mu R_m}{\Delta p} \qquad (4.7)$$

To further prepare the concentrated cell suspension, a freeze-drying device (Freeze dry, Christ/Gamma2-16, Osterode am Harz, Germany) was utilized.

Figure 4.1 Schematic diagram of dead-end (A) and cross-flow microfiltration (B) experiments.
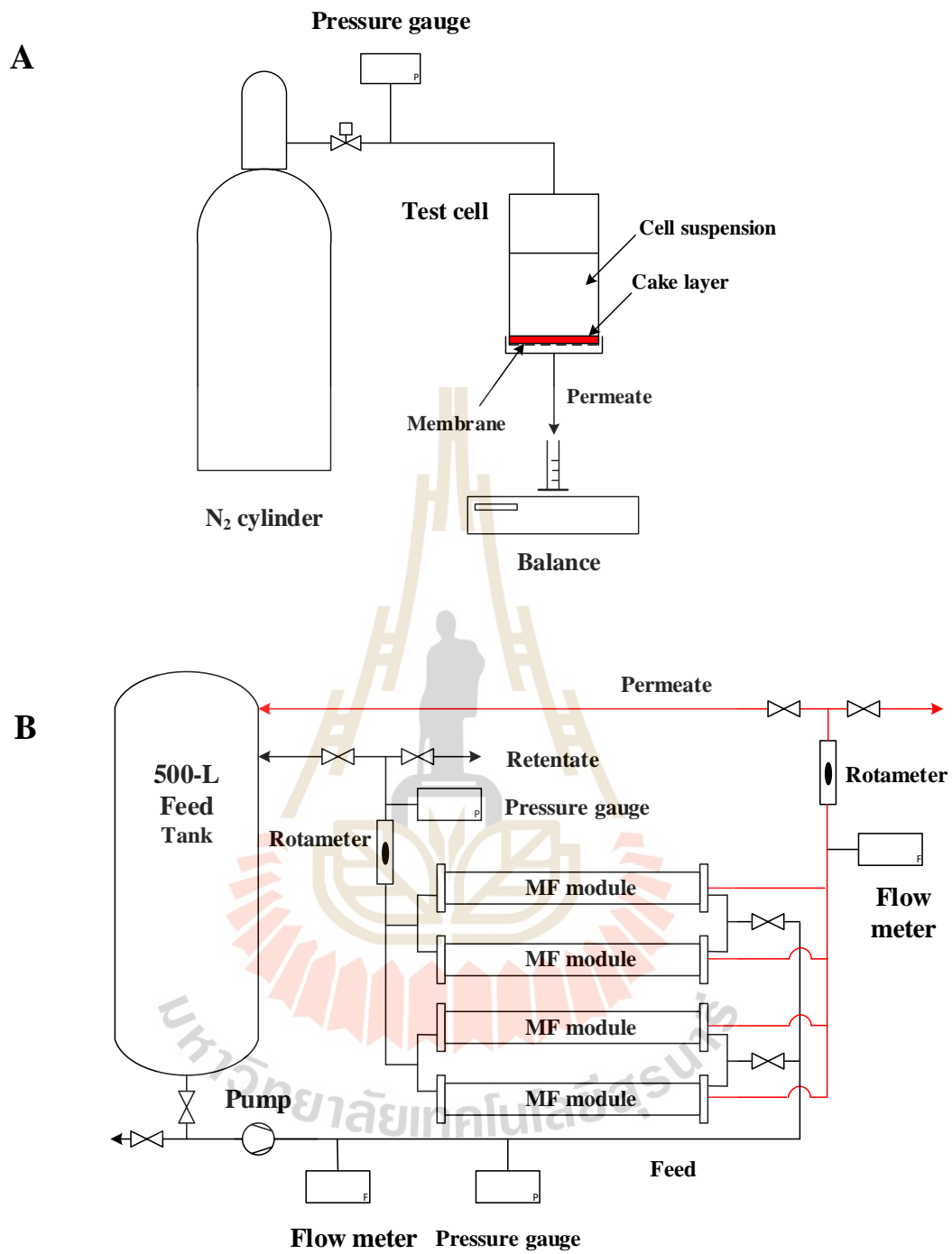
4.3.3 Response Surface methodology (RSM) – Box-Behnken

The optimization of *R. paludigena* CM33 cell disruption were studied by Box-Behnken Design. The optimal conditions effect on carotenoid concentration were studied through the Box-Behnken using Design expert (Software 13, Stat-Ease Inc., Minneapolis, MN, USA). The independent variables and their levels are shown in Table 4.1. The Box-Behnken design consists of 15 factorial points as given in Table 4.2. The predicted and obtained response regarding carotenoid production and cell disruption with High pressure homogenizer (HPH) were analyzed. The response variables could be fitted into the general form of a quadratic polynomial model shown in Eq. (4.8).

$$y = \beta_0 + \sum_{i=1}^{3} \beta_i x_i + \sum_{i=1}^{3} \beta_{ii} x_i^2 + \Sigma_{i=1}^{2} \sum_{j=i+1}^{3} \beta_{ii} x_i x_j \qquad (4.8)$$

When Y is the response variable measured for each combination of factorial level; β_0, β_i, β_{ii}, and β_{ij} are terms are regression coefficients for linearity, intercept, interaction and square; X_1, X_2, and X_3 are codes of the independent variables.

Table 4.1 Evaluated factors, factor notation, and their levels in Box-Behnken.

Independent variables	Codes	Factor levels		
		-1	0	1
Pressure (psi)	A (X_1)	10,000	20,000	30,000
Feed (%)	B (X_2)	5	12.5	20
Passes (Time)	C (X_3)	4	6	8

Table 4.2 Box-Behnken consisting of 15 experiments for three experimental factors for the carotenoid concentration by *R. paludigena* CM33.

Run	Independent variables			Dependent variables	
	Pressure (psi)	Feed (%)	Passes (Time)	Carotenoid concentration (ug/g)	
				observed	predicted
1	20,000	5	4	1,763.12	1,803.99
2	30,000	5	6	2,014.60	1,823.29
3	30,000	20	6	750.84	650.77
4	20,000	20	8	731.58	746.84
5	10,000	5	6	769.65	812.98
6	10,000	12.5	4	719.44	663.31
7	20,000	20	4	1,773.66	1,722.69
8	30,000	12.5	6	466.82	691.36
9	20,000	12.5	6	462.96	626.60
10	10,000	12.5	8	718.83	596.45
11	30,000	12.5	4	1,425.15	1,491.39
12	20,000	5	8	1,703.19	1,810.30
13	20,000	12.5	6	719.96	626.60
14	20,000	12.5	6	809.16	626.60
15	10,000	20	6	705.56	840.74

4.3.4 Carotenoids purification with high pressure homogenizer and preparative high-performance liquid chromatography.

Based on the above study, fermentation broth was treated with High Pressure Homogenization (HPH) (Microfluidics Model M-110EH-30 Massachusetts, USA) at homogenization pressure 30,000 psi, 5% feed, and 4 passes, , as indicated by the results obtained from the Response Surface Methodology (RSM) (Comuzzo & Calligaris, 2019). After HPH treatment, 25 mL sample were centrifuged at 5,000 rpm for 10 min. The pellets were washed by deionized water, and carotenoid were extracted followed the method by Ribeiro et al. (Ribeiro et al., 2019). At the end of the extraction stage, the sample was further separated and purified.

Preparative high-performance liquid chromatography (prep HPLC) (BÜCHI Pure Flash/Prep HPLC Model C-850 Flawil, Switzerland) was used to separate and purify the carotenoids extracted from *R. paludigena* CM33. The operation process was as follows: The mobile phase consisted of methanol: acetonitrile: ethyl acetate (76:12:12 v/v) (Cipolatti et al., 2019). The separation was dissolved in 100 mL mobile phase. The sample was injected into the HPLC system equipped with EcoFlex C18 50 μm spheric 12 g column. The flow rate was 30 mL/min, the analysis wavelength was 450, 474, 500 and 515 nm. After purification the carotenoids were confirmed by HPLC, LC-MS, and NMR.

4.3.5 Analytical methods

Carotenoids extraction was carried out according to Ribeiro et al. (Ribeiro et al., 2019) Briefly, cells were harvested by centrifugation at 12,000 x g for 5 min (Denville microcentrifuge 260D New Jersey, USA) and re-suspended with 1 mL deionized water, after discarding the supernatant, the cell pellets were frozen at -20 °C for 24 hours. The frozen pellets were then thawed and disrupted before being re-suspended in 2 mL DMSO. The resulting mixture was vortexed for 2 minutes and incubated at 60°C for 15 minutes. Subsequently, 2 mL of acetone, 2 mL of petroleum ether, and 2 mL of 20% NaCl were sequentially added to the mixture. The entire mixture was vortexed for a total of 5 minutes and then centrifuged at 12,000 x g for 5 minutes. Carotenoid concentration was measured by spectrophotometer (Thermo scientific P1000 UV-Vis Wisconsin, USA) at 450 nm wavelength using the absorption coefficient of β-carotene in PE ($A^{1\%}_{1cm}$ = 2592) (Ribeiro et al., 2019).

A SpectraSystem (Thermo scientific P1000 UV-Vis Wisconsin, USA) equipped with a SuperC18 HPLC column (4.6 mm × 150 mm i.d., 5 μm) was used for HPLC analysis. The detection conditions were optimized before analysis. The mobile phase consisted of a mixture of methanol: acetonitrile, and water in a ratio of 72:12:12 (Cipolatti et al., 2019). The flow rate was set to 1 mL/min, the column temperature was maintained at 45 °C, the injection volume was 10 μL, and the analysis wavelength was set to 450 nm (Marova et al., 2012). The concentration of the β-carotene pigment was determined by referencing a β-carotene standard curve. The identification of β-carotene in the compound was based on its relative retention times compared to the standard β-carotene (MilliporeSigma, USA) (Alipour et al., 2017).

Liquid chromatography-mass spectrometry (LC-MS) was used to identify different carotenoid using UHPLC Ultimate 3000 (Thermo Fisher Scientific) Liquid chromatography (LC) coupled with Bruker/micrOTOF – Q II mass spectrometer (MS). Mass spectra of carotenoids were acquired with an m/z detector and 50 – 1700 by a diode array detector and confirmed with their respective standards. The LC-MS analysis of carotenoids was conducted in positive ion mode (APCI), with a capillary voltage of 4500 V for the total ion current (TIC), and a charging voltage of 4500 V. Nitrogen was used as the nebulizer gas (purity 99.9%) with a flow rate of 2 L/min and a vaporizer temperature of 250°C. The identification of individual components was performed by comparing mass spectra with profiles from the NIST 20 mass libraries (Sivathanu & Palaniswamy, 2012).

[1]H Nuclear Magnetic Resonance Spectroscopy (NMR) measurements were performed on a Bruker NMR (Bruker AVANCE III 500 MHz Massachusetts, USA) at 500 MHz. Purified compounds were dissolved in methanol and acetone, and data were processed by Bruker Topspin 3.5 software (Latha & Jeevaratnam, 2010).

4.4 Results and discussion

4.4.1 Microfiltration process

Microfiltration is commonly used in the downstream processing of biotechnological products to eliminate microbial cells from fermentation broth. It is crucial to have a clear understanding of the cake structure as it has a substantial impact on the filtering behavior of the microbial cell cake that forms on the membrane's surface. This understanding plays a vital role in the design and operation of filter equipment and membranes (Katagiri et al., 2021). A microfiltration machine was employed to extract bacterial cells from fermentation broth, which contained dissolved contaminants such as proteins, polysaccharides, coloring compounds, and others. These substances contribute to another form of resistance known as "adsorption resistance, Ra," as they can adsorb onto the membrane wall, reducing permeation flux. The cleaning process was utilized to measure the resistance in series. The decline in permeate flow (J) was slower compared to that observed with pure water during the process. The cell elimination rate held significant importance in this experiment. The changing of flux was shown in Figure 4.2 *R. paludigena* CM33 culture

was transferred to cross- flow filtration system to be ready for the separation. Using a transmembrane pressure of 1 bar, a membrane with a surface area of 18 m² and a pore diameter of 0.1 μm was operated. The time taken was recorded after collecting 25 samples of the permeate. The flux of pure water was measured at a constant value of 100.72 L/m²/h. However, when switching from pure water to fermentation broth, a flow reduction characteristic was observed. The flux experienced a rapid decline in the first 346 seconds, followed by a gradual decrease until the completion of the experiment. The cells were collected for further downstream oil extraction processing. Furthermore, a cleaning technique involving RO water and 1% NaOH was utilized for the machine. The recovered water flux of each cleaning step was monitored until it returned to the initial flux value.

4.4.1.1 Resistance analysis

The resistance-in-series model, which takes into account membrane resistance, adsorption resistance, and cake resistance, has been applied to describe the fouling mechanism in the membrane filtration process. This model is particularly applicable for analyzing the decline in flux during microfiltration of the current broth, which contains numerous macromolecules such as proteins, polysaccharides, and peptides (Juang et al., 2008). Figure 4.3 shows the linear relationship between 1/J and 1/P, indicating the validity of Eq. (2). The measurement of flow using pure water can be utilized to determine the membrane resistance, R_m. Water has a viscosity of 10^{-4} Pa·s. Figure 4.3 illustrates that as 1/P (Pa^{-1}) increased, 1/J (m²s/m³) also increased. The slope can be used to calculate the value of R_m, which is 1.4×10^{15} m^{-1}, with a correlation coefficient of 0.9971.

4.4.1.2 Fouling and cleaning of microfiltration system

The experimental results were presented in Table 4.3, showing the flux values of the fermentation broth. These values were used to create a graph illustrating the relationship between flux and time (Figure 4.4). Additionally, another graph was plotted to depict the relationship between flux and volume concentration ratio (Figure 4.5). Theoretically, when using dead-end filtration, the efficiency is expected to be lower over time due to the formation of a thicker cake layer above

the membrane. The flux of the samples decreased gradually over time, taking approximately 20 minutes to obtain 50 mL of filtrated sample. In contrast, cross-flow filtration is anticipated to have high efficiency initially, which then decreases steadily until reaching a constant level. Both membranes had an outer diameter of approximately 9 mm and featured a zirconia oxide active layer with a mean pore size of 0.23 mm. When a 5 wt.% yeast suspension was subjected to microfiltration using the smooth membrane, the steady flux of the permeate was attained at around 1000 s. In contrast, it took over 2000 s to achieve the steady flux using the stamped membrane (Stopka et al., 2001). In a previous study, microfiltration of beer yeast suspensions was conducted using stamped ceramic membranes (Stopka et al., 2001). Furthermore, previous research has focused on the accumulation of yeast cells on the membrane surface, the morphology of the resulting cake, and the microfiltration process (Valencia et al., 2022). Therefore, microfiltration of the *R. paludigena* CM33 fermentation broth enhances the efficiency of cell harvesting, and the harvested cells can be stored at -20°C for next experiments. On the other hand, cake formation increased and stabilized due to the reduction of cake thickness caused by the flowing phenomenon. However, in the case of 350 L of cross-flow filtration, it significantly deviated from the theoretical expectations. The low efficiency of cross-flow filtration was attributed to membrane fouling. Both the percentage of cake formation and absorption emphasized the need for membrane cleaning and efficiency testing before industrial application. Additionally, there are numerous factors to consider when scaling up to an industrial scale. Typically, downstream processing presents fewer challenges compared to upstream processes, which involve solving multiple factors. Regarding water cleaning, the permeate flow rate was 1,230.22 L/h. The regained flux after water washing was measured as 68.40 L/m²/h, while after 1% NaOH washing, it increased to 80.00 L/m²/h. This corresponds to a percentage of absorption of 12.62% and a percentage of cake formation of 85.38%. The retained cells accumulated on the membrane surface, forming a growing cake layer. The thickness of the cake layer increased, resulting in an elevated resistance to the permeate flow.
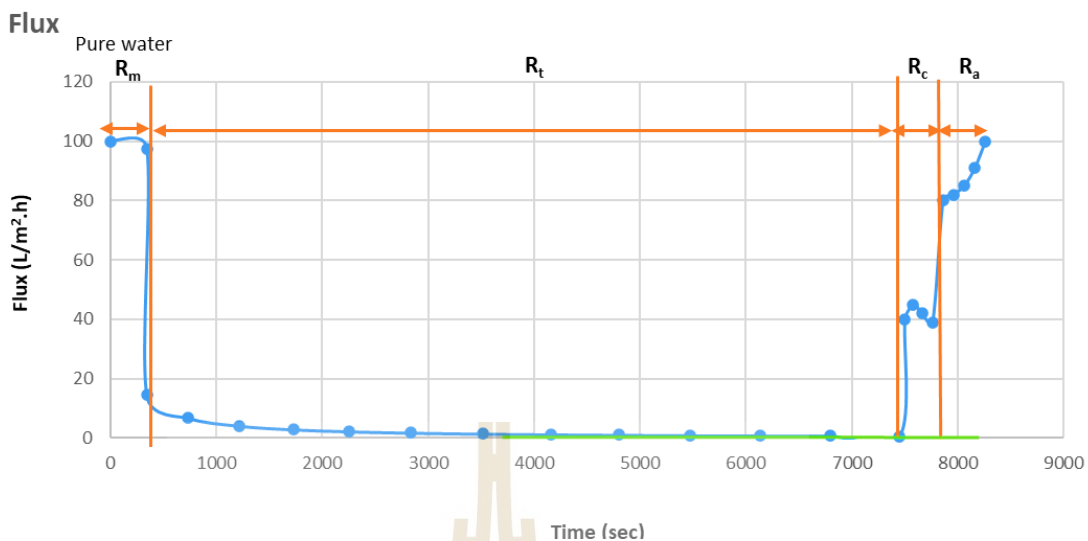
Figure 4.2 The change in flux was observed by employing the cleaning method in the cross-flow filtration system, which utilized a membrane with a surface area of 18 m², a pore diameter of 0.1 μm, and a transmembrane pressure of 1 bar.
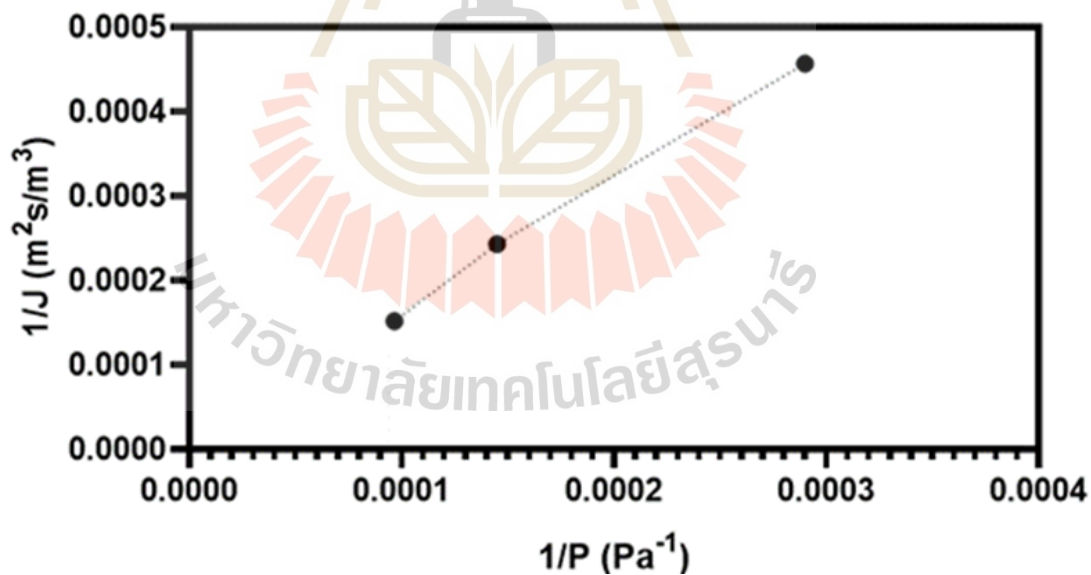
Figure 4.3 Relationship between 1/J Vs 1/P of water.

Table 4.3 Flux and volume concentration ratio of cross-flow filtration.

Volume per time	Permeate volume (L)	Time (min)	Time (s)	Time (h)	Delta time	membrane area (m^2)	Flux	volume concentration ratio (VCR)
				0			80	
25	25	5	46	0.10	0.10	18	14.45	1.08
25	50	12	12	0.20	0.11		6.83	1.17
25	75	20	11	0.34	0.13		4.13	1.27
25	100	28	50	0.48	0.14		2.89	1.40
25	125	37	30	0.63	0.14		2.22	1.56
25	150	47	20	0.79	0.16		1.76	1.75
25	175	58	41	0.98	0.19		1.42	2.00
25	200	69	20	1.16	0.18		1.20	2.33
25	225	80	5	1.33	0.18		1.04	2.80
25	250	91	14	1.52	0.19		0.91	3.50
25	275	102	12	1.70	0.18		0.82	4.67
25	300	113	15	1.89	0.18		0.74	7.00
25	325	124	11	2.07	0.18		0.67	14.00
Washing with H$_2$O				3.07	1.00		68.4	
washing with NaOH				4.07	1.00		80	
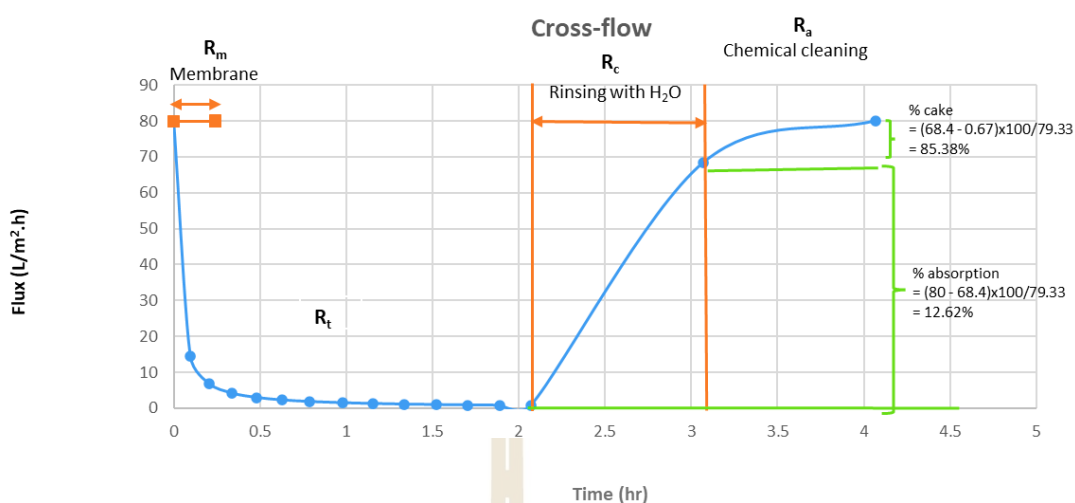
Figure 4.4 Time course of flux in cross-flow filtration, presenting the filtration of *R. paludigena* CM33 broth at 1 bar with a pore diameter of 0.1 μm.
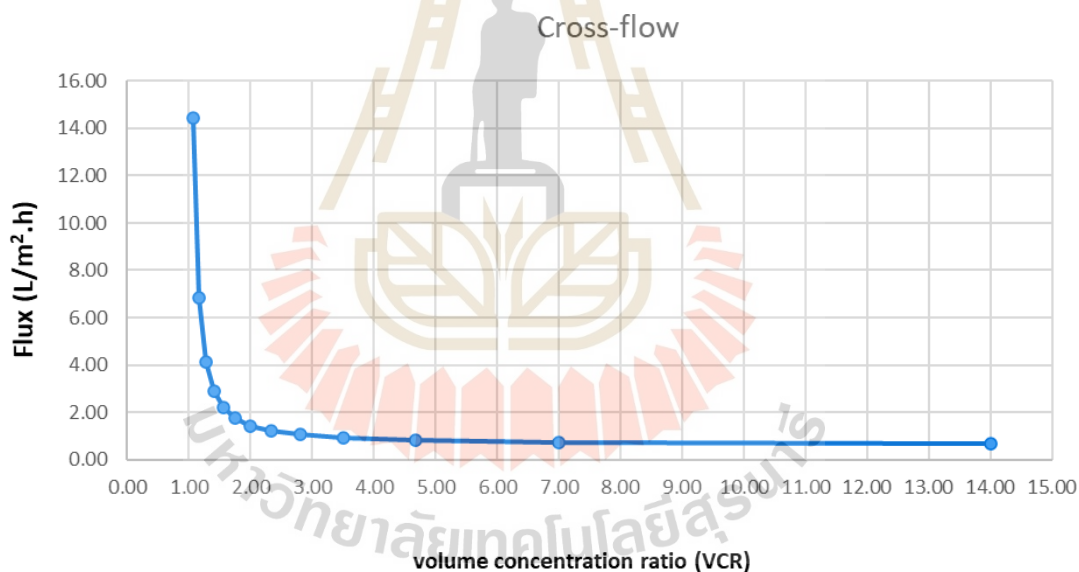
Figure 4.5 Time course of volume concentration ratio in crossflow filtration.

4.4.2 Effects of HPH condition on the concentration of carotenoids in *R. paludigena* CM33

The High-Pressure Homogenizer (HPH) method is used for cell disruption to break down the cell wall. In order to utilize the HPH method, three homogenization cycles were conducted at a homogenization pressure of 80 MPa and a bacterial liquid concentration of 8% (Liu et al., 2019). Therefore, the main factors considered as

independent variables in this study were pressure (X_1), feed (X_2), and passes (X_3). These factors were selected for optimizing the cell disruption and carotenoid production. The combined effect of three independent variables on cell disruption and carotenoids concentration was determined using Box-Behnken Design of Response Surface Methodology (RSM). The results were analyzed using the Analysis of variance (ANOVA) shown in Table 4.4. From Table 4.4, it can be observed that X_1, X_2, and X_3 have positive effects on the resulting responses ($P<0.05$). The Model F-value of 9.31 for carotenoid implies confirms that the model is extremely significant, with a P-value less than 0.05. The lack of insignificance in the lack of fit test indicated the accuracy of the model in predicting carotenoids production. The model successfully predicted the variance occurrence in the test and fitted to the experimental data, as indicated by the obtained P-value of < 0.05. The coefficient of determination was $R^2 = 0.9437$ for carotenoid. The adjusted R-Squared was 0.8424 for carotenoids (Table 4.4). The collected data were subjected to linear regression analysis using Design Expert software 13, and a quadratic polynomial model was used to express the relationship between the variables. The model was expressed in Eq. (4.9), when Y are carotenoids, whereas X_1, X_2, and X_3 represent the variables of pressure, %feed, and passes respectively.

Y carotenoid = 2031.55 + 0.19 pressure + 102.44 feed − 753.69 passes − 0.004 pressure * feed − 0.01 pressure * passes − 16.37 feed * passes − 1.40 pressure^2 + 9.70 feed^2 + 87.17 passes^2 (4.9)

The regression equation of significant parameters on carotenoids concentration was graphically represented in RSM contour plots and 3D surface plots generated by Design Expert Software 13. The relationship and effected between different significant variables on carotenoids concentration were shown in Figure 4.6A-B. The contour and 3D surface graphs were plotted with combination of parameters and a fixed passes concentration, while the remaining parameters were kept constant at the maximum level. Figure 4.6 (A-B) shows that the maximum carotenoids concentration was observed in the contours and 3D surface when the pressure and %feed concentration was in the middle range. The optimized parameters predicted by RSM were 30,000 psi of pressure, 5% of feed and 4 of passes (Figure 4.6C). The

carotenoids concentration obtained from the experiment were found to be close the predicated value. Similar results the yeast strain GYB40-10s utilized HPH with a pressure of up to 100 MPa to enhance energy yield (Ekpeni et al., 2015). In addition, the extraction of β-glucan from Saccharomyces cerevisiae cells was enhanced through autolysis using HPH treatment (200 - 600 bar, 3 passes) (Dimopoulos et al., 2020). Furthermore, the efficiency of cell disruption technology for oil recovery from *Yarrowia lipolytica* yeast using HPH was investigated (Drévillon et al., 2019). The results indicate that condition is a useful approach for optimizing cell disruption and increasing carotenoid extraction with HPH in *R. paludigena* CM33. Therefore, these results from RSM, with a pressure of 30,000 psi, a feed concentration of 5%, and 4 passes, can be applied for the carotenoid purification experiment.

Table 4.4 Analysis of variance (ANOVA) and Significance level of the Response Surface Linear model exhibiting carotenoid concentration.

Source	Sum of squares	Degree of freedom	Mean square	F-value	p-value	
Carotenoid concentration (ug/L)						
Model	3762000	9	418000	9.31	0.0121	significant
A	281300	1	281300	6.27	0.0542	significant
B	655200	1	655200	14.60	0.0124	significant
C	300000	1	330000	7.35	0.0422	significant
Residual	224400	5	44871.32	–	–	
Lack of Fit	159800	3	53251.32	1.65	0.3992	not significant
Prue Error	64617.66	2	32308.83	–	–	
Cor Total	3986000	14	–	–	–	
R^2 = 0.9437; R^2_{adj} = 0.8424						
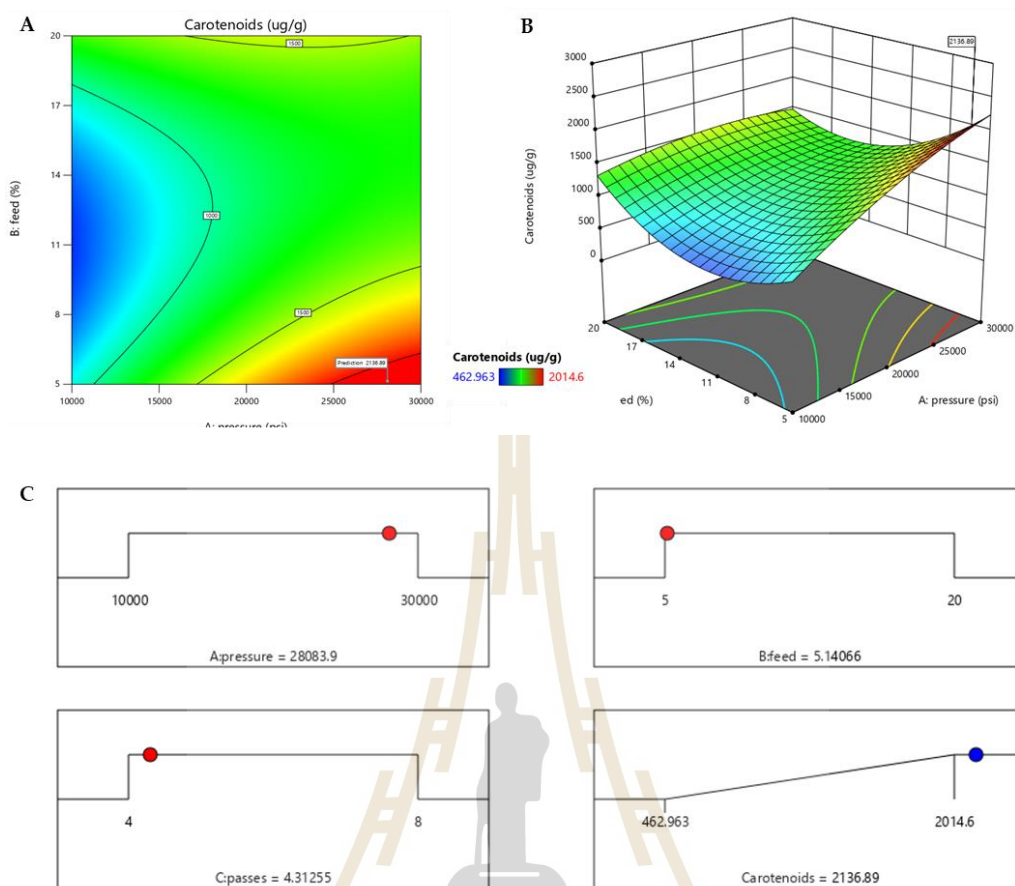
Figure 4.6 (A) The effect of different significant variables on the response surface contour plot was evaluated using Response Surface Methodology for carotenoids production.; (B) The RSM 3D surface plots obtained using Design-Expert software illustrate the effects of different significant variables on carotenoids production by *R. paludigena* CM33 (C) The optimized parameters predicted by RSM were 30,000 psi pressure, 4 passes, and a 5% feed of *R. paludigena* CM33 disruption cells.

4.4.3 Carotenoids Purification with HPH and Prep HPLC and carotenoids analysis by HPLC, LC-MS, and NMR

The carotenoids were purified using HPH and Prep HPLC, which are highly effective and scalable methods for cell disruption and compound separation. HPH is particularly advantageous, providing efficient disruption and release of intracellular components (Nemer et al., 2021), while Prep HPLC is a liquid chromatography

technique, it utilizes a preparative column with high loading and high resolution to achieve high-purity separation (Tong et al., 2015). HPH employed a pressure of 30,000 psi, underwent 4 passes, and utilized a 5% feed ratio to disrupt the resilient yeast cell walls effectively. This indicates that HPH caused complete cell disruption, as observed in the microscope images of cell disruption after the four passes, as shown in Figure 4.7 A-D, respectively. Multiple passes through a high-pressure homogenizer are typically performed on the samples to achieve the desired results (Nemer et al., 2021). Similar to a previous study, carotenoid extraction was conducted using HPH at a pressure of 80 MPa (11,603 psi) applied to an 8% biomass concentration and involving 3 passes of *Sporidiobolus pararoseus* cells (Liu et al., 2019). Furthermore, HPH was explored as a cell disruption method for the extraction of carotenoids from *Desmodesmus* sp. F51 (Xie et al., 2016). Furthermore, Optimal conditions for separating **β**-carotene using Prep HPLC were established by optimizing parameters, including the mobile phase system (methanol: acetonitrile: ethyl acetate) and a flow rate of 30 mL/min. The detection mode was set at 450 nm, 474 nm, 500 nm, and 515 nm. The characteristics of the compound samples after undergoing the Prep HPLC process are shown in Figure 4.8A-B. After subsequent analysis, it was determined that the observed compound corresponded to **β**-carotene, with a retention time of 4.90 minutes (Figure 4.9A-B). Following Prep HPLC, the compound was compared to a standard **β**-carotene (MilliporeSigma, USA) dissolved in methanol. The analytical HPLC analysis demonstrated excellent resolution for **β**-carotene, indicating a concentration of 12.76 mg/L and a purity of 94.80%, as compared to the retention time of the **β**-carotene standard at 7.53 min (Figure 4.9D). In addition, Both LC-MS and ^{1}H NMR analyses were utilized to determine the structure of the purified **β**-carotene compound. These analytical techniques serve as valuable tools for the characterization of carotenoids (Sivathanu & Palaniswamy, 2012). The LC-MS results displayed a molecular weight of 537.45 m/z for **β**-carotene, as shown in Figure 4.10A, which was comparable to the molecular weight of the **β**-carotene standard at 537.46 m/z. The ^{1}H NMR analysis was conducted using a Bruker 500 MHz instrument to confirm the **β**-carotene, as depicted in Figure 4.10B. The molecular structure of the **β**-carotene was successfully determined, as evidenced by the typical chromatogram pattern observed, indicative of **β**-carotene. The resonance at 5 ppm in the ^{1}H NMR spectrum corresponds to protons

on a double bond, while the resonance of protons attached to methyl groups is observed between 1 and 2 ppm (Wang et al., 2021). Additionally, the ^{1}H NMR spectra of β-carotene displayed resonances in the range of 1.5 to 2.5 ppm, which correspond to the protons attached to the ring (Figure 4.10B). The concentration of β-carotene pigment synthesized from *R. glutinis* 32 accounted for more than 80% of the total carotenoids (Bhosale & Gadre, 2001a, 2001b). The results indicate that both Prep HPLC and cooperative HPH are effective methods for separating carotenoids structures from *R. paludigena* CM33 cells. The confirmation of the purified compound as β-carotene was achieved through LC-MS and NMR analysis.
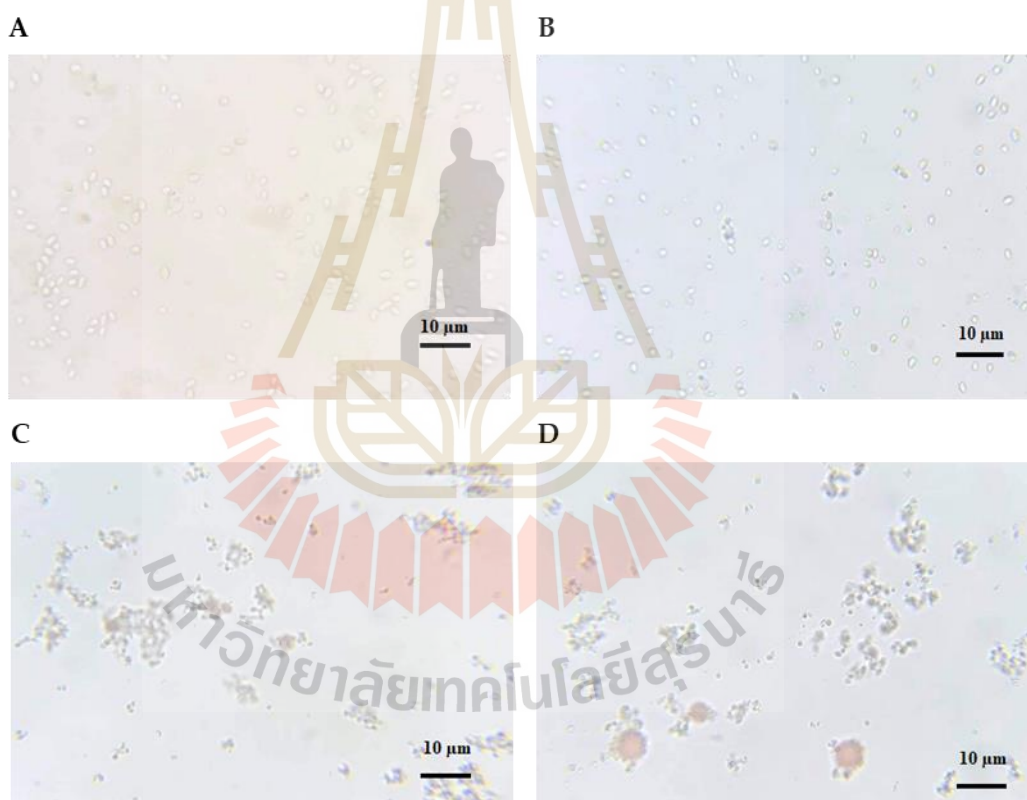
Figure 4.7 Microscopic images (A) after the first pass, (B) after the second pass, (C) after the third pass, and (D) after the fourth pass, all passes were used HPH at a pressure of 30,000 psi and a 5% feed cell concentration of *R. paludigena* CM33 cells.
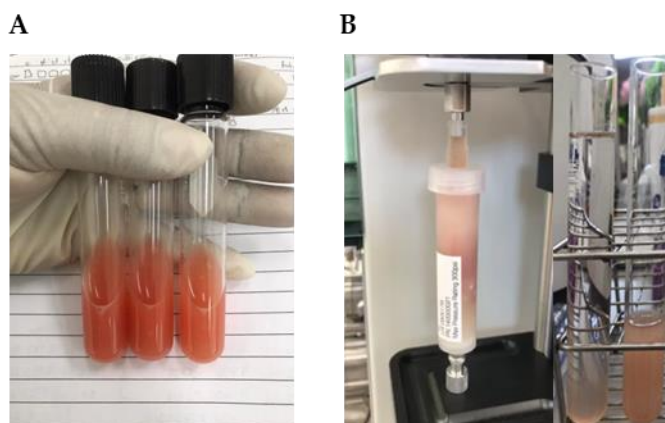
Figure 4.8 (A) *R. paludigena* CM33 samples after HPH treatment, and (B) The compound sample after Prep HPLC process.
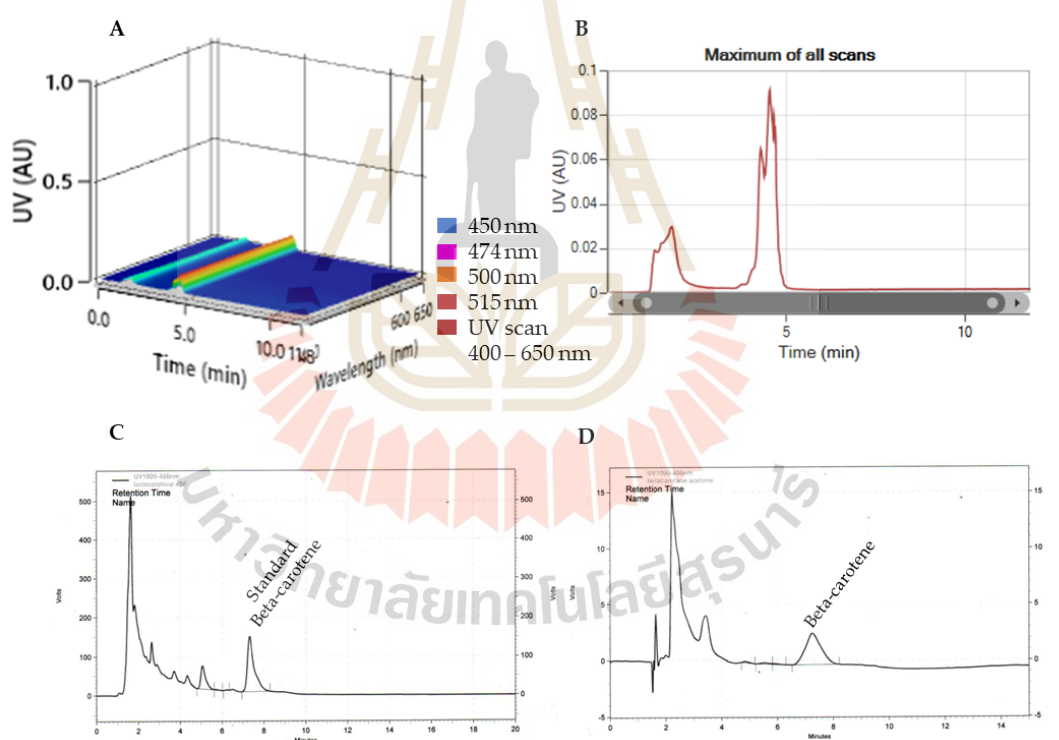
Figure 4.9 Preparative HPLC chromatogram of carotenoids from *R. paludigena* CM33; A) and B) β-carotene and HPLC chromatogram of purified β-carotene after preparative HPLC; C) standard β-carotene D) β-carotene sample after preparative HPLC was analyzed.
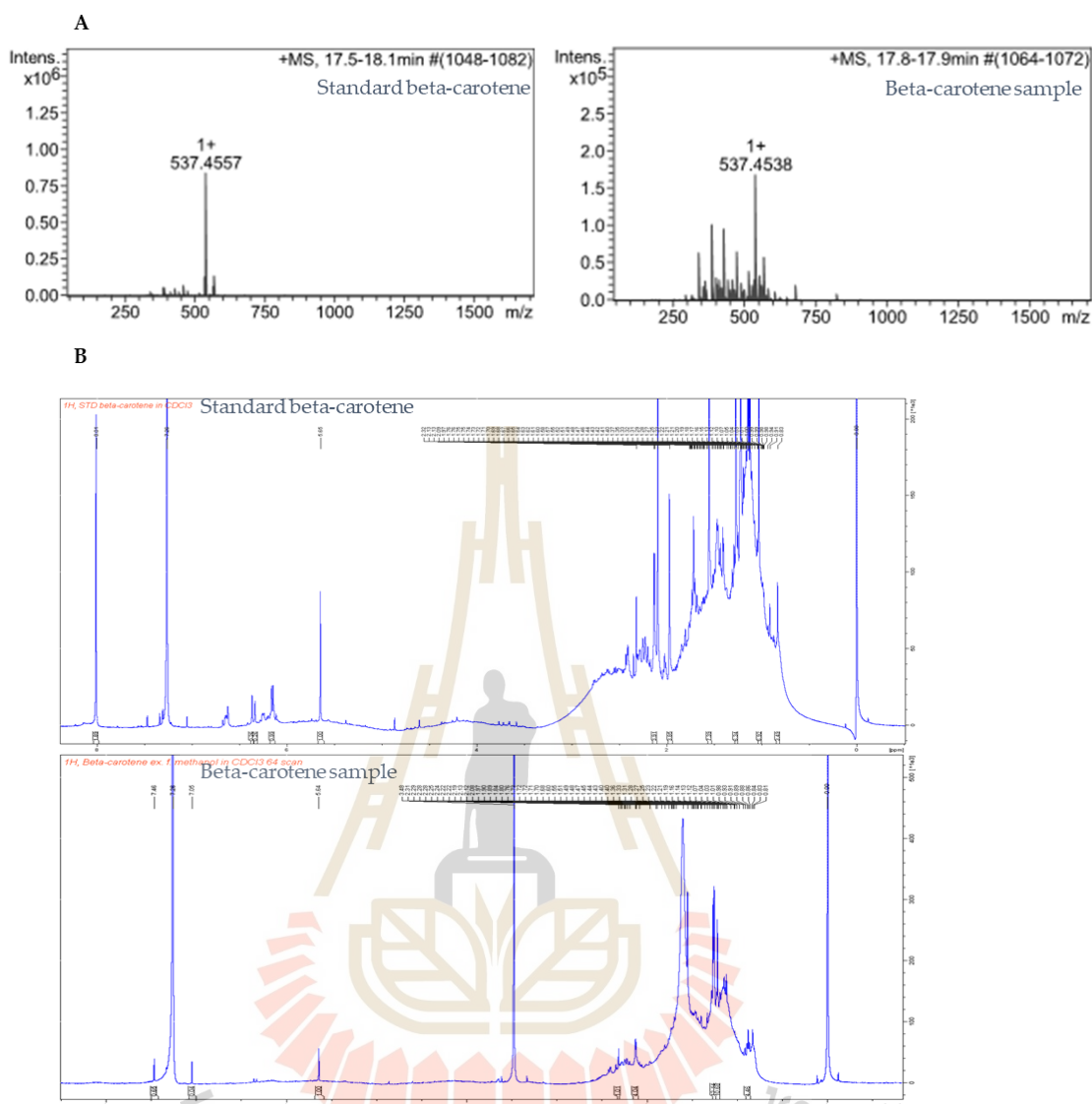
Figure 4.10 A) Mass spectrum of β-carotene standard and β-carotene sample and B) ¹H NMR spectrum of β-carotene standard and β-carotene sample.

4.5 Conclusion

In this study, an alternative method for yeast harvesting using membrane techniques was investigated. Microfiltration was employed to separate yeast from the fermented broth at the conclusion of a batch fermentation process. The study aimed to examine the factors influencing the performance of crossflow filtration. During the cleaning process, cells were cultivated and suspended in saline until a steady state was achieved. It was observed that when the circulation flow rate fell below a critical value, a portion of the crossflow filtration module's channel became blocked by the

cell cake, resulting in a low steady-state flux. In the case of crossflow filtration of yeast cell suspensions, the flux exhibited a gradual decline, and after 12 hours of filtration. Furthermore, this study investigated the use of high-pressure homogenization (HPH) for cell disruption to extract carotenoids. Response surface methodology (RSM) was successfully applied to enhance carotenoid production. The study revealed that using a pressure of 30,000 psi, a feed concentration of 5%, and performing 4 passes resulted in increased cell disruption and carotenoid production. Following preparative high-performance liquid chromatography (prep HPLC), the analysis using analytical HPLC demonstrated excellent resolution for β-carotene, with a concentration of 12.76 mg/L and a purity of 94.80%. The carotenoids identified in this study, primarily β-carotene, were confirmed through HPLC, LC-MS, and NMR analyses. These findings highlight the potential of microfiltration, high-pressure homogenization (HPH), and preparative HPLC in efficient the downstream processing of carotenoids in *R. paludigena* CM33.
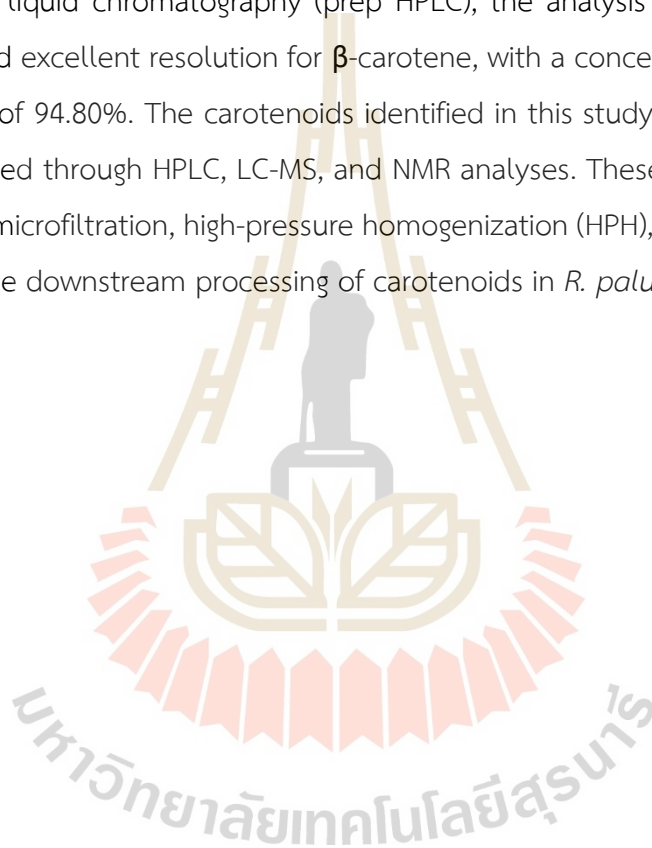
CHAPTER 5

INVESTIGATING THE PROBIOTIC PROPERTEIES OF *Rhodotorula paludigena* CM33 FOR WHITE SHRIMP

5.1 Abstract

Yeast is a health-promoting and bio-therapeutic probiotic that is commonly used in aquaculture. *Rhodotorula paludigena* CM33 can accumulate amounts of intracellular carotenoids and lipid, which are regarded as nutritionally beneficial compounds in various aspects. The aim of this study was to evaluate the impact of different levels of *R. paludigena* CM33 (RD) incorporated in a dietary composition at 0% (control), 1% (1% RD), 2% (2% RD), and 5% (5% RD) on the growth of shrimp (*Litopenaeus vannamei*), their immune-related gene expression, intestinal health, resistance to *Vibrio parahaemolyticus* (VP_{AHPND}) infection, and meat composition. The results showed significant improvements in the specific growth rate, weight gain, and survival of shrimp fed with 1% RD, 2% RD, and 5% RD, which were higher than the control group after 4 weeks of administration. The administration of 5% RD group resulted in a decrease in cumulative mortality upon VP_{AHPND} challenge when compared to the control group. Furthermore, the expression levels of immune-responsive genes, including proPO system (prophenoloxidase-2: PO2), antioxidant enzyme (superoxide dismutase: SOD, glutathione peroxidase: GPX, and catalase: CAT), JAK/STAT pathway (signal transducer and activator of transcription: STAT, gamma interferon inducible lysosomal thiol reductase: GILT), IMD pathway (inhibitor of nuclear factor kappa-B kinase subunit β and epsilon: IKKb and IKKe), and Toll pathway (Lysozyme) genes, were up-regulated in the 5% RD group. In the context of microbiota, microbiome analysis revealed that the main phyla in shrimp intestines were Proteobacteria, Firmicutes, Bacteroidota, Campilobacterota, Actinobacteriota, and Verrucomicrobiota. At the genus level, *Vibrio* was found to be reduced in the 5% RD group, whereas the abundance of

potentially beneficial bacteria *Bifidobacterium* was increased. The 5% RD group showed a significant increase in the levels of crude protein and crude lipid, both of which are essential nutritious components. Our results show the capability of *R. paludigena* CM33 as a probiotic supplement in shrimp feed in improving growth, antimicrobial responses against VP_{AHPND}, and meat quality by increasing protein and lipid content in shrimp.

5.2 Introduction

Carotenoids, natural pigments utilized in high-value industries such as cosmetics, pharmaceuticals, food supplements, and chemical industries, have drawn significant interest. The biochemistry of carotenoid synthesis has been extensively reviewed in previous studies. Pacific white shrimp (*L. vannamei*) is one of the most commonly farmed crustaceans with the majority of production takes place in Asia and Latin America. This shrimp is cultured worldwide because of its high commercial demand, rapid growth, and high nutritional value (Jin et al., 2018). The major markets are located in Japan, the United States of America, and the European Union (Food & Organization, 2020). For many years, the disease outbreaks have wounded a number of shrimp aquaculture industries, resulting in the considerable economic losses (Amaya et al., 2007; Jin et al., 2018). One of the approaches being harnessed to deal with these complications is the use of antibiotics. Nevertheless, this practice has led to several opposing impacts on environments due to the remnants of these compounds (Thuy et al., 2011). Hence, probiotics have become an emphasized choice in the aquaculture industry as an alternative strategy for managing aquatic diseases (Ninawe & Selvin, 2009).

The positive effects on the gut of an animal are brought about by live microorganisms known as probiotics, which can improve health profiles in the host and prevent diseases (Knipe et al., 2021). Numeral probiotics have been revealed to possess beneficial effects to their host for instance, the enhancing immune statuses are perceived from receiving prebiotics or probiotics, which are able to improve maturation, immune response, and resistance to diseases (Chien & Shiau, 2005; Jin et al., 2018; Ju et al., 2011). Many studies have developed approaches to increasing the amounts of probiotic strains, such as *Bifidobacteria* and *Lactobacilli*, which can be

given as supplements capable of changing the gut microbiota in mammals (Jaskari et al., 1998; Jayachandran et al., 2018; Snart et al., 2006). *Lactobacillus plantarum* and *L. pentosus* have been found to produce antimicrobial compounds such as hydrogen peroxide, and bacteriocins, which could hinder the proliferation of pathogens (De Vuyst & Leroy, 2007). Currently, common eukaryotic probiotics, such as yeasts, are used to improve animal and human health. In the context of aquaculture, *Bacillus* and yeast species are generally utilized as probiotics in aquaculture (Nimrat et al., 2021). For instance, the body composition and growth performance of shrimp can be affected by dietary supplementation of 0.1% *Bacillus licheniformis* and 0.5% *Rhodotorula mucilaginosa* (Chen et al., 2020). They are thus compelling choices to be employed to replace antibiotic usages in animal farming.

The pigmented yeasts belonging in *Rhodotorula* genus have been acknowledged to be good sources of carotenoids (Wang et al., 2019b). *Rhodotorula* sp. can synthesize various forms of commercially important carotenoids, including β-carotene, astaxanthin, torularhodin, and torulene (Frengova & Beshkova, 2009). These molecules such as β-carotene and astaxanthin can influence the gene expression, antioxidant capacity, and growth performance in shrimp (Niu et al., 2014). Furthermore, these red yeasts have been identified in shrimp and in their culturing environments such as *R. paludigenum*, *R. toruloides*, and found to accumulate carotenoid pigments (Yang et al., 2011). These yeasts are thus compelling choices to be implemented as probiotic supplementation in marine animals. *R. paludigena* CM33 is one of *Rhodotorula* strains, which has been studied on its capability to produce bio-oils and biochar through pyrolysis process (Poopisut et al., 2023). Furthermore, its spray-dried form and the oils extracted from this yeast displayed vivid red color, which could refer to the high carotenoid contents accumulated within *R. paludigena* CM33 (Poopisut et al., 2023). However, no information on the effect of *R. paludigena* on growth, disease resistance and immunity intestinal health in shrimp was available despite to the fact this finding could provide guidance for harnessing this nutritious microorganism in shrimp production. Nevertheless, this yeast had yet to be studied whether it could be beneficial in shrimp or not. Therefore, this study focused on the advantage of *R. paludigena* CM33 as a potential probiotic supplement in shrimp feed with the aims of revealing its effects on the growth of shrimp, immune-related gene expression, disease

resistance, intestinal microbiota, body composition, and meat quality in *L. vannamei*. This study presents a fascinating chance to evaluate its potential as a probiotic in shrimp and provides a solid support towards its capability as a probiotic supplementation in an attempt to prevent the use of antibiotics in shrimp farming.

5.3 Materials and methods

5.3.1 Ethics statement

The animal study was conducted in accordance with animal use protocol number SUT-IACUC-66-04 and was approved by the Suranaree University of Technology Animal Care and Use Committee. Additionally, the study's biosecurity concerns were reviewed and approved by Suranaree University of Technology with approval number SUT-IBC-66-02.

5.3.2 Animals

Before the feeding trial, healthy *L. vannamei* shrimp weighing 2-3 g were obtained from a shrimp farm located in Chachoengsao Province, Thailand. The shrimp were acclimatized in rearing tanks with constant aeration, water with a salinity of 20-ppt, and an ambient temperature of 28±2°C, and were fed with commercial feed prior to use in the experiments.

5.3.3 Probiotic preparation and experimental diet preparation

The oleaginous yeast *R. paludigena* CM33, which had been isolated by our laboratory, was cultured according to Poopisut et al. (Poopisut et al., 2023). Briefly, the microorganisms were cultured on yeast peptone dextrose (YPD) medium containing 20 g/L glucose, 10 g/L yeast extract, and 10 g/L peptone (Poopisut et al., 2023) at 30°C for 2 days. The cells were transferred to a 500-L fermenter containing 350 L of culture medium (40 g/L crude glycerol, 0.20 g/L KH_2PO_4, 0.55 g/L yeast extract, 1.0 g/L $MgSO_4 \cdot 7H_2O$, and 0.25 g/L $(NH_4)_2SO_4$). The fermenter was incubated at 30°C with an aeration rate of 0.1 vvm for 7 days. The yeast cells were harvested with a 200-L evaporator for 4 hours at 65°C. The cells were freeze dried (Freeze dry, Christ/Gamma2-16, Osterode am Harz, Germany) (Holmgren, 2014) and stored at a temperature of -20°C until utilized. The lyophilized *R. paludigena* CM33 (RD) were subjected to

determining its contents including protein, lipid, ash, and moisture via proximate analysis and the carotenoid substances were analyzed, which are shown in Table 5.1.

Four different diets were formulated by supplementing shrimp feed with RD. The commercial shrimp feed (9092L, Charoen Pokphand Foods, Thailand) consisting of 36% protein, 4% fat, 5% ash, and 12% moisture was used. Supplementations including 0%, 1%, 2%, and 5% (w/w) RD solid weight were supplied on shrimp pellets, which were designated as the control, 1% RD, 2% RD, and 5% RD groups, respectively, and coated with 1% (w/w) alpha starch. The formulated feeds were dried in a hot air oven at a temperature of 60°C for 8 h or until completely dried. After drying, yeast viability was assessed every 7 days by plating on YPD and calculated from three replicates as $CFU.g^{-1}$ as shown in Table 5.2 and stored at a temperature of -20°C until utilized.

Table 5.1 Proximate compositions of *R. paludigena* CM33.

Parameters	*R. paludigena* CM33
	Freeze-dried cells
Moisture (g/100g)	10.71±0.07
Protein (g/100g)	13.82±0.04
Total fat (g/100g)	43.21±0.66
Total carbohydrate (g/100g)	30.93±0.95
Ash (g/100g)	2.97±0.00
Crude fiber (g/100g)	0.21±0.02
Energy (Kcal/100g)	567.87±2.46
Carotenoids (mg/g)	15.39±0.04
β-carotene (mg/g)	10.16±0.08
Torulene (mg/g)	3.25±0.01
Astaxanthin (mg/g)	Not Detected
Other	0.86±0.00

Table 5.2 Total plate count of freeze drying and spray drying at different temperature stores.

Types	Conditions	Temperature	Yeast viability ($\log_{10}$ CFU.mL^{-1}) during storage (weeks)							
			1	2	3	4	5	6	7	8
Freeze drying	1%	Room temp.	5.71±0.27	5.35±0.85	5.77±0.41	5.75±0.72	5.80±0.80	5.07±0.01	5.05±0.01	4.75±0.01
		4 ℃	5.50±0.01	5.50±0.95	5.50±0.36	5.38±0.40	5.35±0.81	5.19±0.01	5.09±0.01	4.80±1.02
		-20 ℃	5.54±0.31	5.80±0.50	6.15±0.84	6.00±1.15	6.05±0.07	5.91±0.01	5.91±0.01	5.58±0.01
	2%	Room temp.	5.64±1.17	6.17±1.31	6.24±1.71	6.23±1.69	6.30±1.86	5.34±1.61	5.34±1.65	5.21±1.52
		4 ℃	5.15±1.52	5.29±1.82	5.26±1.81	5.30±1.75	5.33±1.77	5.31±1.59	5.34±1.62	5.21±1.47
		-20 ℃	6.11±1.69	6.27±1.92	6.22±1.43	6.19±1.77	6.23±1.74	5.85±2.00	5.87±2.03	5.19±1.99
	5%	Room temp.	6.72±2.29	6.59±2.37	6.64±2.56	6.88±2.99	6.83±2.77	6.23±0.01	6.12±0.01	5.90±0.01
		4 ℃	6.74±1.68	6.71±1.80	6.64±2.15	6.86±2.13	6.88±2.31	6.26±0.01	6.27±0.01	6.23±1.87
		-20 ℃	6.61±1.67	6.75±1.60	6.32±1.60	6.68±2.43	6.72±2.50	6.27±1.28	6.23±1.46	6.09±0.01
Spray drying	1%	Room temp.	3.61±1.59	3.82±1.04	4.07±0.79	4.01±0.86	3.91±1.17	3.98±1.42	3.95±1.52	3.19±0.01
		4 ℃	2.79±2.26	3.35±1.60	3.96±0.93	3.32±1.66	3.39±1.76	3.22±0.01	3.22±1.45	3.19±0.05
		-20 ℃	3.50±2.63	3.88±1.11	4.31±1.24	4.64±0.35	4.64±0.32	4.53±0.33	4.43±0.44	3.98±0.08
	2%	Room temp.	2.65±1.06	2.52±1.15	2.75±0.56	2.95±1.15	3.05±0.96	3.43±0.01	3.05±1.15	3.22±0.02
		4 ℃	3.35±1.11	2.35±0.93	2.82±1.80	2.75±1.06	3.16±1.62	3.12±0.02	2.65±0.55	3.19±0.02
		-20 ℃	2.82±0.41	2.75±1.50	2.65±1.41	2.89±0.01	3.09±1.41	2.65±0.01	2.52±0.67	2.05±0.03
	5%	Room temp.	3.18±0.99	2.82±1.33	4.12±0.24	3.18±1.62	4.19±0.32	3.04±1.15	3.09±0.02	3.22±0.01
		4 ℃	3.60±0.41	3.55±0.36	3.77±0.36	3.95±0.04	3.90±0.03	3.13±0.59	3.12±0.01	3.22±0.02
		-20 ℃	3.49±1.41	3.39±0.55	3.46±0.42	3.64±0.31	3.83±0.11	3.57±0.59	3.52±0.02	3.00±0.03

All experiments were performed in three replications (CFU = colony forming unit).

5.3.4 Growth performance analysis

To analyze growth performance, 100 shrimp were distributed into four tanks containing 300 L of water with 20-ppt salinity. The shrimp were fed with an amount of feed equivalent to 5% of their average body weight for four weeks. Before the first feeding, the feed intake, and mortality were monitored. The shrimp growth parameters were calculated from the weight gain (WG, g), specific growth rate (SGR, %.day^{-1}), survival rate (SR, %), average daily gain (ADG, g), and food conversion ratio (FCR) (Zheng et al., 2021) as follows:

$$\text{Weight gain (WG, g)} = \frac{\text{final weight} - \text{initial weight}}{\text{day}} \quad (5.1)$$

$$\text{Average daily gain (ADG, g)} = \frac{\text{final weight} - \text{initial weight}}{\text{experimental duration (day)}} \quad (5.2)$$

$$\text{Specific growth rate (SGR, \%day}^{-1}) = \frac{(\ln(\text{final weight}) - \ln(\text{initial weight}))}{\text{day}} \times 100 \quad (5.3)$$

$$\text{Survival rate (SR, \%)} = \frac{\text{Final amount of shrimp}}{\text{Initial amount of shrimp}} \times 100 \quad (5.4)$$

$$\text{Food conversion ratio (FCR)} = \text{Dried weight of feed fed} - \text{Wet weight gain of shrimp} \quad (5.5)$$

To examine the colonization of RD during feeding, nine shrimp of each treatment were independently cultured apart from the other experiments. The intestines were collected every 7 days and dotted them on YPD agar. The yeast viability in shrimp intestine was calculated from three replications and expressed as CFU.mL^{-1}.

5.3.5 Field emission scanning electron microscope (FE–SEM) analysis of shrimp intestines

The colonization of RD in shrimp intestine was observed in each treatment (0%, 1%, 2%, and 5% RD). The intestinal tissue of nine shrimp was fixed with 5% glutaraldehyde in 200 mM monobasic sodium phosphate and 200 mM dibasic sodium phosphate for 24 h. After being cut longitudinally, the digestive tracts were displayed on a specimen stub prior to desiccation. They were coated with 20 μm of gold using an ion coater (MSR-1S, Vacuum Device., Japan) and then examined by field emission scanning electron microscope (FE-SEM) (JEOL, JSM 7800F, Tokyo, Japan). The images were acquired at a nominal magnification of 5,000x using a 3.0 kV acceleration voltage in secondary electron (SE) mode (Adilah et al., 2022).

5.3.6 *Vibrio parahaemolyticus* (VP$_{AHPND}$) challenge

After feeding, shrimp were monitored for cumulative mortality upon VP$_{AHPND}$ challenge. The bacteria were incubated at 30°C and 220 rpm in tryptic soy broth (TSB) supplemented with 1.5% NaCl for culturing. The optical density (OD) at a wavelength of 600 nm (OD$_{600}$) was used to determine the bacterial concentration, which is an OD$_{600}$ of 2.0 is equivalent to 1×10^8 CFU.mL^{-1} (Boonchuen et al., 2018). Bacterial inoculant (final concentration: 1×10^6 CFU.ml^{-1}) was added to sample tanks containing 15 shrimps (LD$_{50}$ = 24 h). The challenges were divided into VP$_{AHPND}$ infection and non-VP$_{AHPND}$ infection, which both included the shrimp from control, 1% RD, 2% RD, and 5% RD. The cumulative mortality of shrimp was recorded every 12 hours for 120 hours.

At 24 hours post-inoculation, the hepatopancreas and stomach were collected from each group to determine the total *Vibrio* count. The collected specimens were serially diluted with sterilized 0.85% (w/v) NaCl, spread on Difco TCBS agar (BD), and incubated at 30°C for 14 hours. The resulting green colonies were counted and reported as colony-forming units (CFU.mL^{-1}) from three replications (n = 9).

5.3.7 Quantitative real-time PCR (qRT- PCR) analysis of immune gene expression

After 4 weeks of feeding trials, hemolymph was collected from nine shrimp of each treatment in the presence of an equal volume of MAS solution (27 mM sodium citrate, 115 mM glucose, 9 mM EDTA, 336 mM NaCl, pH 7.0) (Boonchuen et al., 2020). Hemocytes were harvested by centrifuging at 800 x g for 10 minutes at 4°C. The total RNA was extracted using a FavorPrep Tissue Total RNA mini kit (Favorgen) according to the manufacturer's protocol. RNA purity and quantity were determined by a Nanodrop 2000 Spectrophotometer (ThermoScientific) and agarose gel electrophoresis. The cDNA was synthesized using the iScript reverse transcription supermix for quantitative real-time PCR (qRT-PCR) (Bio-Rad) was used. The qRT-PCR amplification was performed using specific pair primers (Table 5.3) and 2x Luna Universal qPCR Master Mix (New England Biolabs) with the following conditions: 95°C for 3 min, 40 cycles of 95°C for 30 s, and 60°C (57°C for SOD) for 30 s. The relative expression was calculated from three replicates using $2^{-\Delta\Delta Ct}$ method with elongation factor-1 alpha (EF-1α) serving as the internal control gene (Livak & Schmittgen, 2001).

Table 5.3 The list primers used in this study.

Primer name	Sequence (5' to 3')	Annealing temperature (°C)
LvCatal-F	CCCTGATGGCTATCGTCA	60
LvCatal-R	TCAGCCTTCTTGCTGCTA	
LvGPX-F	TCGGCAAAGTCGACGTCAA	60
LvGPX-R	GCAGTCGCTCCTTCAGGTACTTA	
LvSOD-F	GCAGGTCGCCGTAGTAAG	57
LvSOD-R	AGTTCGCAAATGCAGCA	
LvHSP70-F	CTCCTGCGTGGGTGTGTT	60
LvHSP70-R	GCGGCGTCACCAATCAGA	
LvHSP90-F	TGGGCTTCTACTCCGCCTACC	60
LvHSP90-R	ACGGTGAAAGAGCCTCCAGCA	
LvPO-F	ACTGACCTGGAAATCTGGCG	60
LvPO-R	TCCTCCTTGTGAGCGTTGTC	
LvPO2-F	CCGTGAACAACTCCGGAAGA	60
LvPO2-R	CTGAGATTCGAGTCGGCCTC	
IMD-F	CGGCTCTGCGGTTCACAT	60
IMD-R	CCTCGACCTTGTCTCGTTCCT	
LvIKKb-F	ACCACACTTTCCACCTTTGG	60
LvIKKb-R	TCCCGATGAAGGAAGAACAC	
LvIKKe-F	TTGGCTTCTTTCCAGGACAC	60
LvIKKe-R	TTTTATGGCTGCCAGGAGTC	
LvMyD88-F1	GCTGTTCCACCGCCATTT	60
LvMyD88-R1	GCATCATAGTGCTGTAGTCCAAGA	
Dorsal-F	GATGGAATGATAGAATGGGAAGC	60
Dorsal-R	CACTGGTACTCTTGTCTGGTGGTC	
PEN4-F	ATATTTTCTTTCTTTCTTTCCCAGGG	60
PEN4-R	GTCCTCTGTGACAACAATCCCC	
LYZ-F	TACGCGACCGATTACTGGCTAC	60
LYZ-R	AGTCTTTGCTGCGACCACATTC	
STAT-F	TATATCCGAATGTGCCTA	60
STAR-R	ATAGTTTGTGGTGTGTTG	
GILT-F	TCCTTCACCTGCCAACA	60
GILT-R	CGAGAGAAGGCAGTTGA	
EF-1α-F	CGCAAGAGCGACAACTATGA	60
EF-1α-R	TGGCTTCAGGATACCAGTCT	

5.3.8 Enzymatic activities

Nine shrimp were randomly selected from the control and 5% RD groups to measure phenoloxidase (PO), catalase (CAT) activity, and superoxide dismutase (SOD). The determination of PO activity was carried out using the method described by Boonchuen et. al, (Boonchuen et al., 2022) with a spectrophotometer to record the formation of dopachrome converted from L-3,4-dihydroxyphenylalanine (L-DOPA; Fluka). The enzyme activity was measured by recording the absorbance at 490 nm after incubating the sample for 90 min and recorded as A490/mg total protein/min.

Superoxide dismutase (SOD) activity was determined by using the protocol reported by Beauchamp et al. (Beauchamp & Fridovich, 1971). Briefly, 3 mL of reaction mixture (13 µM methionine, 0.75 mM Nitro Blue Tetrazolium (NBT), and 20 µM riboflavin in 50 mM phosphate buffer at pH 7.8), and 100 µL of hemocyte were placed under fluorescent light for 1 min. The enzyme activity was measured with absorbance at 560 nm and calculated in units per mg protein.

Catalase (CAT) activity was examined based on catalase peroxidatic action by measuring the production of formaldehyde (Johansson & Borg, 1988). A standard curve was plotted using formaldehyde at concentrations of 5, 10, 15, 45, 60, and 75 µM in 25 mM KH_2PO_4, 0.1% bovine serine albumin, and 1 mM EDTA at pH 7.5. The samples were measured in a 96-well plate using 20 µL and 150 µL of the reaction mixture, which contained 66.7% 100 mM KH_2PO_4 at pH 7.0, 20% methanol, and 13.3% 4.2 mM H_2O_2. The samples were shaken for 20 min and then the reaction was stopped by adding 30 µL of 10 M KOH. Subsequently, 30 µL of chromagen; Purpald (4-amino-3-hydrazino-5-mercapto-1,2,4-triazole) (Sigma-Aldrich) was added. The mixture was then incubated at room temperature for 20 min. The reaction was oxidized with 10 µL of potassium periodate and incubated for 5 min, and the absorbance at 550 nm was measured. The activity was recorded as units per mg protein. Experiments were conducted in triplicate.

5.3.9 Microbiome analysis

After feeding trials for 2 and 4 weeks, genomic DNA was extracted from the intestines of twelve shrimp of each group; control and 5% RD, using a FavorPerp Stool DNA Isolation Mini Kit (Favorgen) by following the manufacturer's protocol. The DNA

integrity was evaluated by 1% agarose gel electrophoresis. The DNA concentration was determined by a NanoDrop 2000 Spectrophotometer (ThermoScientific). The V3-V4 region of 16S rRNA genes was amplified with the common primer pair (Forward primer, 5′-CCTACGGGNGGCWGCAG-3′; reverse primer, 5′-GGACTACHVGGGTWTCTAAT-3′). A total volume of 50 µL PCR components contained 10 µL buffer, 0.2 µL Q5 high-fidelity DNA polymerase, 10 µL high GC enhancer, 1 µL dNTP, 10 µM of each primer and 60 ng genome DNA. Thermal cycling conditions were as follows: an initial denaturation at 95 °C for 2 min, followed by 30 cycles at 95 °C for 40 s, 50 °C for 30 s and 72 °C for 1 min, with a final extension at 72 °C for 7 min. Finally, all PCR products were quantified by Qubit dsDNA HS Reagent and pooled together. High-throughput sequencing analysis of bacterial rRNA genes was performed on the purified, pooled sample using the Illumina Hiseq 2500 platform (2 × 250 paired ends) according to the standard protocols.

Quality filtering on the raw tags were performed using the fastp (Version 0.20.0) software to obtain high-quality clean tags. Paired-end reads were merged using FLASH (Version 1.2.11, http://ccb.jhu.edu/software/FLASH/) (Magoč and Salzberg, 2011). The clean tags were compared with the reference database (Silva database https://www.arbsilva.de/ for 16S/18S,Unite database https://unite.ut.ee/ for ITS) using Vsearch (Version 2.15.0) to detect chimera sequences, and then the chimera sequences were removed to obtain the effective tags (Haas et al., 2011). The high-quality effective tags were clustered into operational taxonomic units (OTUs) at 97% sequence identity by DADA2 or deblur module in the QIIME2 software (Version QIIME2-202006) and taxonomic annotation was carried out on OTUs based on the taxonomy databases (http://scikit-bio.org/docs/latest/generated/skbio.diversity.alpha. observed_otus.html), and the taxa relative abundances of community compositions in samples were identified at different taxonomic level (phylum, class, order, family, genus, and species) respectively and displayed with R software (Version 3.5.3).

Alpha diversity was applied in analyzing the complexity of species diversity for samples through 3 indices, including Chao1, Shannon, and Simpson. Unique species among groups were shown by Venn analysis. Beta diversity was calculated based on weighted UniFrac distances, visualized via principle coordinate analysis (PCoA) which was plotted in R software (Version 2.15.3), and MetaStat analysis was plotted in R software (Version 3.5.3) (Li et al., 2020).

5.3.10 Proximate and color analysis

The proximate compositions of shrimp meat, including moisture, protein, fat, and ash, were determined using nine shrimp for each parameter according to the method of the Association of Official Analytical Chemists (AOAC) (AOAC, 2000) The crude protein (N x 6.25) was analyzed by the Kjeldahl method using an Auto Kjeldahl System (Buchi 323, Distillation Unit, Flawil, switzerland). Moisture was determined by the air oven method. Aluminum moisture dishes were preheated for 30 min at 103 – 105°C and were cooled in a desiccator for 15 min. After cooling, the weights of the aluminum moisture dishes were taken, and approximately 5.0 g of the shrimp sample was weighed into dishes. The moisture dishes and contents were subjected to oven drying at a temperature of 103 – 105°C for 4 h after which they were removed and cooled in a desiccator for 15 min. Crude lipid was analyzed by via the petroleum ether extraction method using a Soxhlet extraction system. (OPSIS, SX360, Sweden) Ash was analyzed by incineration in a muffle furnace at 550 – 600°C for 3 h after which they were removed and cooled in a desiccator and expressed as % wet-weight basis. For color, both raw and cooked shrimp meat (boiled at 100°C for 7 min) (Niamnuy et al., 2007) were investigated by using a Hunter Lab test (Color Quest XE, Virginia, USA) with nine samples per group. The results were expressed as L* (lightness), a* (redness), and b* (yellowness) (Wachirasiri et al., 2017). The experiments were performed in triplicate.

5.3.11 Statistical analysis

Significant differences were established using a one-way analysis of variance (ANOVA) at the 5% level of probability, and differences between means were compared using Tukey's range test for growth performance, VP_{AHPND} challenge, gene expression, antioxidant enzyme activity, alpha diversity, proximate analysis, and color analysis. All results are presented as the mean ± standard deviation (SD). The survival percentage is displayed as the mean ± 1 standard error (S.E.) at each time point. The statistical analysis of the survival rate in each experiment group was done using the log-rank (Mantel-Cox) test (Bland & Altman, 2004). Statistical analysis was carried out in Minitab (Minitab version 19 Sydney, Australia) and GraphPad Software (GraphPad Software version 19 Massachusetts, USA) for Windows.

5.4 Results

5.4.1 Growth performance and colonization of RD in shrimp intestine

The effects of difference amount of *R. paludigena* CM33 in shrimp feed on the growth performance of *L. vannamei* were examined. The viable cell numbers of freeze-dried *R. paludigena* CM33 yeast were in the range of 2.82 to 6.88 log(CFU.mL^{-1}) (Table 5.2). After 4 weeks of feeding, significantly higher weight gain, ADG, SGR, and survival rate of shrimp fed 1% RD, 2% RD, and 5% RD were observed in comparison to the control group. The increases were around 1.25, 1.5, and 1.15-fold, respectively. FCR was lower by around 1.5-fold when compared to the control group.

Colonies of yeast microbes resembling *R. paludigena* CM33 were not detected in the intestine of the control group during the experiment. After feeding, the populations in the intestine of the 2% RD and 5% RD were in the range of 5.89±0.08x10^3 and 5.44±0.16x10^4 CFU.mL^1, respectively, which were significantly higher than those of 1% RD and the control group (Table 5.4). Intestinal morphological characteristics of shrimp were analyzed using FE–SEM. The internal surfaces of the 1% RD, 2% RD, and 5% RD groups showed yeast cell colonies in the upper microvilli of the midgut epithelium (Figure 5.1A-D).

Table 5.4 Growth performance of *L. vannamei* fed with the experimental different diets of *R. paludigena* CM33 for 4 weeks.

Parameters	Treatments			
	Control	1% RD	2% RD	5% RD
IBW (g)	3.00±0.50[a]	2.86±0.47[a]	2.59±0.43[a]	2.78±0.84[a]
FBW (g)	4.75±1.45[a]	5.08±0.75[a]	5.09±0.90[a]	5.13±1.13[a]
WG (g)	1.75±0.29[d]	2.22±0.12[c]	2.50±0.18[b]	2.35±0.05[a]
ADG (g)	0.06±0.01[c]	0.08±0.01[b]	0.09±0.01[a]	0.09±0.01[a]
SGR (%g.day^{-1})	8.00±1.07[d]	8.21±0.45[c]	9.25±0.67[a]	8.70±0.17[b]
FCR	2.40±0.42[a]	1.62±0.03[c]	1.45±0.09[d]	1.59±0.30[b]
Survival rate (%)	92.25±0.41[d]	95.73±0.76[b]	95.23±0.16[c]	97.50±0.35[a]
Total plate count	*R. paludigena* CM33 (CFU.mL^{-1})			
Day 0	n.d.	n.d.	n.d.	n.d.
Day 14	n.d.[d]	1.33±0.01x10^3 [c]	5.78±0.06x10^3 [b]	5.78±0.15x10^4 [a]
Day 28	n.d.[d]	1.44±0.01x10^3 [c]	5.89±0.08x10^3 [b]	5.44±0.16x10^4 [a]

All values were presented as the mean ± SD (n = 9). Means in the same row sharing different superscripts are significantly different ($P<0.05$) as determined by Tukey's range test. The experiment was conducted in three replications (n.d. = Not detected, CFU = colony forming unit, IBW = initial body weight, FBW = final body weight, WG = weight gain, ADG = average daily gain, SGR = specific growth rate, and FCR = food conversion ratio).
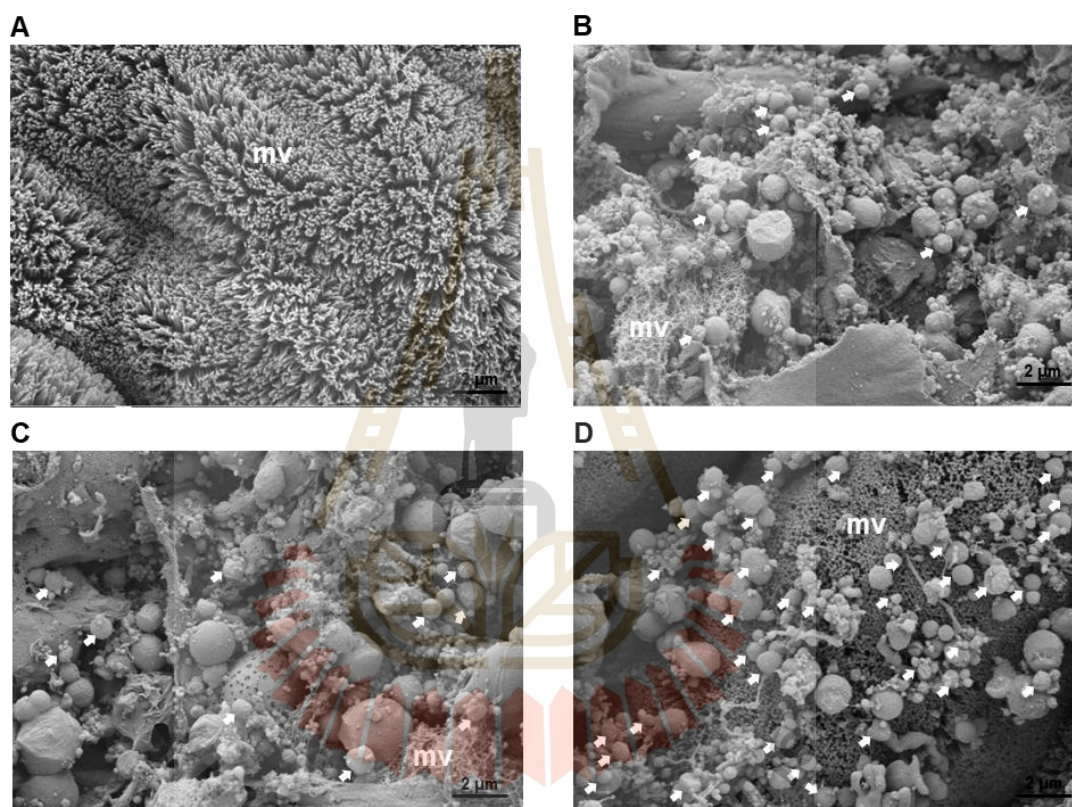
Figure 5.1 Field emission scanning electron microscope results of intestinal sections of *L. vannamei*. (A) Control, (B) 1% RD, (C) 2% RD, and (D) 5% RD. Yeast are visible in the intestines of 1% RD, 2% RD, and 5% RD groups (white arrow). The images (magnification x 5,000) demonstrate the findings of field emission scanning electron microscopy in secondary electron (SE) mode at an acceleration voltage of 3.0 kV. Scale bars represent 2 μm. Representative images from three replicates are shown (mv = microvilli).

5.4.2 The impact of RD feeding on cumulative mortality with VP$_{AHPND}$ infection

After feeding for 4 weeks, shrimp were challenged with VP$_{AHPND}$. Shrimp mortality was inspected at every 12 hours post infection (hpi). At 48 h, the survival rates of the control, 1% RD, and 2% RD groups were 0%, 6.67%, and 20%, respectively. 100% mortality of 1% RD, and 2% RD groups was observed at 72 and 96 hpi, respectively. In the 5% RD group, 40% survival was observed at 48 to 120 hpi, which was significantly higher than in the control, 1% RD, and 2% RD groups (Figure 5.2). To confirm the effect of RD supplementation on VP$_{AHPND}$ resistance, the numbers of *Vibrio* (CFU.mL^{-1}) in the hepatopancreas and stomach were observed, which were lower in all RD groups at 24 hpi (Figure 5.3). According to the significant reduction in shrimp mortality upon VP$_{AHPND}$ infection, the control and 5% RD group was used in further experiments to discern immune-related gene expression, the activity of antioxidant enzymes, and changes in intestinal microbiome.
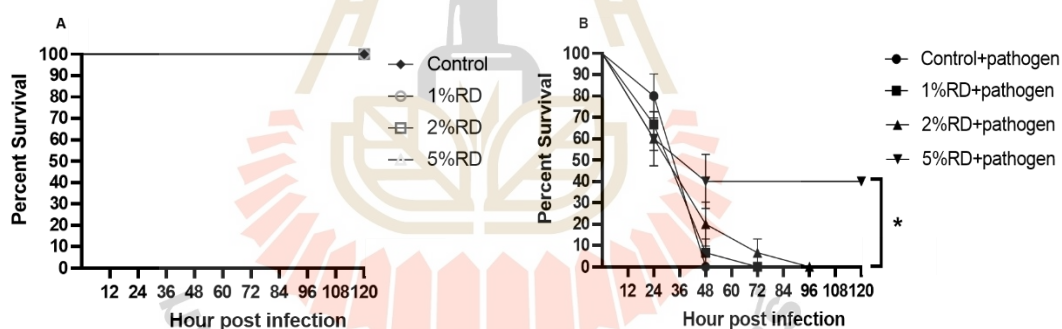
Figure 5.2 The effect of *R. paludigena* CM33 on shrimp mortality. VP$_{AHPND}$-infected shrimp were observed for 120 hpi. Shrimp were divided into eight groups of 15 each: (A) without VP$_{AHPND}$ infection: control (♦), 1% RD (○), 2% RD (□), and 5% RD (△) for 120 h; (B) with VP$_{AHPND}$ infection: control (●), 1% RD (■), 2% RD (▲), and 5% RD (▼). The survival percentage is displayed as mean ± 1 standard error (S.E.) at each time point. Asterisks indicate significant differences between data of each treatment (*P*<0.05).
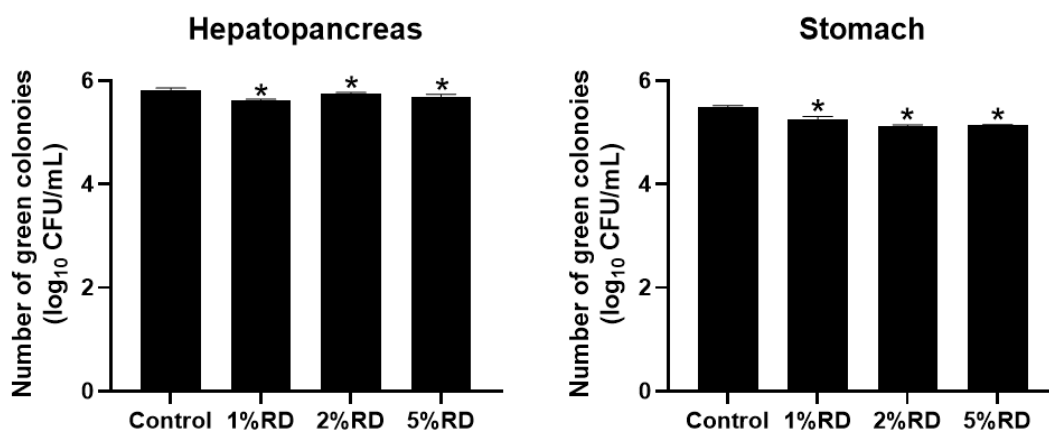
Figure 5.3 The effect of *R. paludigena* CM33 on shrimp mortality. Total *Vibrio* count in hepatopancreas and stomach was elucidated by spread plating on TCBS agar. The green colonies were counted as the total number of viable green colony forming units (CFUs). All experiments were performed in triplicate. Bars represent mean ± SD (n = 9).

5.4.3 Modulation of immune-related genes and antioxidant enzyme activity from dietary RD feeding.

Figure 5.4 and Figure 5.5 shows the results of gene expression analysis of immune-related andantioxidant genes, including Toll pathway (MyD88, Dorsal, and Lysozyme), IMD pathway (immune deficiency: IMD, inhibitor of nuclear factor kappa-B kinase subunit beta and epsilon: IKKb and IKKe), JAK/STAT pathway (signal transducer and activator of transcription: STAT and gamma interferon inducible lysosomal thiol reductase: GILT), Toll/IMD pathway (penaeidin-4: PEN4), antioxidant enzyme (superoxide dismutase: SOD, glutathione peroxidase: GPX, and catalase: CAT), and proPO system (prophenoloxidase-1: PO1 and prophenoloxidase-2: PO2) in hemolymph. The expression levels of PO2, SOD, GPX, CAT, STAT, GILT, IKKb, IKKe, and lysosome were significantly up-regulated by 2 to 8-fold in the 5% RD group in comparison with the control group, whereas the expression of PO1 showed no significant difference between the 5% RD and control groups (Figure 5.4). In the analysis of enzymatic, PO, SOD, and catalase activity, the 5% RD group displayed significantly higher results than the control group by about 4, 3, and 3-fold, respectively (Figure 5.5).
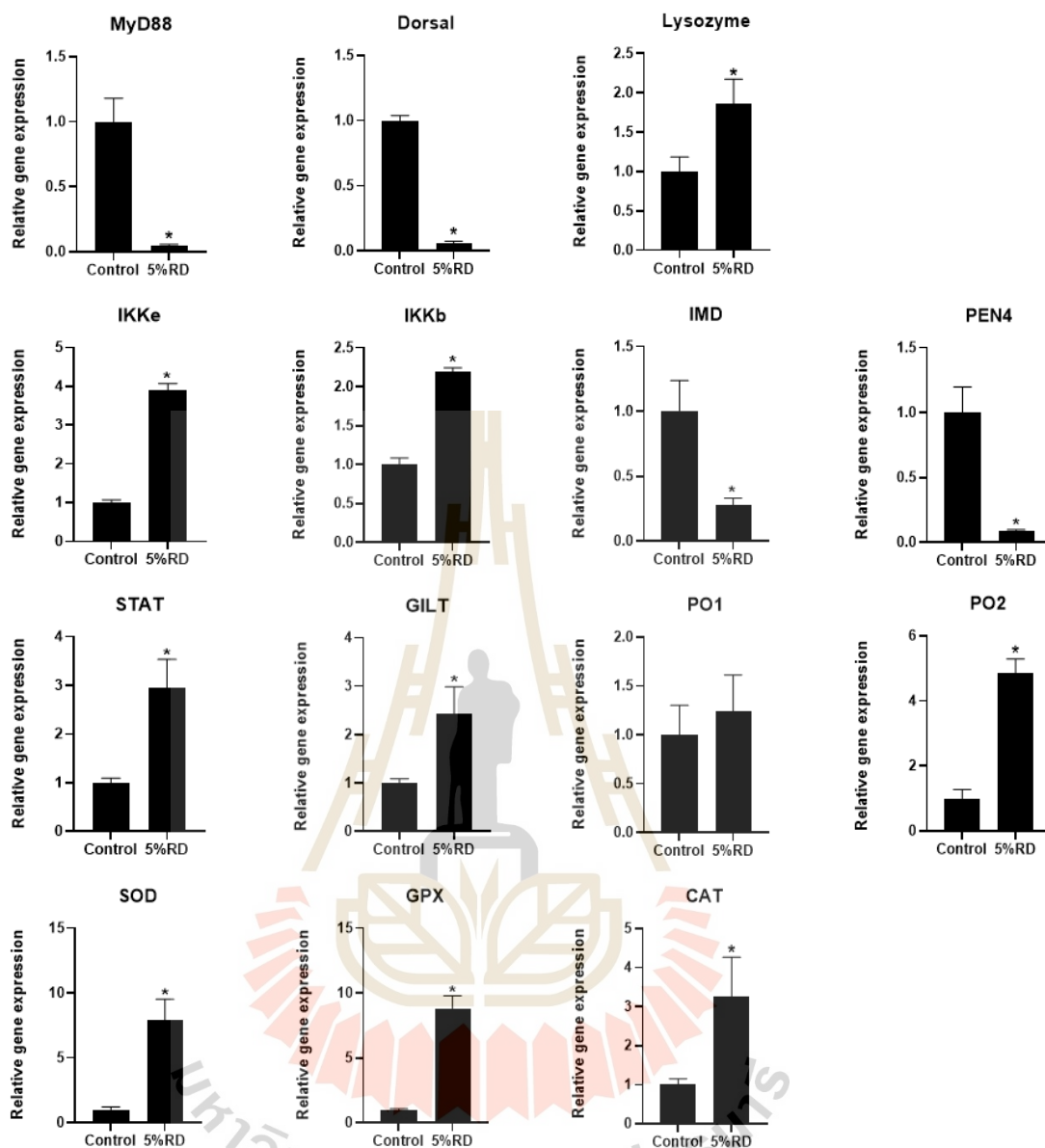
Figure 5.4 The effects of different experimental diets on *R. paludigena* CM33 and the gene expression effects in the hemocytes of *L. vannamei* were studied for 4 weeks. The expression profile of MyD88, Dorsal, lysozyme, IMD, IKKb, IKKe, PEN4, STAT, GILT, PO1, PO2, GPX, SOD, and CAT by qRT-PCR was normalized against EF-1 α. Triplicate replications (n = 9) were performed, and results are displayed as means ± SD. Asterisks indicate significant differences between data of each treatment (*P*<0.05).
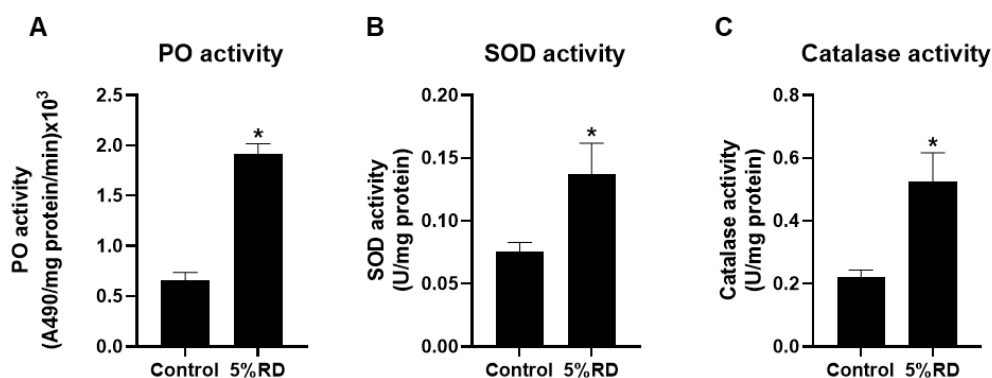
Figure 5.5 The effects of experimental different diets of *R. paludigena* CM33. PO activity (A), SOD activity (B), and catalase activity (C) effects in the hemocytes of *L. vannamei* for 4 weeks. PO activity was examined at 4 weeks of the different treatments, and the activity was measured as A490/mg total protein/min. SOD activity and catalase activity were examined at 4 weeks of the different treatments, and the activity was measured U/mg protein. Triplicate replications (n = 9) were performed, and results are displayed as means ± SD. Asterisks indicate significant differences between data of each treatment (*P*<0.05).

5.4.4 Intestinal microbiota in RD-fed shrimp

The OTU and alpha diversity data from the intestinal microbiota of *L. vannamei* are presented in Table 5.5 A total of 1,908,035 high-quality effective sequencing reads were obtained from 12 samples, ranging from 86,685 to 137,338. OTUs in the 5% RD1 (2 weeks) and 5% RD2 (4 weeks) groups were significantly higher than in the control group. The 5% RD1 and 5% RD2 treatment groups showed significantly improved Chao and Shannon estimator indices compared to the control group. In addition, the Simpson estimator index ranged between 0.77 and 0.96 (Table 5.5).

The relative taxa abundance of bacteria in *L. vannamei* intestine is shown in Figure 5.6. The main phyla in shrimp intestine among the six groups were Proteobacteria, Bacteroidota, Firmicutes, Actinobacteria, Campilobacterota, and Verrucomicobiota. At the genus level (Figure 5.6), *Motilimonas*, *Bifidobaterium*, *Rhodobacteraceae*, *Pseudoalteromonas*, and *Lactobacillius* were abundant in the 5%

RD1 (2weeks) and 5% RD2 (4 weeks) groups. Beta diversity was demonstrated by PCoA, which revealed discrete clustering of intestinal microbiota in shrimp between the 5% RD and control groups (Figure 5.7).

The two principal coordinates explained 72.39% of the differences. Bacteria communities from different diets along PC-2 were divided into two major clusters with a total of 27.57% variation (control and 5% RD). However, the boxplot obtained by MetaStat analysis revealed that *Vibrio* was significantly decreased in the 5% RD2 group when compared to the control (Figure 5.8A), while *Bifidobacterium* was significantly increased in the 5% RD2 group when compared to the control (Figure 5.8B).

Table 5.5 Effects of different diets on the diversity of intestinal microbiome in shrimp.

Treatments	Control 1 (2. weeks)	5% RD 1 (2. weeks)	Control 2 (4. weeks)	5% RD 2 (4. weeks)
Raw read	128,258	102,420	119,292	127,039
Clean read	119,737	90,572	112,868	122,381
Tags	119,568	87,226	110,789	120,858
OTU	337.00 ± 93.64^{b}	704.67 ± 151.44^{a}	433.00 ± 31.75^{b}	743.67 ± 100.50^{a}
Chao	330.09 ± 64.44^{b}	705.87 ± 152.19^{a}	437.92 ± 33.77^{b}	746.58 ± 99.81^{a}
Shannon	3.87 ± 1.34^{b}	6.67 ± 1.08^{a}	4.42 ± 0.67^{ab}	5.98 ± 0.21^{ab}
Simpson	0.77 ± 0.17^{a}	0.96 ± 0.02^{a}	0.84 ± 0.11^{a}	0.94 ± 0.02^{a}

All values were presented as the mean ± SD (n = 12). Means in the same row sharing different superscripts were significantly different ($P<0.05$) as determined by Tukey's range test. All experiments were performed in quadruplicate.
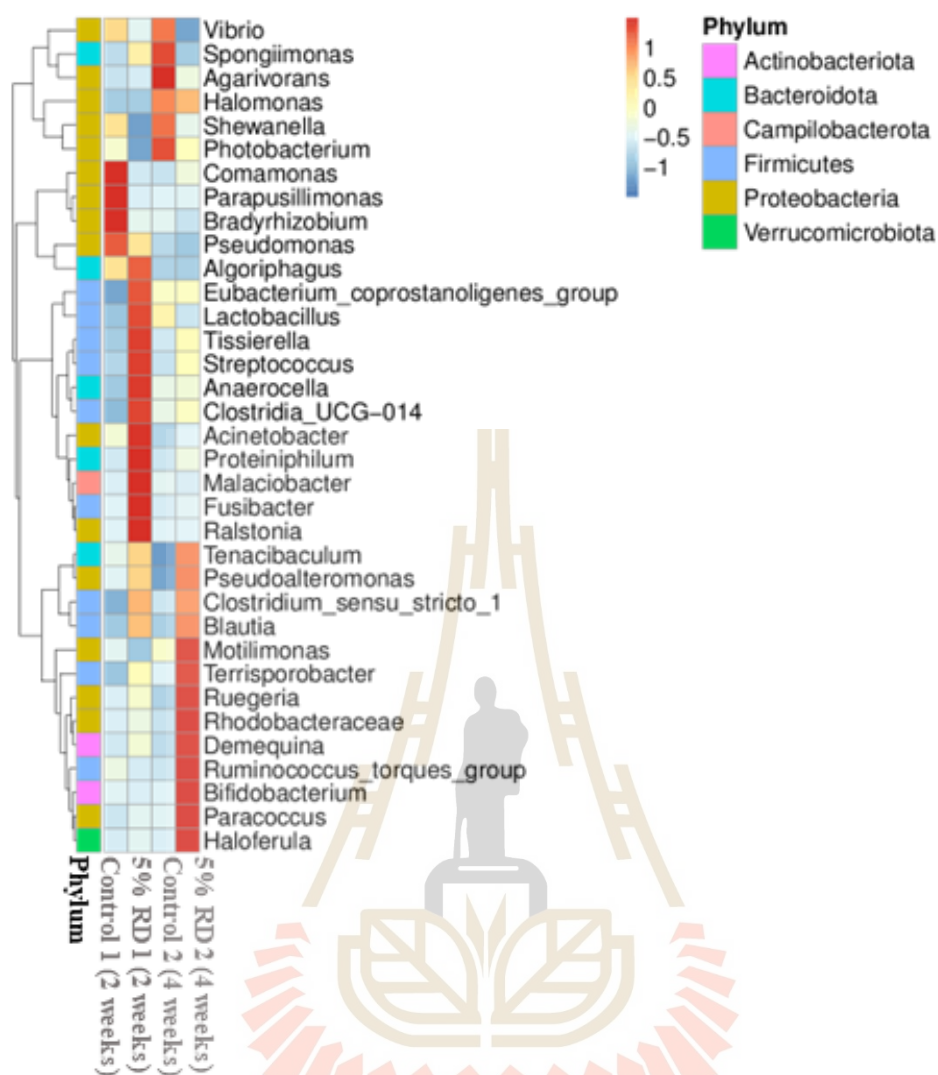
Figure 5.6 Intestinal microbiota composition of *L. vannamei* fed with the experimental different diets of R. *paludigena* CM33 for 2 and 4 weeks. Taxonomical composition at genus level of the microbiome on different diets of *R. paludigena* CM33 and control group for 2 and 4 weeks.
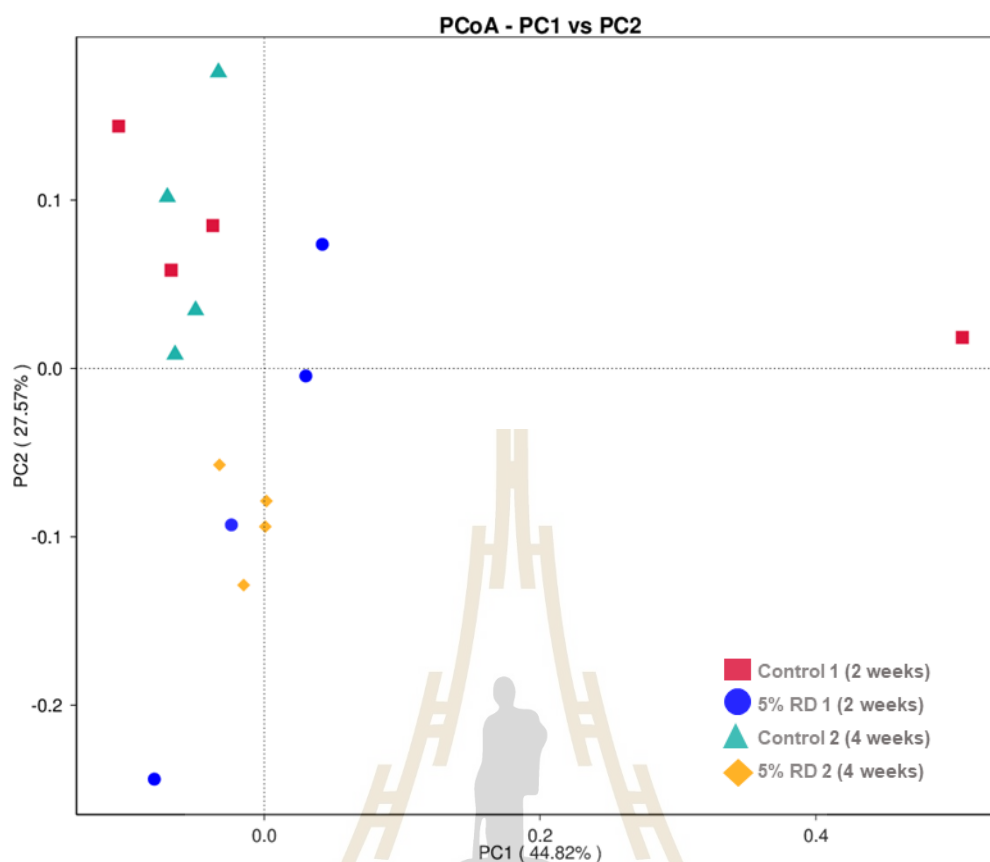
Figure 5.7 Principle coordinate analysis (PCoA) based on weighted UniFrac distances
of intestinal bacteria communities of *L. vannamei* fed different diets. Each
point represents a sample with different diets: control for 2 weeks, 5% RD
for 2 weeks, control for 4 weeks, and 5% RD for 4 weeks. Horizontal
coordinates and vertical coordinates mean the two characteristic values
that led to the biggest differences among samples, and the main influence
degree was reflected by a percentage (n = 12 for each group).
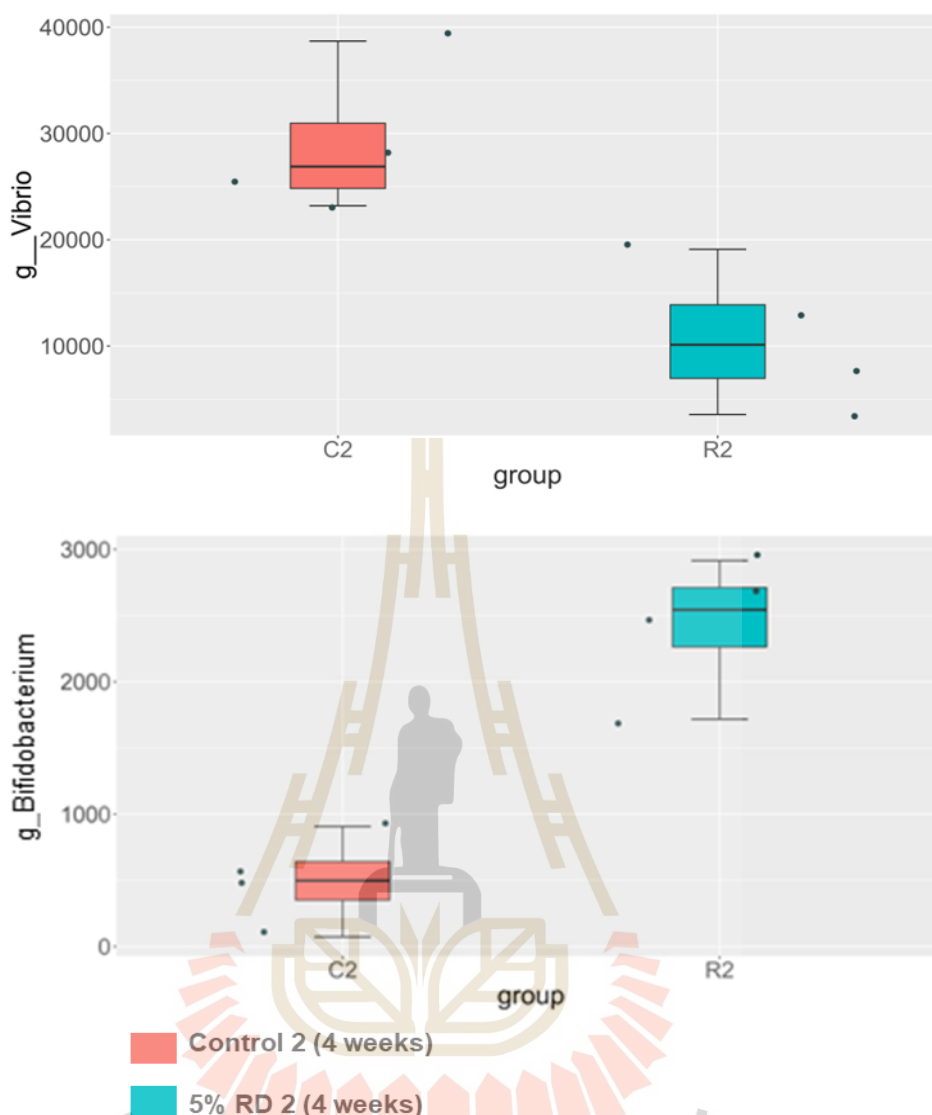
Figure 5.8 MetaStat analysis of microbiota data based on weighted UniFrac distances between control for 4 weeks and 5% RD for 4 weeks in the *Vibrio* level (A) and Bifidobacterium level (B).

5.4.5 Meat composition and color of RD-treated shrimp

Proximate compositions of shrimp are presented in Table 5.6 The results showed that the contents of moisture, crude protein, and crude lipid of the 5% RD and control groups were significantly different ($P<0.05$). Their ranges were 76.21±0.07% to 76.58±0.12%, 73.12±0.62% to 77.48±0.74%, and 4.97±0.13% to 6.20±0.22%, respectively. There was no difference in ash content between these 2 samples ($P<0.05$), accounting for 5.78±0.19 to 5.49±0.20.

The moisture content of the 5% RD group was lower than in the control group. The significantly higher crude lipid and crude protein of the 5% RD shrimp were around 1.25 and 1.10-fold higher, respectively. The color values of the raw and boiled shrimp in the 5% RD and control groups are shown in Table 5.6. There were no differences in color between these 2 samples in both raw and cooked form ($P<0.05$). For raw shrimp, the lightness (L*), redness (a*), and yellowness (b*) were around 53.76±3.40, -2.84±0.41, and -4.68±0.39, respectively. After boiling, L*, a*, and b* were around 84.82±2.38, 3.16±1.51, and 8.93±2.15, respectively.

Table 5.6 Proximate analysis and color of Pacific white shrimp *L. vannamei* fed with experimental different diets of *R. paludigena* CM33 for 4 weeks.

Parameters	Treatments	
	Control	5% RD
Moisture (%)	76.58±0.12[a]	76.21±0.07[b]
Crude protein (%)	73.12±0.62[a]	77.48±0.74[b]
Crude lipid (%)	4.97±0.13[a]	6.20±0.22[b]
Ash (g)	5.78±0.19[a]	5.49±0.20[a]
Color (Raw)		
L*	52.49±2.77[a]	53.76±3.40[a]
a*	-2.31±0.74[a]	-2.84±0.41[a]
b*	-4.07±1.08[a]	-4.68±0.39[a]
Color (Boiled)		
L*	84.24±2.33[a]	84.82±2.38[a]
a*	3.67±1.74[a]	3.16±1.51[a]
b*	9.33±3.01[a]	8.93±2.15[a]

All values are presented as the mean ± SD (n = 9). Means in the same row sharing with different superscripts were significantly different ($P<0.05$) as determined by Tukey's range test. All experiments were carried out in three replications (L* = lightness, a* = (+) red or (-) green, and b* = (+) yellow or (-) blue).

5.5 Discussion

Yeast is regarded to be one of probiotics able to enhance animal health and promote growth (Chaitanawisuti et al., 2011). Furthermore, its anti-inflammatory ability is discerned in aquatic animals (Dawood et al., 2020; Qiang et al., 2019). Previous research reported enhanced growth performance with 1% hydrolysate yeast (*R. mucilaginosa*) supplementation, as well as increased feed utilization and growth in juvenile Nile tilapia (Chen et al., 2019). In *L. vannamei*, 1-2% dietary *Saccharomyces cerevisiae* supplementation could significantly enhance the growth performance (Jin et al., 2018), weight gain rate (WG), SGR, survival rate, and low FCR (Ayiku et al., 2020). Likewise, our study showed significant improvement of growth parameters such as WG, ADG, SGR, FCR, and survival when shrimp were fed with *R. paludigena* CM33 (Table 5.4). These results demonstrated that *R. paludigena* CM33 supplementation in feed can improve growth performance in shrimp.

Probiotics have the potential to decrease the likelihood of the bacterial infections in shrimp, thereby reducing the risk of infectious diseases (Prabawati et al., 2022). Previously, the supplementation of *B. subtilis* P2.24 was able to increase survival by 40% after injecting *V. parahaemolyticus* (Aribah & Wahyudi, 2022). The *B. subtilis* E20 supplementation decreased shrimp mortality after a *V. alginolyticus* injection (Adilah et al., 2022). Furthermore, a mixture of *L. plantarum* and galactooligosaccharide fed to the shrimp showed a decrease in mortality after *V. harveyi* infection (Huynh et al., 2019). In addition, shrimp fed 2% *S. cerevisiae* had 70% survival against *V. harveyi* infection (Ayiku et al., 2020). In our study, 5% RD increased the shrimp survival rate (40% survival) after challenging with VP_{AHPND}, which was higher than the control group (Figure 5.2). These results indicated that 5% RD could be used as a potential feed additive to improve the resistance of shrimp against VP_{AHPND} infection.

During pathogenic invasion, the innate immune system is harnessed by shrimp to handle with the infection through various pathways such as the prophenoloxidate (proPO) system, Toll/IMD pathways, and JAK/STAT. In these pathways, the major components and downstream products are lysozyme, IkB kinase-β (IKKb), IkB kinase-ϵ (IKKe), IMD, Dorsal, anti-lipopolysaccharide (ALF), gamma-interferon-inducible lysosomal thiol reductase (GILT), signal transducer and activator of transcription (STAT), penaiedin 4 (PEN4), and phenoloxidase (PO) (Li & Xiang, 2013; Wang et al., 2013).

Antioxidant enzymes (e.g., superoxide dismutase (SOD), glutathione peroxidase (GPX), and catalase (CAT)) are responsible for eradicating radical species that are generated in response to biotic and abiotic stresses (Huchzermeyer et al., 2022). Hence, these genes and enzymes have been regarded as imperative targets for monitoring the health status of shrimp. Probiotics have been found to increase immune gene expression and the activities of antioxidant enzymes, which promotes resistance to infectious diseases (Yuan et al., 2019). Previously, The upregulation of proPO was observed in shrimp that were fed with *L. plantarum,* resulting in an enhanced resistance against *V. alginolyticus* infection (Chiu et al., 2007). Furthermore, the increased transcriptional levels of lysozyme, PO1, and PO2 were observed in shrimp given *B. subtilis* E20 (Liu et al., 2010). Chiu et al. discerned the effect of dietary *L. plantarum* on the upregulation of PO and SOD activity and resistance to *V. alginolyticus* infection (Chiu et al., 2007). Moreover, the elevated expression of proPO, SOD, GPX, and CAT and increased GPX and SOD activities were found in shrimp given hydrolyzed *R. mucilaginosa* and *B. licheniformis* (Chen et al., 2020). In this study, the 5% RD group showed significantly upregulated transcriptional levels of immune-related genes, such as lysozyme, IKKb, IKKe, STAT, GILT, and PO2 genes and antioxidant genes such as SOD, CAT, and GPX while PO1 was not significantly induced when compared to the control (Figure 5.4). Increased activities of PO, SOD, and catalase were also observed in the 5% RD-fed shrimp (Figure 5.5). Thus, 5% RD could have a positive impact on the health status of *L. vannamei* by inducing the activities of antioxidant enzymes and immune responses.

Our study showed the downregulated expression of myeloid differentiation primary response protein (MyD88), Dorsal, ALF, IMD, and PEN4 in the 5% RD group (Figure 5.4). Similar expression patterns of these genes have been perceived in Ussuri catfish that had been given dietary yeast culture, which showed a reduction of the transcript level of Myd88 (Bu et al., 2020). Likewise, decreased expression levels of MyD88, Toll-like receptor, Nuclear factor κb p65, and caspase-1 were recognized in juvenile shrimp fed with yeast culture (Guo et al., 2022). The decreased expression of these genes might imply the alleviation of stresses that resulted from the supplementation of probiotics; nevertheless, the involvement and the consequences of these trends remain elusive and need further investigation.

Probiotics can affect the microbiota throughout the shrimp's digestive tract (Imaizumi et al., 2021). There have been extensive reports of how rich nutrients in yeast-extract supplementation enhance microbiota structure and microbial diversity in the intestine of *L. vannamei* (Zheng et al., 2021). Previously, probiotic supplementation resulted in the most abundant intestinal bacteria communities in shrimp, which were in phyla such as Proteobacteria, Bacteroidetes, Actinobacteria, and Firmicutes (Ayiku et al., 2020) and in genera such as *Bifidobacteria* (Boonanuntanasarn et al., 2016). *Bifidobacteria* secretes antimicrobial and antioxidant agents that contribute to intestinal health of the host (Fan et al., 2019). The population of *Vibrio*, which is a major cause of bacterial disease in shrimp farming, was decreased after probiotic supplementation (Aribah & Wahyudi, 2022). In addition, previous studies have demonstrated that a decrease in *Vibrio* in shrimp intestinal microbiota led to upregulation of prophenoloxidase and serine proteinase, as well as an increase in superoxide dismutase (SOD) and phenoloxidase (PO) activity in shrimp hemolymph (Tepaamorndech et al., 2020). However, in some studies, a high correlation has been found between the expression of immune genes and certain bacteria in the intestinal microbiota of shrimp (Zheng et al., 2023). Notably, the microbiota have local effects on the development of gut immunity in mammals (Hall et al., 2008; Uematsu et al., 2008). And, changes in intestinal microbiota has led to differences in the gene functions (Yu et al., 2022). In the context of shrimp, the administration of probiotic, *Bacillus velezensis* BV007, could alter the intestinal microbiota and instigate the expression of immune-related genes (Chen et al., 2021). From our results, the addition of 5% RD affected the biodiversity of the intestinal microbiota. High proportions of three major intestinal bacteria (Firmicutes, Proteobacteria, and Bacteroidetes) were found in the 5% RD group. At the genus level, the relative abundance of beneficial bacteria, *Bifidobacterium,* was increased when shrimp were fed with 5% RD, while *Vibrio*, which are predominantly pathogenic bacteria of shrimp, was decreased. However, no significant differences of *Vibrio* between 2-week feeding trial and control group were observed. These data could imply to the synergistic impact of 5% RD on the elevation of helpful microbes while reducing unfavorable bacteria in the intestinal microbiota, where more significant consequences were perceived in 4-week group when compared to 2-week group. Therefore, the alterations of these microbial networks after feeding

for 4 weeks in 5% RD could be one of imperative features resulting in the reduction of shrimp mortality upon VP$_{AHPND}$ infection. In addition, we found that dietary 5% RD impacted antioxidant enzymes and immune responses compared with the control group. Herein, these results suggested that microbiota in the intestinal of shrimp may be a key factor to associate immune-related gene expression.

Shrimp are regarded as a good source of quality macromolecules such as proteins and lipids, which have comparable levels to those of fish, eggs, and other meats (Ali et al., 2017). Previous research has reported that supplementation of 1–3% yeast extract can increase crude lipid and crude protein in shrimp (Zheng et al., 2021). In this study, 5% RD led to significantly higher protein and lipid contents in shrimp meat, suggesting the potential to improve the nutritional value of this meat. The increase in protein and lipid and constant ash content after yeast supplementation agree with the study by Ayiku et al. (Ayiku et al., 2020). Additionally, elevated levels of crude lipid were found in shrimp that had received a yeast-formulated diet (Zheng et al., 2021).

The discrepancies in the quantities and sources of lipids and proteins could influence body compositions (Cheng & Hardy, 2004; Jin et al., 2015; Zhang et al., 2013). In the context of *Rhodotorula*, various bio-oils, proteins, and other nutritious compounds such as β-glucan, β-carotenoids, and MOS are highly accumulated and can be produced by RD (Chen et al., 2019; Frengova & Beshkova, 2009). These components might be responsible for the increment of crude protein and crude lipid in RD groups. However, which substances predominantly increase the body compositions remain vague and need to be examined further. Previously, the red pigmented yeasts such as *R. paludigenum, R. toruloides, R. sphaerocarpum* have been isolated from shrimp and their culturing environments and found to contain carotenoids in the range of 124.5 to 422.6 µg/g (approximately 0.124 to 0.423 mg/g) (Yang et al., 2011). According to our analysis, it was found that the predominant carotenoid found in *R. paludigena* CM33 was β-carotene, which was at the concentration of 15.39 mg/g, while astaxanthin was not detected (Table 5.1). Hence, *R. paludigena CM33* contains the high quantity of carotenoids when compared to the ones that have been isolated from the marine. When considering the color changes from the application of dietary carotenoids in shrimp, astaxanthin had a more pronounced impact on color enhancement in shrimp

compared to β-carotene (Niu et al., 2014). However, when *R. paludigena* CM33 being used in feeding, no significant differences were found in color values between the 5% RD and control groups. Therefore, RD could promote the growth and nutrient composition of *L. vannamei* while preserving their color, which is one of the qualities that make consumers perceive shrimp as palatable.

5.6 Conclusion

In summary, this study provides compelling evidence that the inclusion of *R. paludigena* CM33 in the diet leads to significant improvements in growth performance, antioxidant enzyme activities, immune responses, body compositions, crude lipid, crude protein, microbiota communities, and resistance against VP_{AHPND} in shrimp. These findings highlight the potential of *R. paludigena* CM33 as an effective probiotic for shrimp, capable of enhancing the immune system and increasing survival rates.
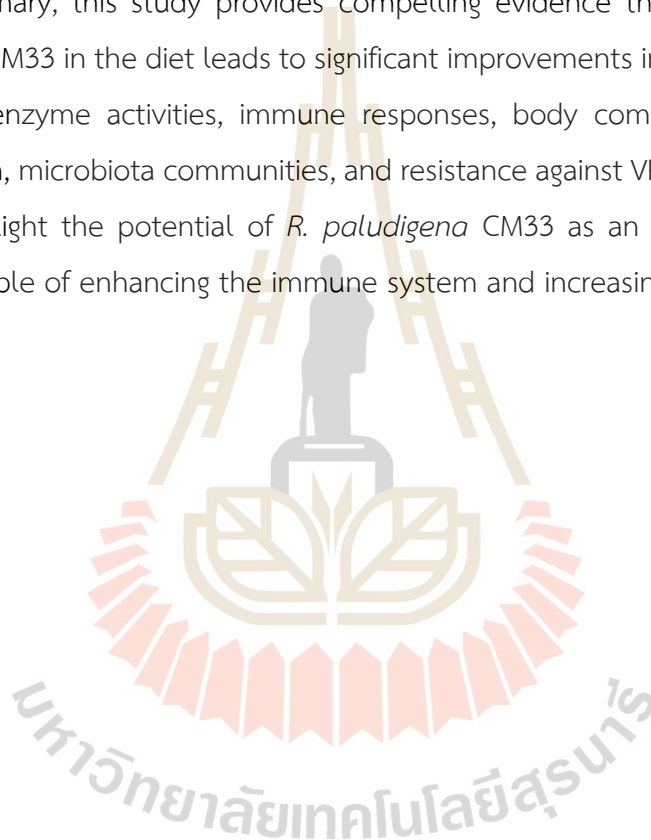
CHAPTER 6

CONCLUSION

6.1 Optimizing the utilization of crude glycerol in the cultivation of *R. paludigena* CM33 for carotenoid production in a 500-L fermenter

6.1.1 Crude glycerol, a byproduct of the biodiesel industry, was used in this work as a substrate for the growth of *R. paludigena* CM33. Response surface methods (RSM) were employed to optimize the growth conditions, and it was shown that using 40 g/L of crude glycerol significantly increased the carotenoid content. This shows the potential of employing crude glycerol as a different and more affordable substrate to increase the production of carotenoids by *R. paludigena* CM33.

6.1.2 In this study, the maximum concentrations of biomass (cell dry weight) and carotenoids were obtained at 45.38±1.05 g/L and 15.39±0.03 mg/g, respectively, using a fed-batch procedure conducted in a 500-L fermenter.

6.1.3 These findings demonstrate the potential of crude glycerol as an additional substrate for enhancing carotenoid synthesis in *R. paludigena* CM33.

6.2 Optimization of the harvesting, extraction, and separation of carotenoids from *R. paludigena* CM33 cells

6.2.1 The microfiltration process was utilized for the efficient harvesting of *R. paludigena* CM33 cells. The results revealed that the cake accounted for 85.38% of the overall resistance, while the adsorption resistance accounted for 12.62%. This highlights the enhanced efficiency of cell harvesting through microfiltration of the *R. paludigena* CM33 fermentation broth.

6.2.2 The high-pressure homogenizer (HPH) was utilized in this study to disrupt the cells, followed by the purification of carotenoids using preparative high-performance liquid chromatography (prep HPLC). The results demonstrated that enhanced cell disruption was achieved by applying a pressure of 30,000 psi, performing 4 passes, and utilizing a 5% yeast cell feed.

6.2.3 Using HPLC, LC-MS, and NMR studies, the carotenoids, mainly β-carotene, that were discovered in this study were verified. These results highlight the potential of preparative HPLC, high-pressure homogenization (HPH), and microfiltration in enhancing carotenoids' downstream processing in *R. paludigena* CM33.

6.3 The potential of *R. paludigena* CM33 as a probiotic for white shrimp

6.3.1 After 4 weeks of administration, the results revealed significant improvements in the specific growth rate, weight gain, and survival of shrimp fed with 1%, 2%, and 5% RD, which were higher than those of the control group.

6.3.2 The shrimp were challenged with VP_{AHPND} after 4 weeks of feeding, and shrimp mortality was recorded at 12-hour intervals post-infection (hpi). When comparing the 5% RD group to the control group at 120 hours, the cumulative mortality following the VP_{AHPND} challenge was lower. Supplementation of *R. paludigena* CM33 reduced shrimp mortality against VP_{AHPND} infection.

6.3.3 In the 5% RD group, the application of RD in feed led to the modulation of immune-related gene expressions and enzymatic activities. The expression levels of immune-responsive genes, including proPO system (prophenoloxidase-2: PO2), antioxidant enzymes (superoxide dismutase: SOD, glutathione peroxidase: GPX, and catalase: CAT), JAK/STAT pathway (signal transducer and activator of transcription: STAT, gamma interferon inducible lysosomal thiol reductase: GILT), IMD pathway (inhibitor of nuclear factor kappa-B kinase subunit beta and epsilon: IKKb and IKKe), and Toll pathway (Lysozyme) genes, were up-regulated in the 5% RD group.

6.3.4 Microbiome analysis revealed the predominant phyla present in the shrimp intestines, including Proteobacteria, Firmicutes, Bacteroidota, Campilobacterota, Actinobacteriota, and Verrucomicrobiota. At the genus level, the abundance of *Vibrio* was reduced in the 5% RD group, while the potentially beneficial bacteria *Bifidobacterium* showed an increase. These findings indicate that 5% RD supplementation had a positive influence on the intestinal microflora of the shrimp, promoting a favorable microbial community.

6.3.5 In the 5% RD group, there was a notable and significant increase observed in the levels of crude protein and crude lipid, both of which are essential and nutritious components. This finding suggests that the inclusion of 5% RD in the diet positively influenced the nutritional composition of the samples.

6.3.6 The results demonstrate the potential of *R. paludigena* CM33 as a probiotic supplement in shrimp feed, as it has shown positive effects on various aspects. Firstly, it improves growth performance in shrimp. Secondly, it enhances the shrimp's antimicrobial responses against VP_{AHPND}, a harmful pathogen. Lastly, it positively influences the meat quality of shrimp by increasing the protein and lipid content. These findings highlight the potential benefits of incorporating *R. paludigena* CM33 into shrimp feed as a probiotic supplement.
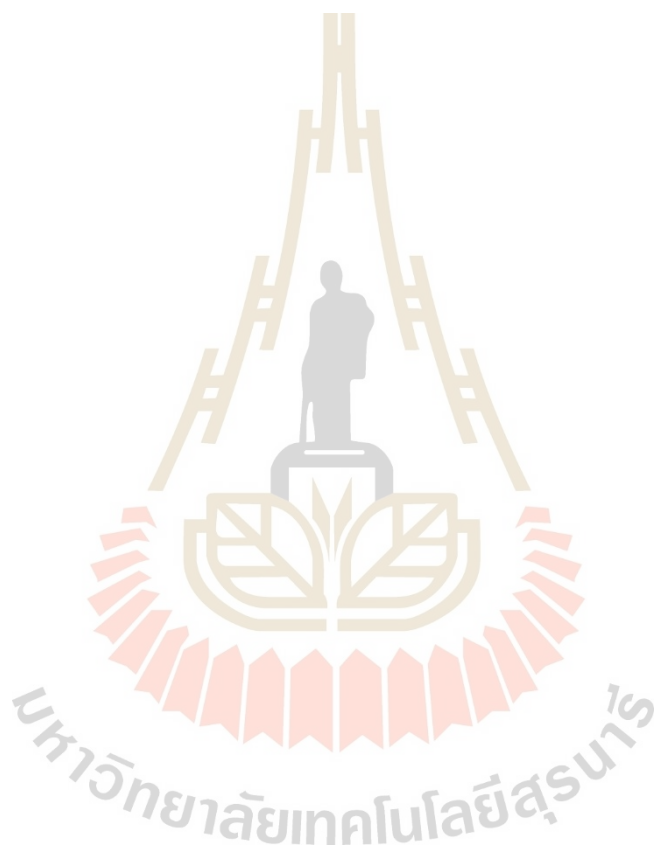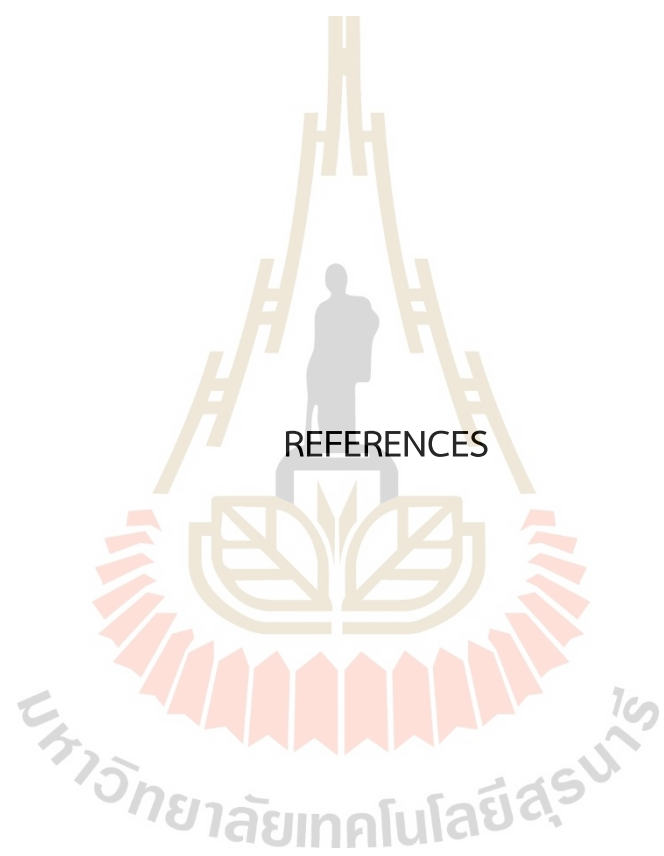
REFERENCES

REFERENCES

Adilah, R. N., Chiu, S. T., Hu, S. Y., Ballantyne, R., Happy, N., Cheng, A. C., & Liu, C. H. (2022). Improvement in the probiotic efficacy of *Bacillus subtilis* E20-stimulates growth and health status of white shrimp, *Litopenaeus vannamei* via encapsulation in alginate and coated with chitosan. *Fish & Shellfish Immunology, 125*, 74-83.

AG, B. L. (2020). *Pure Chromatography Systems*. https://buchi.showpad.com/share/ qGHpfek6E7IbHQCwmCeb3

Aksu, Z., & Eren, A. T. (2005). Carotenoids production by the yeast *Rhodotorula mucilaginosa*: use of agricultural wastes as a carbon source. *Process Biochemistry, 40*(9), 2985-2991.

Ali, S. S. R., Ramachandran, M., Chakma, S. K., & Sheriff, M. (2017). Proximate composition of commercially important marine fishes and shrimps from the Chennai coast, India. *International Journal of Fisheries and Aquatic Studies, 5*(5), 113-119.

Alipour, S., Habibi, A., Taavoni, S., & Varmira, K. (2017). β-carotene production from soap stock by loofa-immobilized *Rhodotorula rubra* in an airlift photobioreactor. *Process Biochemistry, 54*, 9-19.

Allahkarami, S., Sepahi, A. A., Hosseini, H., & Razavi, M. R. (2021). Isolation and identification of carotenoid-producing *Rhodotorula* sp. from Pinaceae forest ecosystems and optimization of *in vitro* carotenoid production. *Biotechnology Reports, 32*, e00687.

Amaya, E. A., Davis, D. A., & Rouse, D. B. (2007). Replacement of fish meal in practical diets for the Pacific white shrimp *(Litopenaeus vannamei)* reared under pond conditions. *Aquaculture, 262*(2-4), 393-401.

Anderson, D. P. (1992). Immunostimulants, adjuvants, and vaccine carriers in fish: applications to aquaculture. *Annual review of fish diseases, 2*, 281-307.

Anitha, M., Kamarudin, S., & Kofli, N. (2016). The potential of glycerol as a value-added commodity. *Chemical Engineering Journal, 295*, 119-130.

AOAC. (2000). Offcial Methods of analysis of the Association of Official Analytical Chemists International. *sixteenth ed*(Association of Official Analytical Chemists).

Aribah, D., & Wahyudi, A. T. (2022). The effectiveness of marine bacterial microcapsules in controlling vibriosis disease caused by the infection of *Vibrio parahaemolyticus* in white shrimp *Litopenaeus vannamei*. *Aquaculture, 549*, 737795.

Asche, F., Oglend, A., & Smith, M. D. (2022). Global markets and the commons: the role of imports in the US wild-caught shrimp market. *Environmental Research Letters, 17*(4), 045023.

Ayiku, S., Shen, J.-f., Tan, B.-p., Dong, X.-h., & Liu, H.-y. (2020). Effects of dietary yeast culture on shrimp growth, immune response, intestinal health and disease resistance against *Vibrio harveyi*. *Fish & Shellfish Immunology, 102*, 286-295.

Bamford, D. H., & Zuckerman, M. (2021). *Encyclopedia of virology*. Academic Press.

Bccresearch. (2022, 30 December 2022). Carotenoids Market Size. https://www.bccresearch.com/market-research/food-and-beverage/the-global-market-for-carotenoids.html.

Beauchamp, C., & Fridovich, I. (1971). Superoxide dismutase: improved assays and an assay applicable to acrylamide gels. *Analytical biochemistry, 44*(1), 276-287.

Bezerra, M. A., Santelli, R. E., Oliveira, E. P., Villar, L. S., & Escaleira, L. A. (2008). Response surface methodology (RSM) as a tool for optimization in analytical chemistry. *Talanta, 76*(5), 965-977.

Bhosale, P., & Bernstein, P. S. (2005). Microbial xanthophylls. *Applied microbiology and biotechnology, 68*, 445-455.

Bhosale, P., & Gadre, R. (2001a). Optimization of carotenoid production from hyper-producing *Rhodotorula glutinis* mutant 32 by a factorial approach. *Letters in applied Microbiology, 33*(1), 12-16.

Bhosale, P., & Gadre, R. (2001b). β-carotene production in sugarcane molasses by a *Rhodotorula glutinis* mutant. *Journal of Industrial Microbiology and Biotechnology, 26*, 327-332.

Bioninja. (2021). *Diagram of a Standard Fermenter*. Retrieved 13 May 2023 from https://www.buchi.com/th-th/node/3687

Bland, J. M., & Altman, D. G. (2004). The logrank test. *Bmj, 328*(7447), 1073.

Boonanuntanasarn, S., Wongsasak, U., Pitaksong, T., & Chaijamrus, S. (2016). Effects of dietary supplementation with β-glucan and synbiotics on growth, haemolymph chemistry, and intestinal microbiota and morphology in the P acific white shrimp. *Aquaculture Nutrition, 22*(4), 837-845.

Boonchuen, P., Jaree, P., Tassanakajon, A., & Somboonwiwat, K. (2018). Hemocyanin of *Litopenaeus vannamei* agglutinates *Vibrio parahaemolyticus* AHPND (VP~AHPND~) and neutralizes its toxin. *Developmental & Comparative Immunology, 84*, 371-381.

Boonchuen, P., Maralit, B. A., Jaree, P., Tassanakajon, A., & Somboonwiwat, K. (2020). MicroRNA and mRNA interactions coordinate the immune response in non-lethal heat stressed *Litopenaeus vannamei* against AHPND-causing *Vibrio parahaemolyticus*. *Scientific reports, 10*(1), 1-15.

Boonchuen, P., Sakhor, H., Jaree, P., & Somboonwiwat, K. (2022). Shrimp Vago5 activates an innate immune defense upon bacterial infection. *Fish & Shellfish Immunology, 120*, 122-132.

Borregaard, N., Elsbach, P., Ganz, T., Garred, P., & Svejgaard, A. (2000). Innate immunity: from plants to humans. *Immunology today, 21*(2), 68-70.

Breil, C., Meullemiestre, A., Vian, M., & Chemat, F. (2016). Bio-based solvents for green extraction of lipids from oleaginous yeast biomass for sustainable aviation biofuel. *Molecules, 21*(2), 196.

Breitenbach, J., Pollmann, H., & Sandmann, G. (2019). Genetic modification of the carotenoid pathway in the red yeast *Xanthophyllomyces dendrorhous*: engineering of a high-yield zeaxanthin strain. *Journal of biotechnology, 289*, 112-117.

Britton, G. (2008). Functions of intact carotenoids. *Carotenoids: volume 4: natural functions*, 189-212.

Brown, M. (2011). Modes of action of probiotics: recent developments. *Journal of Animal and Veterinary Advances, 10*(14), 1895-1900.

Bu, X., Huang, J., Tao, S., Yang, J., Liao, Y., Liu, H., & Yang, Y. (2020). Yeast cultures alleviate gossypol induced inflammatory response in liver tissue of Ussuri catfish (*Pseudobagrus ussuriensis*). *Aquaculture, 518*, 734828.

Buzzini, P. (2001). Batch and fed-batch carotenoid production by *Rhodotorula glutinis*– *Debaryomyces castellii* co-cultures in corn syrup. *Journal of applied Microbiology, 90*(5), 843-847.

Buzzini, P., & Martini, A. (2000). Production of carotenoids by strains of *Rhodotorula glutinis* cultured in raw materials of agro-industrial origin. *Bioresource technology, 71*(1), 41-44.

Campos, J., Tejada, L. G., Bao, J., & Lidén, G. (2023). Fed-batch strategies for biodetoxification in production of optically pure lactic acid from softwood hydrolysate using *Pediococcus acidilactici. Process Biochemistry, 125*, 162-170.

Cassano, A., & Basile, A. (2013). Integrating different membrane operations and combining membranes with conventional separation techniques in industrial processes. In *Handbook of Membrane Reactors* (pp. 296-343). Elsevier.

Cerenius, L., Lee, B. L., & Söderhäll, K. (2008). The proPO-system: pros and cons for its role in invertebrate immunity. *Trends in immunology, 29*(6), 263-271.

Chaitanawisuti, N., Choeychom, C., & Piyatiratitivorakul, S. (2011). Effect of dietary supplementation of brewers yeast and nucleotide singularly on growth, survival and *vibriosis* resistance on juveniles of the gastropod spotted babylon (*Babylonia areolata*). *Aquaculture International, 19*, 489-496.

Chauhan, A., & Singh, R. (2019). Probiotics in aquaculture: a promising emerging alternative approach. *Symbiosis, 77*(2), 99-113.

Chen, L., Lv, C., Li, B., Zhang, H., Ren, L., Zhang, Q., Zhang, X., Gao, J., Sun, C., & Hu, S. (2021). Effects of *Bacillus velezensis* Supplementation on the Growth Performance, Immune Responses, and Intestine Microbiota of *Litopenaeus vannamei. Frontiers in Marine Science, 8*, 744281.

Chen, M., Chen, X.-Q., Tian, L.-X., Liu, Y.-J., & Niu, J. (2020). Enhanced intestinal health, immune responses and ammonia resistance in Pacific white shrimp (*Litopenaeus vannamei*) fed dietary hydrolyzed yeast (*Rhodotorula mucilaginosa*) and *Bacillus licheniformis. Aquaculture Reports, 17*, 100385.

Chen, X.-Q., Zhao, W., Xie, S.-W., Xie, J.-J., Zhang, Z.-H., Tian, L.-X., Liu, Y.-J., & Niu, J. (2019). Effects of dietary hydrolyzed yeast (*Rhodotorula mucilaginosa*) on growth performance, immune response, antioxidant capacity and histomorphology of juvenile Nile tilapia (*Oreochromis niloticus*). *Fish & Shellfish Immunology, 90*, 30-39.

Cheng, Z., & Hardy, R. (2004). Protein and lipid sources affect cholesterol concentrations of juvenile Pacific white shrimp, *Litopenaeus vannamei* (Boone). *Journal of animal science, 82*(4), 1136-1145.

Chien, Y.-H., & Shiau, W.-C. (2005). The effects of dietary supplementation of algae and synthetic astaxanthin on body astaxanthin, survival, growth, and low dissolved oxygen stress resistance of kuruma prawn, *Marsupenaeus japonicus* Bate. *Journal of Experimental Marine Biology and Ecology, 318*(2), 201-211.

Chiu, C.-H., Guu, Y.-K., Liu, C.-H., Pan, T.-M., & Cheng, W. (2007). Immune responses and gene expression in white shrimp, *Litopenaeus vannamei*, induced by *Lactobacillus plantarum. Fish & Shellfish Immunology, 23*(2), 364-377.

Chopra, J., Rangarajan, V., & Sen, R. (2022). Recent developments in oleaginous yeast feedstock based biorefinery for production and life cycle assessment of biofuels and value-added products. *Sustainable Energy Technologies and Assessments, 53*, 102621.

Cipolatti, E. P., Remedi, R. D., dos Santos Sá, C., Rodrigues, A. B., Ramos, J. M. G., Burkert, C. A. V., Furlong, E. B., & de Medeiros Burkert, J. F. (2019). Use of agroindustrial byproducts as substrate for production of carotenoids with antioxidant potential by wild yeasts. *Biocatalysis and Agricultural Biotechnology, 20*, 101208.

Comuzzo, P., & Calligaris, S. (2019). Potential applications of high pressure homogenization in winemaking: A review. *Beverages, 5*(3), 56.

Cuzon, G., Lawrence, A., Gaxiola, G., Rosas, C., & Guillaume, J. (2004). Nutrition of *Litopenaeus vannamei* reared in tanks or in ponds. *Aquaculture, 235*(1-4), 513-551.

Dawood, M. A., Abdo, S. E., Gewaily, M. S., Moustafa, E. M., SaadAllah, M. S., AbdEl-Kader, M. F., Hamouda, A. H., Omar, A. A., & Alwakeel, R. A. (2020). The influence of dietary β-glucan on immune, transcriptomic, inflammatory and histopathology disorders caused by deltamethrin toxicity in Nile tilapia (*Oreochromis niloticus*). *Fish & shellfish immunology, 98*, 301-311.

de la Peña, L. D., Cabillon, N. A. R., Catedral, D. D., Amar, E. C., Usero, R. C., Monotilla, W. D., Calpe, A. T., Fernandez, D. D., & Saloma, C. P. (2015). Acute hepatopancreatic necrosis disease (AHPND) outbreaks in *Penaeus vannamei* and *P. monodon* cultured in the Philippines. *Diseases of Aquatic Organisms, 116*(3), 251-254.

De Vuyst, L., & Leroy, F. (2007). Bacteriocins from lactic acid bacteria: production, purification, and food applications. *Microbial Physiology, 13*(4), 194-199.

Deepika, A., Sreedharan, K., & Rajendran, K. (2022). Molecular characterisation, ontogeny and tissue level expression analysis of a downstream signalling molecule of the Toll-pathway, Dorsal (an NF-κB homologue) in black tiger shrimp (*Penaeus monodon*).

Dhar, A. K., Cowley, J. A., Hasson, K. W., & Walker, P. J. (2004). Genomic organization, biology, and diagnosis of Taura syndrome virus and yellowhead virus of penaeid shrimp. *Advances in virus research, 63*, 353.

Dhar, P., Singh, R. V., Peng, K.-C., Wu, Z., & Chellappa, R. (2019). Learning without memorizing. Proceedings of the IEEE/CVF conference on computer vision and pattern recognition,

Dias, C., Reis, A., Santos, J. A., & da Silva, T. L. (2020). Concomitant wastewater treatment with lipid and carotenoid production by the oleaginous yeast *Rhodosporidium toruloides* grown on brewery effluent enriched with sugarcane molasses and urea. *Process Biochemistry, 94*, 1-14.

Dimopoulos, G., Tsantes, M., & Taoukis, P. (2020). Effect of high pressure homogenization on the production of yeast extract via autolysis and beta-glucan recovery. *Innovative Food Science & Emerging Technologies, 62*, 102340.

dos S Filho, L. G. A., Diniz, F. M., & Pereira, A. M. (2023). Immunostimulants derived from plants and algae to increase resistance of pacific white shrimp (*Litopenaeus vannamei*) against vibriosis. *Studies in Natural Products Chemistry, 77*, 297-337.

Drévillon, L., Koubaa, M., Nicaud, J.-M., & Vorobiev, E. (2019). Cell disruption pre-treatments towards an effective recovery of oil from *Yarrowia lipolytica* oleaginous yeast. *Biomass and Bioenergy, 128*, 105320.

Ekasari, J., Azhar, M. H., Surawidjaja, E. H., Nuryati, S., De Schryver, P., & Bossier, P. (2014). Immune response and disease resistance of shrimp fed biofloc grown on different carbon sources. *Fish & Shellfish Immunology, 41*(2), 332-339.

Ekpeni, L. E., Benyounis, K., Nkem-Ekpeni, F. F., Stokes, J., & Olabi, A.-G. (2015). Underlying factors to consider in improving energy yield from biomass source through yeast use on high-pressure homogenizer (hph). *Energy, 81*, 74-83.

El-Saadony, M. T., Swelum, A. A., Ghanima, M. M. A., Shukry, M., Omar, A. A., Taha, A. E., Salem, H. M., El-Tahan, A. M., El-Tarabily, K. A., & Abd El-Hack, M. E. (2022). Shrimp production, the most important diseases that threaten it, and the role of probiotics in confronting these diseases: a review. *Research in veterinary science*.

Elshopakey, G. E., Risha, E. F., Abdalla, O. A., Okamura, Y., Hanh, V. D., Ibuki, M., Sudhakaran, R., & Itami, T. (2018). Enhancement of immune response and resistance against *Vibrio parahaemolyticus* in kuruma shrimp (*Marsupenaeus japonicus*) by dietary supplementation of β-1, 4-mannobiose. *Fish & Shellfish Immunology, 74*, 26-34.

Fan, L., Wang, Z., Chen, M., Qu, Y., Li, J., Zhou, A., Xie, S., Zeng, F., & Zou, J. (2019). Microbiota comparison of Pacific white shrimp intestine and sediment at freshwater and marine cultured environment. *Science of the Total Environment, 657*, 1194-1204.

Faramarzi, M., Kiaalvandi, S., & Iranshahi, F. (2011). The effect of probiotics on growth performance and body composition of common carp (*Cyprinus carpio*). *Journal of Animal and Veterinary Advances, 10*(18), 2408-2413.

Flegel, T. W. (2012). Historic emergence, impact and current status of shrimp pathogens in Asia. *Journal of Invertebrate Pathology, 110*(2), 166-173.

Food, & Organization, A. (2020). Sustainability in action. *State of World Fisheries and Aquaculture. Rome, 200*.

Frengova, G. I., & Beshkova, D. M. (2009). Carotenoids from *Rhodotorula* and *Phaffia*: yeasts of biotechnological importance. *Journal of Industrial Microbiology and Biotechnology, 36*(2), 163.

Gassel, S., Schewe, H., Schmidt, I., Schrader, J., & Sandmann, G. (2013). Multiple improvement of astaxanthin biosynthesis in *Xanthophyllomyces dendrorhous* by a combination of conventional mutagenesis and metabolic pathway engineering. *Biotechnology letters, 35*, 565-569.

Gong, G., Zhang, X., & Tan, T. (2020). Simultaneously enhanced intracellular lipogenesis and β-carotene biosynthesis of *Rhodotorula glutinis* by light exposure with sodium acetate as the substrate. *Bioresource technology, 295*, 122274.

Gosalawit, C., Imsoonthornruksa, S., Gilroyed, B. H., Mcnea, L., Boontawan, A., & Ketudat-Cairns, M. (2021). The potential of the oleaginous yeast *Rhodotorula paludigena* CM33 to produce biolipids. *Journal of biotechnology, 329*, 56-64.

Guo, Y., Zhang, L., Liang, Y., Li, P., Zhang, T., Meng, F., Liu, B., Zhang, H., Fu, W., & Wang, W. (2022). Effects of dietary yeast culture on health status in digestive tract of juvenile Pacific white shrimp *Litopenaeus Vannamei*. *Fish and Shellfish Immunology Reports, 3*, 100065.

Haas, B. J., Gevers, D., Earl, A. M., Feldgarden, M., Ward, D. V., Giannoukos, G., Ciulla, D., Tabbaa, D., Highlander, S. K., & Sodergren, E. (2011). Chimeric 16S rRNA sequence formation and detection in Sanger and 454-pyrosequenced PCR amplicons. *Genome research, 21*(3), 494-504.

Hall, J. A., Bouladoux, N., Sun, C. M., Wohlfert, E. A., Blank, R. B., Zhu, Q., Grigg, M. E., Berzofsky, J. A., & Belkaid, Y. (2008). Commensal DNA limits regulatory T cell conversion and is a natural adjuvant of intestinal immune responses. *Immunity, 29*(4), 637-649.

Hannibal, L., Lorquin, J., D'Ortoli, N. A., Garcia, N., Chaintreuil, C., Masson-Boivin, C., Dreyfus, B., & Giraud, E. (2000). Isolation and characterization of canthaxanthin biosynthesis genes from the photosynthetic bacterium *Bradyrhizobium* sp. strain ORS278. *Journal of Bacteriology, 182*(13), 3850-3853.

Hasson, K., Fan, Y., Reisinger, T., Venuti, J., & Varner, P. (2006). White-spot syndrome virus (WSSV) introduction into the Gulf of Mexico and Texas freshwater systems through imported, frozen bait-shrimp. *Diseases of Aquatic Organisms, 71*(2), 91-100.

Hauton, C. (2012). The scope of the crustacean immune system for disease control. *Journal of Invertebrate Pathology, 110*(2), 251-260.

Hawksworth, D. L., Kirk, P., Sutton, B. C., & Pegler, D. (1996). Ainsworth & Bisby's dictionary of the fungi. *Revista do Instituto de Medicina Tropical de São Paulo, 38*, 272-272.

Holmgren, L. (2014). Influence of the metabolic inhibitor sesamin on the fatty acid profile of the oleaginous yeast *Rhodotorula glutinis*.

Hu, S., Luo, X., Wan, C., & Li, Y. (2012). Characterization of crude glycerol from biodiesel plants. *Journal of agricultural and food chemistry, 60*(23), 5915-5921.

Huchzermeyer, B., Menghani, E., Khardia, P., & Shilu, A. (2022). Metabolic pathway of natural antioxidants, antioxidant enzymes and ROS providence. *Antioxidants, 11*(4), 761.

uynh, T. G., Hu, S. Y., Chiu, C. S., Truong, Q. P., & Liu, C. H. (2019). Bacterial population in intestines of white shrimp, *Litopenaeus vannamei* fed a synbiotic containing *Lactobacillus plantarum* and galactooligosaccharide. *Aquaculture Research, 50*(3), 807-817.

Igreja, W. S., Maia, F. d. A., Lopes, A. S., & Chisté, R. C. (2021). Biotechnological production of carotenoids using low cost-substrates is influenced by cultivation parameters: A review. *International Journal of Molecular Sciences, 22*(16), 8819.

Imaizumi, K., Tinwongger, S., Kondo, H., & Hirono, I. (2021). Analysis of microbiota in the stomach and midgut of two penaeid shrimps during probiotic feeding. *Scientific Reports, 11*(1), 9936.

Jaskari, J., Kontula, P., Siitonen, A., Jousimies-Somer, H., Mattila-Sandholm, T., & Poutanen, K. (1998). Oat β-glucan and xylan hydrolysates as selective substrates for *Bifidobacterium* and *Lactobacillus* strains. *Applied microbiology and biotechnology, 49*(2), 175-181.

Jayachandran, M., Chen, J., Chung, S. S. M., & Xu, B. (2018). A critical review on the impacts of β-glucans on gut microbiota and human health. *The Journal of nutritional biochemistry, 61*, 101-110.

Jayasree, L., Janakiram, P., & Madhavi, R. (2006). Characterization of *Vibrio* spp. associated with diseased shrimp from culture ponds of Andhra Pradesh (India). *Journal of the world aquaculture society, 37*(4), 523-532.

Jin, M., Xiong, J., Zhou, Q.-C., Yuan, Y., Wang, X.-X., & Sun, P. (2018). Dietary yeast hydrolysate and brewer's yeast supplementation could enhance growth performance, innate immunity capacity and ammonia nitrogen stress resistance ability of Pacific white shrimp (*Litopenaeus vannamei*). *Fish & shellfish immunology, 82*, 121-129.

Jin, Y., Tian, L.-x., Xie, S.-w., Guo, D.-q., Yang, H.-j., Liang, G.-y., & Liu, Y.-j. (2015). Interactions between dietary protein levels, growth performance, feed utilization, gene expression and metabolic products in juvenile grass carp (*Ctenopharyngodon idella*). *Aquaculture, 437*, 75-83.

Johansson, L. H., & Borg, L. H. (1988). A spectrophotometric method for determination of catalase activity in small tissue samples. *Analytical biochemistry, 174*(1), 331-336.

Ju, Z. Y., Deng, D. F., Dominy, W. G., & Forster, I. P. (2011). Pigmentation of Pacific white shrimp, *Litopenaeus vannamei*, by dietary astaxanthin extracted from *Haematococcus pluvialis*. *Journal of the World Aquaculture Society, 42*(5), 633-644.

Juang, R.-S., Chen, H.-L., & Chen, Y.-S. (2008). Membrane fouling and resistance analysis in dead-end ultrafiltration of *Bacillus subtilis* fermentation broths. *Separation and Purification Technology, 63*(3), 531-538.

Kan, H., Kim, C.-H., Kwon, H.-M., Park, J.-W., Roh, K.-B., Lee, H., Park, B.-J., Zhang, R., Zhang, J., & Söderhäll, K. (2008). Molecular Control of Phenoloxidase-induced Melanin Synthesis in an Insect. *Journal of Biological Chemistry, 283*(37), 25316-25323.

Katagiri, N., Tomimatsu, K., Date, K., & Iritani, E. (2021). Yeast cell cake characterization in alcohol solution for efficient microfiltration. *Membranes, 11*(2), 89.

Kim, S.-J., Kim, G.-J., Park, D.-H., & Ryu, Y.-W. (2003). High-level production of astaxanthin by fed-batch culture of mutant strain *Phaffia rhodozyma* AJ-6-1.

Kitcha, S., & Cheirsilp, B. (2013). Enhancing lipid production from crude glycerol by newly isolated oleaginous yeasts: strain selection, process optimization, and fed-batch strategy. *Bioenergy Research, 6*, 300-310.

Knipe, H., Temperton, B., Lange, A., Bass, D., & Tyler, C. R. (2021). Probiotics and competitive exclusion of pathogens in shrimp aquaculture. *Reviews in Aquaculture, 13*(1), 324-352.

Kongjao, S., Damronglerd, S., & Hunsom, M. (2010). Purification of crude glycerol derived from waste used-oil methyl ester plant. *Korean Journal of Chemical Engineering, 27*, 944-949.

Koyuncu, I., Sengur, R., Turken, T., Guclu, S., & Pasaoglu, M. (2015). Advances in water treatment by microfiltration, ultrafiltration, and nanofiltration. In *Advances in membrane technologies for water treatment* (pp. 83-128). Elsevier.

Krishna, C. (2005). Solid-state fermentation systems—an overview. *Critical reviews in biotechnology, 25*(1-2), 1-30.

Kulkarni, A., Krishnan, S., Anand, D., Kokkattunivarthil Uthaman, S., Otta, S. K., Karunasagar, I., & Kooloth Valappil, R. (2021). Immune responses and immunoprotection in crustaceans with special reference to shrimp. *Reviews in Aquaculture, 13*(1), 431-459.

Kumar, R., Huang, M.-Y., Chen, C.-L., Wang, H.-C., & Lu, H.-P. (2023). Resilience and probiotic interventions to prevent and recover from shrimp gut dysbiosis. *Fish & Shellfish Immunology*, 108886.

Kumar, R., Ng, T. H., & Wang, H. C. (2020). Acute hepatopancreatic necrosis disease in penaeid shrimp. *Reviews in Aquaculture, 12*(3), 1867-1880.

Kurtzman, C. P., Fell, J. W., & Boekhout, T. (2011). *The yeasts: a taxonomic study.* Elsevier.

Lammari, N., Tarhini, M., Miladi, K., Louaer, O., Meniai, A. H., Sfar, S., Fessi, H., & Elaïssari, A. (2021). Encapsulation methods of active molecules for drug delivery. In *Drug delivery devices and therapeutic systems* (pp. 289-306). Elsevier.

Landsman, A., St-Pierre, B., Rosales-Leija, M., Brown, M., & Gibbons, W. (2019). Impact of aquaculture practices on intestinal bacterial profiles of Pacific whiteleg shrimp *Litopenaeus vannamei. Microorganisms, 7*(4), 93.

Latha, B., & Jeevaratnam, K. (2010). Purification and characterization of the pigments from *Rhodotorula glutinis* DFR-PDY isolated from natural source. *Global Journal of Biotechnology & Biochemistry, 5*(3), 166-174.

Lee, D., Yu, Y.-B., Choi, J.-H., Jo, A.-H., Hong, S.-M., Kang, J.-C., & Kim, J.-H. (2022). Viral shrimp diseases listed by the OIE: A review. *Viruses, 14*(3), 585.

Li, F., & Xiang, J. (2013). Signaling pathways regulating innate immune responses in shrimp. *Fish & Shellfish Immunology, 34*(4), 973-980.

Li, M., Shao, D., Zhou, J., Gu, J., Qin, J., Chen, W., & Wei, W. (2020). Signatures within esophageal microbiota with progression of esophageal squamous cell carcinoma. *Chinese Journal of Cancer Research, 32*(6), 755.

Li, N., Cui, R., Zhang, F., Meng, X., & Liu, B. (2022). A novel enzyme from *Rhodotorula mucilaginosa* Aldolase: Isolation, identification and degradation for patulin in apple juice. *Process Biochemistry, 116*, 148-156.

Lightner, D. V. (1999). The penaeid shrimp viruses TSV, IHHNV, WSSV, and YHV: current status in the Americas, available diagnostic methods, and management strategies. *Journal of Applied Aquaculture, 9*(2), 27-52.

Liu, C., Cheng, Y., Du, C., Lv, T., Guo, Y., Han, M., Pi, F., Zhang, W., & Qian, H. (2019). Study on the wall-breaking method of carotenoids producing yeast *Sporidiobolus pararoseus* and the antioxidant effect of four carotenoids on SK-HEP-1 cells. *Preparative Biochemistry and Biotechnology, 49*(8), 767-774.

Liu, C., Hu, B., Cheng, Y., Guo, Y., Yao, W., & Qian, H. (2021). Carotenoids from fungi and microalgae: A review on their recent production, extraction, and developments. *Bioresource technology, 337*, 125398.

Liu, H., Guo, S., Wang, R., He, Y., Shi, Q., Song, Z., & Yang, M. (2021). Pathogen of *Vibrio harveyi* infection and C-type lectin proteins in whiteleg shrimp (*Litopenaeus vannamei*). *Fish & Shellfish Immunology, 119*, 554-562.

Liu, J., Zhang, K., Ren, X., Luo, G., & Shen, J. (2004). Bioimprinted protein exhibits glutathione peroxidase activity. *Analytica chimica acta, 504*(1), 185-189.

Liu, K.-F., Chiu, C.-H., Shiu, Y.-L., Cheng, W., & Liu, C.-H. (2010). Effects of the probiotic, *Bacillus subtilis* E20, on the survival, development, stress tolerance, and immune status of white shrimp, *Litopenaeus vannamei* larvae. *Fish & shellfish immunology, 28*(5-6), 837-844.

Livak, K. J., & Schmittgen, T. D. (2001). Analysis of relative gene expression data using real-time quantitative PCR and the $2^{-\Delta\Delta_{CT}}$ method. *methods, 25*(4), 402-408.

Lorenz, E., Runge, D., Marbà-Ardébol, A.-M., Schmacht, M., Stahl, U., & Senz, M. (2017). Systematic development of a two-stage fed-batch process for lipid accumulation in *Rhodotorula glutinis*. *Journal of biotechnology, 246*, 4-15.

Luo, T., Li, F., Lei, K., & Xu, X. (2007). Genomic organization, promoter characterization and expression profiles of an antiviral gene PmAV from the shrimp *Penaeus monodon*. *Molecular immunology, 44*(7), 1516-1523.

Machado, W. R. C., Murari, C. S., Duarte, A. L. F., & Del Bianchi, V. L. (2022). Optimization of agro-industrial coproducts (molasses and cassava wastewater) for the simultaneous production of lipids and carotenoids by *Rhodotorula mucilaginosa*. *Biocatalysis and Agricultural Biotechnology*, 102342.

Maldonade, I. R., Rodriguez-Amaya, D. B., & Scamparini, A. R. (2008). Carotenoids of yeasts isolated from the Brazilian ecosystem. *Food chemistry, 107*(1), 145-150.

Malisorn, C., & Suntornsuk, W. (2008). Optimization of β-carotene production by *Rhodotorula glutinis* DM28 in fermented radish brine. *Bioresource technology, 99*(7), 2281-2287.

Manowattana, A., Techapun, C., Laokuldilok, T., Phimolsiripol, Y., & Chaiyaso, T. (2020). Enhancement of β-carotene-rich carotenoid production by a mutant *Sporidiobolus pararoseus* and stabilization of its antioxidant activity by microencapsulation. *Journal of Food Processing and Preservation, 44*(8), e14596.

Marova, I., Carnecka, M., Halienova, A., Certik, M., Dvorakova, T., & Haronikova, A. (2012). Use of several waste substrates for carotenoid-rich yeast biomass production. *Journal of Environmental Management, 95*, S338-S342.

Mata-Gómez, L. C., Montañez, J. C., Méndez-Zavala, A., & Aguilar, C. N. (2014). Biotechnological production of carotenoids by yeasts: an overview. *Microbial Cell Factories, 13*(1), 1-11.

Mohapatra, S., Chakraborty, T., Kumar, V., DeBoeck, G., & Mohanta, K. N. (2013). Aquaculture and stress management: a review of probiotic intervention. *Journal of animal physiology and animal nutrition, 97*(3), 405-430.

Moliné, M., Flores, M. R., Libkind, D., Carmen Diéguez, M. d. C., Farías, M. E., & van Broock, M. (2010). Photoprotection by carotenoid pigments in the yeast *Rhodotorula mucilaginosa*: the role of torularhodin. *Photochemical & Photobiological Sciences, 9*(8), 1145-1151.

Mussagy, C. U., Kurnia, K. A., Dias, A. C., Raghavan, V., Santos-Ebinuma, V. C., & Pessoa Jr, A. (2022). An eco-friendly approach for the recovery of astaxanthin and β-carotene from *Phaffia rhodozyma* biomass using bio-based solvents. *Bioresource technology, 345*, 126555.

Nemer, G., Louka, N., Vorobiev, E., Salameh, D., Nicaud, J.-M., Maroun, R. G., & Koubaa, M. (2021). Mechanical cell disruption technologies for the extraction of dyes and pigments from microorganisms: A review. *Fermentation, 7*(1), 36.

Niamnuy, C., Devahastin, S., & Soponronnarit, S. (2007). Effects of process parameters on quality changes of shrimp during drying in a jet-spouted bed dryer. *Journal of food science, 72*(9), E553-E563.

Nie, J., Chen, D., Ye, J., Lu, Y., & Dai, Z. (2021). Preparative separation of three terpenoids from edible brown algae *Sargassum fusiforme* by high-speed countercurrent chromatography combined with preparative high-performance liquid chromatography. *Algal Research, 59*, 102449.

Nimrat, S., Khaopong, W., Sangsong, J., Boonthai, T., & Vuthiphandchai, V. (2021). Dietary administration of *Bacillus* and yeast probiotics improves the growth, survival, and microbial community of juvenile whiteleg shrimp, *Litopenaeus vannamei*. *Journal of Applied Aquaculture, 33*(1), 15-31.

Ninawe, A. S., & Selvin, J. (2009). Probiotics in shrimp aquaculture: avenues and challenges. *Critical reviews in microbiology, 35*(1), 43-66.

Niu, J., Wen, H., Li, C.-H., Liu, Y.-J., Tian, L.-X., Chen, X., Huang, Z., & Lin, H.-Z. (2014). Comparison effect of dietary astaxanthin and β-carotene in the presence and absence of cholesterol supplementation on growth performance, antioxidant capacity and gene expression of *Penaeus monodon* under normoxia and hypoxia condition. *Aquaculture, 422*, 8-17.

Nordberg, J., & Arnér, E. S. (2001). Reactive oxygen species, antioxidants, and the mammalian thioredoxin system. *Free radical biology and medicine, 31*(11), 1287-1312.

Park, P., Kim, E., & Chu, K. (2007). Chemical disruption of yeast cells for the isolation of carotenoid pigments. *Separation and Purification Technology, 53*(2), 148-152.

Poontawee, R., Lorliam, W., Polburee, P., & Limtong, S. (2023). Oleaginous yeasts: Biodiversity and cultivation. *Fungal Biology Reviews, 44*, 100295.

Poopisut, P., Boonyanan, P., Boontawan, P., Sukjit, E., Promsampao, N., Chollacoop, N., Ketudat-Cairns, M., Pattiya, A., & Boontawan, A. (2023). Oleaginous yeast, *Rhodotorula paludigena* CM33, platform for bio-oil and biochar productions via fast pyrolysis. *Biotechnology for Biofuels and Bioproducts, 16*(1), 17.

Prabawati, E., Hu, S.-Y., Chiu, S.-T., Balantyne, R., Risjani, Y., & Liu, C.-H. (2022). A synbiotic containing prebiotic prepared from a by-product of king oyster mushroom, *Pleurotus eryngii* and probiotic, *Lactobacillus plantarum* incorporated in diet to improve the growth performance and health status of white shrimp, *Litopenaeus vannamei*. *Fish & Shellfish Immunology, 120*, 155-165.

Prabhala, R. H., Braune, L. M., Garewal, H. S., & Watson, R. R. (1993). Influence of beta-carotene on immune functions. *Annals of the New York Academy of Sciences, 691*, 262-263.

Qiang, J., Wasipe, A., He, J., Tao, Y.-F., Xu, P., Bao, J.-W., Chen, D.-j., & Zhu, J.-H. (2019). Dietary vitamin E deficiency inhibits fat metabolism, antioxidant capacity, and immune regulation of inflammatory response in genetically improved farmed tilapia (GIFT, *Oreochromis niloticus*) fingerlings following *Streptococcus iniae* infection. *Fish & shellfish immunology, 92*, 395-404.

Rattanachai, A., Hirono, I., Ohira, T., Takahashi, Y., & Aoki, T. (2005). Peptidoglycan inducible expression of a serine proteinase homologue from kuruma shrimp (*Marsupenaeus japonicus*). *Fish & Shellfish Immunology, 18*(1), 39-48.

Raviadaran, R., Chandran, D., Shin, L. H., & Manickam, S. (2018). Optimization of palm oil in water nano-emulsion with curcumin using microfluidizer and response surface methodology. *Lwt, 96*, 58-65.

Redkar, S. G., & Davis, R. H. (1993). Crossflow microfiltration of yeast suspensions in tubular filters. *Biotechnology progress, 9*(6), 625-634.

Ribeiro, J. E. S., da Silva Sant'Ana, A. M., Martini, M., Sorce, C., Andreucci, A., de Melo, D. J. N., & da Silva, F. L. H. (2019). *Rhodotorula glutinis* cultivation on cassava wastewater for carotenoids and fatty acids generation. *Biocatalysis and Agricultural Biotechnology, 22*, 101419.

Robles-Iglesias, R., Naveira-Pazos, C., Fernández-Blanco, C., Veiga, M. C., & Kennes, C. (2023). Factors affecting the optimisation and scale-up of lipid accumulation in oleaginous yeasts for sustainable biofuels production. *Renewable and Sustainable Energy Reviews, 171*, 113043.

Rodrigues, T. V. D., Amore, T. D., Teixeira, E. C., & de Medeiros Burkert, J. F. (2019). Carotenoid production by *Rhodotorula mucilaginosa* in batch and fed-batch fermentation using agroindustrial byproducts. *Food technology and Biotechnology, 57*(3), 388.

Russotti, G., Osawa, A. E., Sitrin, R. D., Buckland, B. C., Adams, W. R., & Lee, S. S. (1995). Pilot-scale harvest of recombinant yeast employing microfiltration: a case study. *Journal of biotechnology, 42*(3), 235-246.

Ryu, J. H., Ha, E. M., Oh, C. T., Seol, J. H., Brey, P. T., Jin, I., Lee, D. G., Kim, J., Lee, D., & Lee, W. J. (2006). An essential complementary role of NF-κB pathway to microbicidal oxidants in *Drosophila* gut immunity. *The EMBO journal, 25*(15), 3693-3701.

Saenge, C., Cheirsilp, B., Suksaroge, T. T., & Bourtoom, T. (2011). Potential use of oleaginous red yeast *Rhodotorula glutinis* for the bioconversion of crude glycerol from biodiesel plant to lipids and carotenoids. *Process Biochemistry, 46*(1), 210-218.

Sahandi, J., Jafaryan, H., Soltani, M., & Ebrahimi, P. (2019). The use of two *Bifidobacterium* strains enhanced growth performance and nutrient utilization of Rainbow Trout (*Oncorhynchus mykiss*) fry. *Probiotics and antimicrobial proteins, 11*, 966-972.

Sánchez-Paz, A. (2010). White spot syndrome virus: an overview on an emergent concern. *Veterinary research, 41*(6).

Schmitz, A., & Nguyen, L. (2022). Seafood supply and demand disruptions: The Covid-19 pandemic and shrimp. *Aquaculture Economics & Management*, 1-25.

Schweiggert, R. M., & Carle, R. (2016). Carotenoid production by bacteria, microalgae, and fungi. *Carotenoids: nutrition, analysis and technology*, 217-240.

Sivathanu, B., & Palaniswamy, S. (2012). Purification and characterization of carotenoids from green algae *Chlorococcum humicola* by HPLC-NMR and LC-MS-APCI. *Biomedicine & Preventive Nutrition, 2*(4), 276-282.

Snart, J., Bibiloni, R., Grayson, T., Lay, C., Zhang, H., Allison, G. E., Laverdiere, J. K., Temelli, F., Vasanthan, T., & Bell, R. (2006). Supplementation of the diet with high-viscosity beta-glucan results in enrichment for *lactobacilli* in the rat cecum. *Applied and Environmental Microbiology, 72*(3), 1925-1931.

Song, Y.-L., & Li, C.-Y. (2014). Shrimp immune system-special focus on penaeidin. *Journal of marine Science and Technology, 22*(1), 1.

Sreedharan, K., Deepika, A., Paria, A., Babu, P. S., Makesh, M., & Rajendran, K. (2017). Ontogeny and expression analysis of tube (interleukin-1 receptor-associated kinase-4 homolog) from *Penaeus monodon* in response to white spot syndrome virus infection and on exposure to ligands. *Agri Gene, 3*, 21-31.

Stopka, J., Bugan, S., Broussous, L., Schlosser, Š., & Larbot, A. (2001). Microfiltration of beer yeast suspensions through stamped ceramic membranes. *Separation and Purification Technology, 25*(1-3), 535-543.

Sun, H., Yang, M., Gao, Z., Wang, X., Wu, C., Wang, Q., & Gao, M. (2023). Economic and environmental evaluation for a closed Loop of crude glycerol bioconversion to biodiesel. *Journal of biotechnology*.

Tang, W., Wang, Y., Zhang, J., Cai, Y., & He, Z. (2019). Biosynthetic pathway of carotenoids in *Rhodotorula* and strategies for enhanced their production.

Taskin, M., Sisman, T., Erdal, S., & Kurbanoglu, E. B. (2011). Use of waste chicken feathers as peptone for production of carotenoids in submerged culture of *Rhodotorula glutinis* MT-5. *European Food Research and Technology, 233*, 657-665.

Tassanakajon, A., Somboonwiwat, K., Supungul, P., & Tang, S. (2013). Discovery of immune molecules and their crucial functions in shrimp immunity. *Fish & Shellfish Immunology, 34*(4), 954-967.

Tepaamorndech, S., Nookaew, I., Higdon, S. M., Santiyanont, P., Phromson, M., Chantarasakha, K., Mhuantong, W., Plengvidhya, V., & Visessanguan, W. (2020). Metagenomics in bioflocs and their effects on gut microbiome and immune responses in Pacific white shrimp. *Fish & shellfish immunology, 106*, 733-741.

Thompson, J. C., & He, B. B. (2006). Characterization of crude glycerol from biodiesel production from multiple feedstocks. *Applied engineering in agriculture, 22*(2), 261-265.

Thuy, H. T. T., Nga, L. P., & Loan, T. T. C. (2011). Antibiotic contaminants in coastal wetlands from Vietnamese shrimp farming. *Environmental Science and Pollution Research, 18*, 835-841.

Tidwell, J. H., & Allan, G. L. (2001). Fish as food: aquaculture's contribution. *EMBO reports, 2*(11), 958-963.

Tong, S., Zhang, H., Shen, M., Ito, Y., & Yan, J. (2015). Application and comparison of high-speed countercurrent chromatography and high performance liquid chromatography in preparative enantioseparation of α-substitution mandelic acids. *Separation science and technology, 50*(5), 735-743.

Tran, L., Nunan, L., Redman, R. M., Mohney, L. L., Pantoja, C. R., Fitzsimmons, K., & Lightner, D. V. (2013). Determination of the infectious nature of the agent of acute hepatopancreatic necrosis syndrome affecting penaeid shrimp. *Diseases of Aquatic Organisms, 105*(1), 45-55.

Uematsu, S., Fujimoto, K., Jang, M. H., Yang, B.-G., Jung, Y.-J., Nishiyama, M., Sato, S., Tsujimura, T., Yamamoto, M., & Yokota, Y. (2008). Regulation of humoral and cellular gut immunity by lamina propria dendritic cells expressing Toll-like receptor 5. *Nature immunology, 9*(7), 769-776.

Uprety, B. K., Dalli, S. S., & Rakshit, S. K. (2017). Bioconversion of crude glycerol to microbial lipid using a robust oleaginous yeast *Rhodosporidium toruloides* ATCC 10788 capable of growing in the presence of impurities. *Energy Conversion and Management, 135*, 117-128.

Valduga, E., Ribeiro, A. H. R., Cence, K., Colet, R., Tiggemann, L., Zeni, J., & Toniazzo, G. (2014). Carotenoids production from a newly isolated *Sporidiobolus pararoseus* strain using agroindustrial substrates. *Biocatalysis and Agricultural Biotechnology, 3*(2), 207-213.

Valencia, A., LeMen, C., Ellero, C., Lafforgue-Baldas, C., Morris, J. F., & Schmitz, P. (2022). Direct observation of the microfiltration of yeast cells at the micro-scale: Characterization of cake properties. *Separation and Purification Technology, 298*, 121614.

Wachirasiri, K., Wanlapa, S., Uttapap, D., Puttanlek, C., & Rungsardthong, V. (2017). Changing in processing yield and physical properties of frozen white shrimp (*Penaeus vannamei*) treated with lysine and sodium bicarbonate. *International Journal of Food Science & Technology, 52*(3), 763-771.

Wang, D., Li, F., Chi, Y., & Xiang, J. (2012). Potential relationship among three antioxidant enzymes in eliminating hydrogen peroxide in penaeid shrimp. *Cell Stress and Chaperones, 17*, 423-433.

Wang, M.-H., Wang, R.-Y., Wei, X.-Y., Zhao, W., & Fan, X. (2021). Molecular characteristics of the oxidation products of a lignite based on the big data obtained from Fourier transform ion cyclotron resonance mass spectrometry. *Fuel, 295*, 120644.

Wang, M., Mao, W., Wang, X., Li, F., Wang, J., Chi, Z., Chi, Z., & Liu, G. (2019a). Efficient simultaneous production of extracellular polyol esters of fatty acids and intracellular lipids from inulin by a deep-sea yeast *Rhodotorula paludigena* P4R5. *Microbial Cell Factories, 18*, 1-13.

Wang, M., Mao, W., Wang, X., Li, F., Wang, J., Chi, Z., Chi, Z., & Liu, G. (2019b). Efficient simultaneous production of extracellular polyol esters of fatty acids and intracellular lipids from inulin by a deep-sea yeast *Rhodotorula paludigena* P4R5. *Microbial cell factories, 18*(1), 1-13.

Wang, P.-H., Gu, Z.-H., Wan, D.-H., Liu, B.-D., Huang, X.-D., Weng, S.-P., Yu, X.-Q., & He, J.-G. (2013). The shrimp IKK–NF-κB signaling pathway regulates antimicrobial peptide expression and may be subverted by white spot syndrome virus to facilitate viral gene expression. *Cellular & molecular immunology, 10*(5), 423-436.

Wang, Y., Wang, B., Liu, M., Jiang, K., Wang, M., & Wang, L. (2020). Comparative transcriptome analysis reveals the potential influencing mechanism of dietary astaxanthin on growth and metabolism in *Litopenaeus vannamei. Aquaculture Reports, 16*, 100259.

Wei, J., Zhang, X., Yu, Y., Huang, H., Li, F., & Xiang, J. (2014). Comparative transcriptomic characterization of the early development in Pacific white shrimp *Litopenaeus vannamei. PloS one, 9*(9), e106201.

Wirth, F., & Goldani, L. Z. (2012). Epidemiology of *Rhodotorula*: an emerging pathogen. *Interdisciplinary perspectives on infectious diseases, 2012*.

Xie, Y., Ho, S.-H., Chen, C.-N. N., Chen, C.-Y., Jing, K., Ng, I.-S., Chen, J., Chang, J.-S., & Lu, Y. (2016). Disruption of thermo-tolerant *Desmodesmus* sp. F51 in high pressure homogenization as a prelude to carotenoids extraction. *Biochemical Engineering Journal, 109*, 243-251.

Yang, F., Hanna, M. A., & Sun, R. (2012). Value-added uses for crude glycerol--a byproduct of biodiesel production. *Biotechnology for biofuels, 5*(1), 1-10.

Yang, S.-P., Wu, Z.-H., & Jian, J.-C. (2011). Distribution of marine red yeasts in shrimps and the environments of shrimp culture. *Current microbiology, 62*, 1638-1642.

Yeeh, Y. (1999). Rhodotorula.

Yen, H.-W., & Zhang, Z. (2011). Effects of dissolved oxygen level on cell growth and total lipid accumulation in the cultivation of *Rhodotorula glutinis. Journal of bioscience and bioengineering, 112*(1), 71-74.

Yimyoo, T., Yongmanitchai, W., & Limtong, S. (2011). Carotenoid production by *Rhodosporidium paludigenum* DMKU3-LPK4 using glycerol as the carbon source. *Agriculture and Natural Resources, 45*(1), 90-100.

Yu, M.-C., Li, Z.-J., Lin, H.-Z., Wen, G.-L., & Ma, S. (2009). Effects of dietary medicinal herbs and *Bacillus* on survival, growth, body composition, and digestive enzyme activity of the white shrimp *Litopenaeus vannamei. Aquaculture International, 17*, 377-384.

Yu, P., Shan, H., Cheng, Y., Ma, J., Wang, K., & Li, H. (2022). Translucent disease outbreak in *Penaeus vannamei* post-larva accompanies the imbalance of pond water and shrimp gut microbiota homeostasis. *Aquaculture Reports, 27*, 101410.

Yu, Y., Liu, Y., Yin, P., Zhou, W., Tian, L., Liu, Y., Xu, D., & Niu, J. (2020). Astaxanthin attenuates fish oil-related hepatotoxicity and oxidative insult in juvenile Pacific white shrimp (*Litopenaeus vannamei*). *Marine Drugs, 18*(4), 218.

Yuan, Y., Jin, M., Xiong, J., & Zhou, Q. (2019). Effects of dietary dosage forms of copper supplementation on growth, antioxidant capacity, innate immunity enzyme activities and gene expressions for juvenile *Litopenaeus vannamei*. *Fish & Shellfish Immunology, 84*, 1059-1067.

Zhang, S.-p., Li, J.-f., Wu, X.-c., Zhong, W.-j., Xian, J.-a., Liao, S.-a., Miao, Y.-t., & Wang, A.-l. (2013). Effects of different dietary lipid level on the growth, survival and immune-relating genes expression in Pacific white shrimp, *Litopenaeus vannamei*. *Fish & shellfish immunology, 34*(5), 1131-1138.

Zhao, D., & Li, C. (2022). Multi-omics profiling reveals potential mechanisms of culture temperature modulating biosynthesis of carotenoids, lipids, and exopolysaccharides in oleaginous red yeast *Rhodotorula glutinis* ZHK. *LWT, 171*, 114103.

Zheng, J., Jia, Y., Li, F., Chi, M., Cheng, S., Liu, S., Jiang, W., & Liu, Y. (2023). Changes in the gene expression and gut microbiome to the infection of decapod iridescent virus 1 in *Cherax quadricarinatus*. *Fish & Shellfish Immunology, 132*, 108451.

Zheng, L., Xie, S., Zhuang, Z., Liu, Y., Tian, L., & Niu, J. (2021). Effects of yeast and yeast extract on growth performance, antioxidant ability and intestinal microbiota of juvenile Pacific white shrimp (*Litopenaeus vannamei*). *Aquaculture, 530*, 735941.

Zhou, Q., Wang, Y., Hu, J., Bao, Z., & Wang, M. (2023). Development of a real-time enzymatic recombinase amplification assay (RT-ERA) and an ERA combined with lateral flow dipsticks (LFD) assay (ERA-LFD) for rapid detection of acute hepatopancreatic necrosis disease (AHPND) in shrimp *Penaeus vannamei*. *Aquaculture, 566*, 73905.

VITAE

Miss Cheeranan Sriphuttha was born on December 3, 1988, in Udon Thani, Thailand. She graduated with a Bachelor's degree in Biotechnology from Maejo University in 2011. Later, she pursued a Master's degree in Applied Microbiology from Chiang Mai University in 2014. From 2014 to 2020, she worked as a Section Manager at the Central Laboratory Biotechnology Research Center, Charoen Pokphand Food PCL. In 2020, she was awarded the Suranaree University of Technology (SUT) scholarship under the External Grants and Scholarships for Graduate Students (OROG) program. She is currently pursuing her doctoral degree under the supervision of Associate Professor Apicaht Boontawan. Her research topic focuses on enhancing carotenoid production of *Rhodotorula paludigena* CM33 in a pilot-scale using crude glycerol as the substrate and its application as a dietary supplement for *Litopenaeus vannamei*. The chapter 5 in this thesis was published as the research article.

The paper is as follows:

Sriphuttha, C., Limkul, S., Pongsetkul, J., Phiwthong, T., Massu, A., Sumniangyen, N., Boontawan, P., Ketudat-Cairns, M., Boontawan, A., Boonchuen, P., (2023), Effect of fed dietary yeast (*Rhodotorula paludigena* CM33) on shrimp growth, gene expression, intestinal microbial, disease resistance, and meat composition of *Litopenaeus vannamei*, Developmental and Comparative Immunology, 104896.